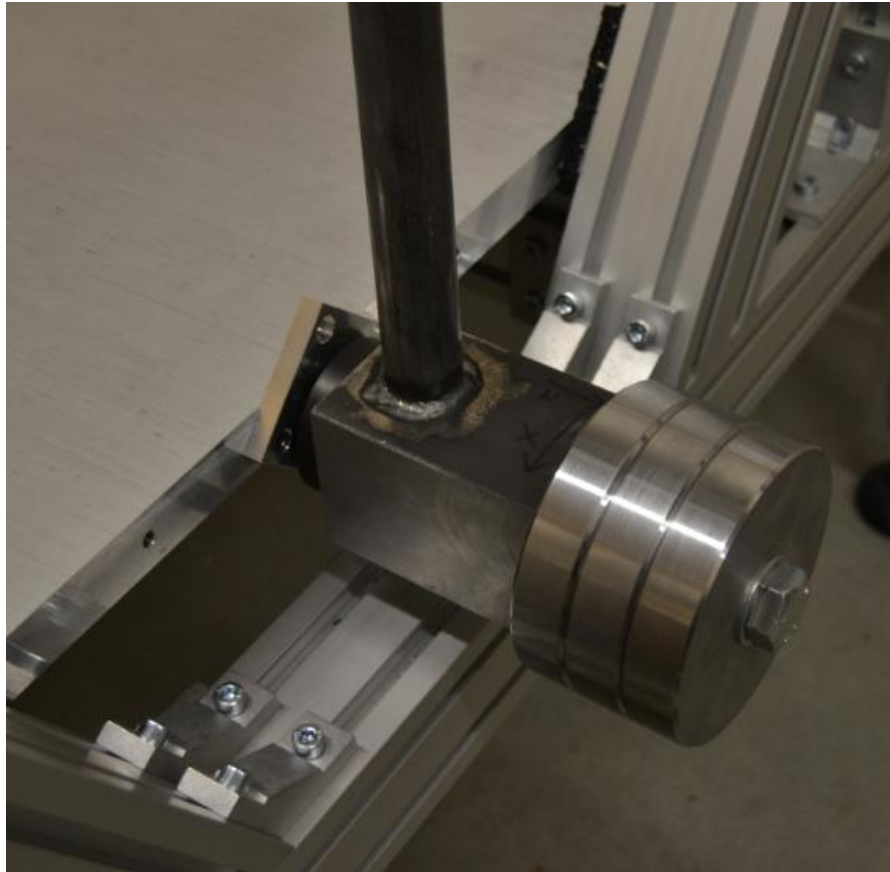


# CHALMERS



## Development of a Shock Test Facility for Qualification of Space Equipment

*Master of Science Thesis in the Master's Programme Applied Mechanics*

**MARTIN JONSSON**

Department of Applied Mechanics

*Division of Dynamics*

CHALMERS UNIVERSITY OF TECHNOLOGY

Göteborg, Sweden 2012

Master's thesis 2012:43



MASTER'S THESIS IN APPLIED MECHANICS

Development of a Shock Test Facility for Qualification  
of Space Equipment

MARTIN JONSSON

Department of Applied Mechanics  
*Division of Dynamics*  
CHALMERS UNIVERSITY OF TECHNOLOGY  
Göteborg, Sweden 2012

Development of a Shock Test Facility for Qualification of Space Equipment  
MARTIN JONSSON

© MARTIN JONSSON, 2012

Master's Thesis 2012:43  
ISSN 1652-8557  
Department of Applied Mechanics  
Division of Dynamics  
Chalmers University of Technology  
SE-412 96 Göteborg  
Sweden  
Telephone: + 46 (0)31-772 1000

Cover:

The pendulum hammer of the shock test facility in the in-plane configuration. Visible are the interchangeable hammer masses, the anvil plate, the hammerhead and parts of the resonant plate and the rig.

Department of Applied Mechanics  
Göteborg, Sweden 2012

Development of a Shock Test Facility for Qualification of Space Equipment  
Master of Science Thesis in the Master's Programme Applied Mechanics  
MARTIN JONSSON  
Department of Applied Mechanics  
Division of Dynamics  
Chalmers University of Technology

## ABSTRACT

Spacecrafts are subject to recurrent high frequency, high amplitude shocks over their lifetime. These shocks have been known to cause failures in systems leading to total or partial loss of entire space missions. With new launch vehicles the shocks are getting more frequent and more severe. Launch vehicle manufacturers are striving to keep as much mass as possible available for value adding payload, so damping materials are kept to a minimum. Hence the required qualification test levels are also increasing which in turn puts higher demands on the shock test facilities.

Requirements for a new shock test facility have been established from research of the shock phenomenon and existing shock test facilities. With a system's engineering approach they have been developed from requirements to concepts. Input from simulations, experts and analysis have been used to bring the development process from a point with a large number of concepts to a point with a final one. The details of this concept were developed into a final design which led to manufacturing of the parts and an actual assembled shock test facility.

The new shock test facility THOR (Testing Hammer for extraOrdinary Rough environments) is a metal-to-metal impact facility capable of qualifying equipment against shock in agreement with any of the shock testing standards and best practices given by NASA, MIL, ECSS or ESA.

The excitation source is the impact between a versatile hammer and a resonant plate which gives a shock that can be tuned to simulate a wide array of mid-field pyroshock environments.

The shock test facility has shown capacity of testing equipment up to 26 kg with control of the SRS for frequencies 100 Hz – 10 kHz. It can achieve shock levels over 3000 g at frequencies 1 kHz – 3 kHz. For smaller specimen the acceleration levels can reach up to 5000 g at 1 kHz and even higher for the highest frequencies.

Key words: Metal-to-Metal Impact, Pyroshock, Qualification Testing, Resonant Plate, Shock, Shock Response Spectrum, Shock Table, Shock Test Facility, Space Equipment, System Engineering



# Contents

ABSTRACT	I
CONTENTS	III
ACKNOWLEDGEMENT	VII
LIST OF ABBREVIATIONS AND SYMBOLS	VIII
LIST OF FIGURES AND TABLES	IX
1 INTRODUCTION	1
1.1 Mission statement	1
1.2 Shock	2
1.3 Shock categorisation	3
1.3.1 Velocity shocks	3
1.3.2 Displacement shocks	3
1.3.3 High frequency shocks	3
1.4 Sources of shock in space missions	5
1.4.1 Effect on equipment	7
1.5 Shock Response Spectrum	7
1.6 Existing shock test facilities	9
1.6.1 Far-field shock test facilities	9
1.6.2 Mid-field shock test facilities	10
1.6.3 Near-field shock test facilities	13
1.7 Shock verification process	13
1.7.1 Qualification test	13
1.7.2 Acceptance test	14
1.7.3 Test levels	14
2 SYSTEM ENGINEERING	19
2.1 Goals with project	20
2.2 Requirements specification	21
2.2.1 Requirement capture	21
2.2.2 Requirement allocation	21
2.2.3 Requirement analysis and validation	23
2.2.4 Requirement maintenance	23
2.3 Concept generation	23
2.3.1 Functional analysis	24
2.3.2 A more systematic look on existing mid-field STFs	26
2.3.3 Brain storming and initial elimination	28
2.3.4 Trade-off studies	28
2.4 Simulation and analysis	32
2.4.1 Selection of parameters and starting point model	34
2.4.2 Parameter simulations	36
2.5 Selection of the final concept	47

2.5.1	Hanging pendulum	47
2.5.2	Foam pad pendulum	48
2.5.3	Hammer combination	49
2.5.4	Numerical trade-off and the final concept	50
2.6	Design process	51
2.6.1	Plate	52
2.6.2	Anvil plate	52
2.6.3	Hammerheads	52
2.6.4	Hammer masses	53
2.6.5	Hammer arm and connector	53
2.6.6	Rig	55
2.6.7	Assembly	57
3	RESEARCH AND DEVELOPMENT PROCESS RESULTS	58
3.1	Final design, parameters and range	58
3.2	Expected results	58
3.3	Data acquisition chain	59
3.3.1	Sensor	60
3.3.2	DAQ hardware	61
3.3.3	DAQ software	61
4	SHOCK TEST FACILITY RESULTS	62
4.1	Actual shock test facility	62
4.2	Characterisation test campaign	62
4.2.1	Repeatability	63
4.2.2	Impact velocity	64
4.2.3	Hammer mass	66
4.2.4	Anvil material	67
4.2.5	Hammerhead material	69
4.2.6	Impact location	70
4.2.7	Foam type	73
4.2.8	Boundary conditions of the plate	74
4.2.9	Mass dummy	75
4.2.10	OOP/IP shift	77
4.3	Goal SRS tuning	79
4.3.1	No dummy OOP	79
4.3.2	Light dummy OOP	81
4.3.3	Heavy dummy OOP	82
4.3.4	No dummy IP	83
4.3.5	Heavy dummy IP	84
5	DISCUSSION	86
5.1	Fulfilment of goals	86
5.1.1	Research the field and define requirements for a new STF	86
5.1.2	Develop STF concepts based on the found requirements and the QuadPack	86

5.1.3	Get data from simulations based on the requirements and concepts	86
5.1.4	Hold elimination process and trade-off studies based on requirements, simulation results and input from experts to select final concept	87
5.1.5	Design the concept details to a level where the STF can be manufactured	87
5.1.6	Test the STF to verify that it gives predicted results	87
5.2	Expected and acquired results comparison	87
5.3	Fulfilment of requirements	92
6	CONCLUSIONS	94
6.1	Future work and recommendations	94
	REFERENCES	96
	APPENDIX A – BRAINSTORMING RESULTS	99
	APPENDIX B – ANALYSIS INFORMATION	104
	APPENDIX C – SUSTAINABLE DEVELOPMENT	106
	APPENDIX D – CHARACTERISATION TEST CAMPAIGN, PLAN AND ANNOTATIONS	107
	APPENDIX E – CALCULATION OF THE PEAK ACCELERATION OF A SDOF SYSTEM	125
	APPENDIX F – ASSEMBLY OF STF	126



## Acknowledgement

First of all I would like to thank ISIS for allowing me to take a huge step towards my dream and goal of working in the space industry by doing this thesis project. It has been a pleasure to twist my head around problems in the creative and international atmosphere that pervades within ISIS. Thank you for letting me come to the Netherlands and work within the heart of the European space industry!

Everyone at ISIS deserves a thank you for being helpful and curious about my project, but special thanks goes to the Mechanical Team that has given me input throughout the project and made no problem unsolvable.

A big factor for the success of this project has been the leader style of my ISIS supervisor Michiel van Bolhuis. By giving me a lot of independency and responsibility I have had the opportunity to grow a lot as an engineer and for that I am ever grateful. By providing support and advice at important toll-gates he made sure that momentum was kept throughout the project.

At a key moment in this project my Chalmers supervisor Mikael Enelund gave me the advice to trust my own judgement which boosted my confidence and made me perform better. That is just one example of the importance of his support that has been a cornerstone throughout my thesis. Thank you!

During the research in this project I found that only a fraction of the knowledge in the field of shock can be found in published sources. The main part is located in the minds, spines and fingertips of the shock experts at the universities, agencies and industries of the world. Some of these experts have aided me with pragmatic advice that I would not have been able to finish my thesis without. For this my sincerest appreciations goes to Christophe De Fruytier at Thalés Alenia Space, Professor Daniel Rixen and Paul van der Valk at Delft University of Technology, Dr Alexander Lacher at Berlin Institute of Technology, Anette Bäger at DLR, Jonas Leijon at RUAG Space AB, Mark Wagner at ESTEC, Jan Kasper at ASTRIUM Satellites, Caroline Jonsson at Epsilon AB and Tobias Andersson at Xdin AB. Thousands of thanks to all of you!

Another important part of the project has been the different software I have used. The thesis would not have been possible without them and they deserve some kudos. For all those times that I came across calculations or problems I could not solve in my head Matlab was always there as a helping friend. Matlab has also been used together with the Data Acquisition Toolbox to develop the DAQ software and a program that simplified the comparison of SRSs. For the FE simulations Abaqus Explicit has been used and Abaqus CAE was used for the pre- and post-processing of the FE data. AutoDesk Inventor has been used throughout the project for virtual prototyping and for making drawings.

Last but not least I would like to take the opportunity to thank you, the reader, for showing interest in my thesis. Stay curious and shock on!

Delft, the rainy October of 2012

Martin Jonsson

## List of Abbreviations and Symbols

<b>Al</b>	Aluminium
<b>CAD</b>	Computer Aided Design
<b>DAQ</b>	Data AcQuisition
<b>ECSS</b>	European Cooperation for Space Standardization
<b>ESA</b>	European Space Agency
<b>FEA</b>	Finite Element Analysis
<b>FEM</b>	Finite Element Method
<b>IEPE</b>	Integrated Electronics PiezoElectric
<b>IP</b>	In Plane
<b>ISIS</b>	Innovative Solutions In Space
<b>MEE</b>	Maximum Expected Environment
<b>n/a</b>	not available/not applicable
<b>NASA</b>	National Aeronautics and Space Administration
<b>OOP</b>	Out Of Plane
<b>SDOF</b>	Single Degree Of Freedom
<b>SRS</b>	Shock Response Spectrum
<b>SS</b>	Stainless Steel
<b>STF</b>	Shock Test Facility
<b>THOR</b>	Testing Hammer for extraOrdinary Rough environments
<b>QM</b>	Qualification Model

## List of Figures and Tables

Figure 1	<i>ISIS – Innovative Solutions In Space</i> .....	1
Figure 2	<i>Typical acceleration time history resulting from shock</i> .....	2
Figure 3	<i>Difference in acceleration time history between near- and far-field shocks [3]</i> .....	4
Figure 4	<i>Typical launch sequence for Ariane 5 [7]</i> .....	5
Figure 5	<i>Example of a clamp band for mounting a spacecraft to a launch vehicle (Source: ESA/EADS-Astrium, used with authorisation from ESA)</i> .....	6
Figure 6	<i>Principle of shock response spectrum calculation. From acceleration time history, through maximum acceleration response of single degree of freedom systems, to shock response spectrum</i> .....	7
Figure 7	<i>Typical shock response spectrum [6]</i> .....	8
Figure 8	<i>From SDOF system to SRS data point [12]</i> .....	8
Figure 9	<i>Electrodynamic shaker (Source: ESA, used with permission of ESA)</i> .....	10
Figure 10	<i>Example of metal-to-metal impact STF's a) mono-plate b) bi-plate c) tunable plate [16]</i> .....	10
Figure 11	<i>Resonant bar, also called Hopkinson bar [16]</i> .....	11
Figure 12	<i>Resonant beam excited by a pneumatic air gun [17]</i> .....	12
Figure 13	<i>German Aerospace Center STF [18]</i> .....	12
Figure 14	<i>Examples of pyrotechnic STF's [16]</i> .....	13
Figure 15	<i>Example of MEE specification from measurements</i> .....	15
Figure 16	<i>Qualification SRSs for Russian launch vehicles compared to the STF SRS requirement</i> .....	16
Figure 17	<i>Qualification SRSs for non-Russian launch vehicles compared to STF SRS requirement</i> .....	17
Figure 18	<i>Qualification SRS described by [100Hz, 1000Hz, 10000Hz], [60g, 3500g, 4500g]</i> .....	17
Figure 19	<i>Shock test tolerances from different sources a) ECSS b) ESA c) MIL d) NASA</i> .....	18
Figure 20	<i>System Engineering functions and boundaries</i> .....	19
Figure 21	<i>Requirement capture</i> .....	21
Figure 22	<i>Development chain from mission start to design concept (This figure is taken from NASA/SP-2007-6105 Rev1, NASA Systems Engineering Handbook, and used with permission of NASA) [21]</i> .....	23
Figure 23	<i>Concept generation process as growing/diminishing list of concepts</i> .....	24
Figure 24	<i>STF sub-functions</i> .....	25
Figure 25	<i>STF function tree</i> .....	25
Figure 26	<i>Mechanical impact</i> .....	26

Figure 27	<i>Shock test setup with resonant plate and pendulum hammer [28]</i> .....	26
Figure 28	<i>RUAG Space AB STF [23]</i> .....	26
Figure 29	<i>From sub-solutions to concept</i> .....	28
Figure 30	<i>Surviving sub-solutions</i> .....	29
Figure 31	<i>STF concept tree showing the 115 surviving concepts</i> .....	30
Figure 32	<i>Thales Alenia Space ETCA shock test facility [26]</i> .....	31
Figure 33	<i>Concept tree after additional trade-off iterations</i> .....	31
Figure 34	<i>Comparison between pendulum and ram hammer</i> .....	32
Figure 35	<i>Concept tree with the three finalist concepts</i> .....	32
Figure 36	<i>Comparison between explicit and implicit solution methods, based on [31]</i> .....	33
Figure 37	<i>Simulation cycle</i> .....	34
Figure 38	<i>Von Mises stress levels [Pa] captured milliseconds after impact</i> .....	36
Figure 39	<i>Starting point simulation SRS. It compares quite well to the requirement SRS also plotted</i> .....	36
Figure 40	<i>Influence of plate thickness on SRS</i> .....	37
Figure 41	<i>Influence on SRS when shortening the plate</i> .....	38
Figure 42	<i>In plane impact. Von Mises stress [Pa] captured milliseconds after impact</i> .....	38
Figure 43	<i>SRS for side impact with three measurement locations. Note that it is the IP acceleration that has been plotted.</i> .....	39
Figure 44	<i>SRS effect of the length of the plate</i> .....	40
Figure 45	<i>Resonant plate dimensions</i> .....	40
Figure 46	<i>Measurement locations (and impact location in brackets)</i> .....	41
Figure 47	<i>Influence of measurement location as can be seen in the former Figure 41</i>	
Figure 48	<i>Examination of different measurement locations</i> .....	42
Figure 49	<i>Different impact locations (and measurement location in brackets) and SRS results for these configurations</i> .....	43
Figure 50	<i>Influence of impact velocity on SRS</i> .....	43
Figure 51	<i>Influence of anvil on SRS</i> .....	44
Figure 52	<i>Influence of hammer mass on SRS</i> .....	45
Figure 53	<i>Curved surface vs. flat surface of misaligned hammer</i> .....	45
Figure 54	<i>Influence of hammer radius of curvature from simulations</i> .....	46
Figure 55	<i>The hanging pendulum concept</i> .....	47
Figure 56	<i>Hanging pendulum concept, a) In plane configuration and b) c) Out of plane configuration</i> .....	48
Figure 57	<i>The foam pad pendulum concept</i> .....	48

Figure 58	<i>Foam pad pendulum concept a) OOP configuration b) IP configuration...</i>	49
Figure 59	<i>The hammer combination concept</i>	49
Figure 60	<i>Hammer combination concept</i>	50
Figure 61	<i>Plate with holes for assembly a) Design 1 b) Design 2</i>	52
Figure 62	<i>Anvil plate a) Design 1 b) Design 2</i>	52
Figure 63	<i>Hammerhead a) Design 1 b) Design 2</i>	53
Figure 64	<i>Hammer masses ab) Design 1 c) Design 2</i>	53
Figure 65	<i>Hammer arm and connector, design 1</i>	53
Figure 66	<i>Hammer arm, design 2</i>	54
Figure 67	<i>a) Hammer connector, design 2 b) Hammer assembly, design 2</i>	54
Figure 68	<i>a) Hammer connector, design 3 b) Hammer assembly, design 3</i>	55
Figure 69	<i>a) Charge angle plate to provide repeatability b) Bearing solution</i>	55
Figure 70	<i>a) Table sketch 1 b) Table sketch 2</i>	56
Figure 71	<i>MK table rig, design 1</i>	56
Figure 72	<i>MK rig, design 2</i>	57
Figure 73	<i>Final design STF a) OOP configuration b) IP configuration</i>	57
Figure 74	<i>Predicted behaviour of STF. The slope over and under the knee frequency as well, as the overall amplitude level, are expected to be controlled by different parameters</i>	59
Figure 75	<i>Zeroshift of shock signal [40]</i>	60
Figure 76	<i>a) Sensor b) Sensor cube c) DAQ-module d) Initial software tests</i>	61
Figure 77	<i>Fully assembled STF in a) OOP configuration b) IP configuration</i>	62
Figure 78	<i>Repeatability of three consecutive shocks</i>	63
Figure 79	<i>Charge angle plate in a) OOP configuration b) IP configuration</i>	65
Figure 80	<i>STF with different charge heights → different impact velocities</i>	65
Figure 81	<i>Influence of Impact velocity</i>	66
Figure 82	<i>Hammer with attached extra mass a) 8 kg b) 10 kg</i>	66
Figure 83	<i>Effect of increasing hammer mass</i>	67
Figure 84	<i>Anvil plates in three different materials</i>	67
Figure 85	<i>a) Influence of anvil material b) Influence of anvil in plastic material</i>	68
Figure 86	<i>Influence of mechanical filter on anvil</i>	68
Figure 87	<i>The two different hammerheads. The hammerhead on the left is the hardened one</i>	69
Figure 88	<i>Influence of hammerhead</i>	69
Figure 89	<i>Influence of soft foam on anvil</i>	70

Figure 90	Impact locations of resonant plate.....	70
Figure 91	Impact location shift between -2y and -3y .....	70
Figure 92	Long term repeatability.....	71
Figure 93	Influence of impact location shift in the x-direction .....	72
Figure 94	Influence of impact location shift in the y-direction .....	72
Figure 95	Influence of impact location shift in the diagonal xy-direction .....	73
Figure 96	Influence of Foam Type .....	73
Figure 97	Resonant plate with its boundary conditions altered a) Free b) Siderails c) Clamps .....	74
Figure 98	Influence of clamping the plate with the siderails .....	74
Figure 99	Resonant plate with clamps .....	75
Figure 100	Influence of clamping the plate with clamps.....	75
Figure 101	Light dummy mounted on resonant plate, 2 kg added to hammer mass ..	76
Figure 102	Influence of light mass dummy.....	76
Figure 103	Heavy dummy on plate, 2 kg added to hammer mass .....	77
Figure 104	Influence of heavy dummy.....	77
Figure 105	IP and OOP impacts .....	78
Figure 106	IP acceleration levels IP impact direction.....	78
Figure 107	Influence of mounting heavy mass dummy on plate.....	79
Figure 108	Results of plan configuration, Shock 56 .....	80
Figure 109	a) Clamping the plate b) Final shock OOP no dummy, Shock 84 .....	81
Figure 110	Plan configuration SRS.....	81
Figure 111	a) Increase of hammer mass b) Comparison of Shock 81 and goal SRS. ....	82
Figure 112	a) Result of the plan configuration test, Shock 91    b) Comparison of Shock 95 and goal SRS .....	83
Figure 113	a) Result of the plan configuration shock. Shock 114    b) Comparison between Shock 117 and goal SRS .....	84
Figure 114	a) Shock 127 is the plan configuration SRS b) Shock 128 is the best shock achieved for the heavy dummy IP .....	85
Figure 115	Cracked anvil plate .....	85
Figure 116	Resonant plate mode at 158 Hz for free boundary conditions.....	88
Figure 117	Resonant plate mode shapes for the frequencies around 1000 Hz .....	88
Figure 118	Relationship between impact and measurement location and apparent modes in the SRS .....	89
Figure 119	Simulation Setup 22 .....	91

<i>Figure 120</i>	<i>Comparison of simulation of Setup 22 and measurement of shock test with the configuration Shock 70 .....</i>	<i>91</i>
<i>Figure 121</i>	<i>Comparison of simulation of Setup 3F and measurement of shock test with the configuration Shock 113 .....</i>	<i>92</i>
<i>Table 1</i>	<i>Pyrotechnic applications in space missions [9].....</i>	<i>6</i>
<i>Table 2</i>	<i>Impact STF's in Aerospace industry [8] .....</i>	<i>11</i>
<i>Table 3</i>	<i>Shock requirements for ESA satellites [8] .....</i>	<i>15</i>
<i>Table 4</i>	<i>Shock test tolerances of the SRS [3], [6] and [19] .....</i>	<i>18</i>
<i>Table 5</i>	<i>Space system requirement classes .....</i>	<i>22</i>
<i>Table 6</i>	<i>Sub-function solutions of existing STF's .....</i>	<i>27</i>
<i>Table 7</i>	<i>Parameter and dimension specification for STF .....</i>	<i>46</i>
<i>Table 8</i>	<i>Apparent advantages and disadvantages.....</i>	<i>48</i>
<i>Table 9</i>	<i>Apparent advantages and disadvantages.....</i>	<i>49</i>
<i>Table 10</i>	<i>Apparent advantages and disadvantages.....</i>	<i>50</i>
<i>Table 11</i>	<i>Results from numerical trade-off .....</i>	<i>51</i>
<i>Table 12</i>	<i>Final parameters and their range .....</i>	<i>58</i>



# 1 Introduction

Modern spacecraft are subject to recurrent high frequency, high amplitude shocks during their operational lifetime. Launch vehicle manufacturers are constantly trying to remove redundant material to make more effective mass available for profit inducing payload. This has led to a minimisation of the damping material and thus the shocks are growing more severe with new launch vehicles. As a consequence the shock qualification levels are getting higher to gain confidence that the equipment can withstand the harsh environment.

As the shocks propagate through the vehicle they are damped, reflected, refracted and dissipated in a highly complex manner. Researchers are constantly pushing the bar on what is possible to capture in computer simulations but high frequency shock is a nut that to some extent remains uncracked. Physical shock tests are hence conventionally used in aerospace industry to qualify space equipment. With the shock and qualification levels growing the demands on the shock test facilities also grow. This report presents the research and development process of a new shock test facility, considering the complete chain from requirement specification to an actual self-built test facility and prototype verification tests.

## 1.1 Mission statement

ISIS - Innovative Solutions In Space, is a spin-off space company from TU Delft – Delft University of Technology, specializing in missions of very small satellites. Part of its business is the development of small satellite deployment systems and providing (services related to) actual launches, through its subsidiary company Innovative Space Logistics. At present, ISIS is developing its second generation of satellite deployment systems. Shock testing has been part of earlier development projects and ISIS is looking to improve its capability for mechanical testing.



*Figure 1* ISIS – Innovative Solutions In Space

The basic objectives that ISIS defined for this project were:

- To define requirements for a new shock test facility from typical use cases
- To develop one specific use case in detail, namely the verification process of the ISIS QuadPack design. The QuadPack is a system to collectively launch and deploy multiple small satellites on small launch vehicles. The verification process ranges from verification planning to analysis and simulation and performing actual tests on prototypes
- To develop a shock test setup including theoretical framework relating test data to conclusions on behaviour to actual shock loads on subjects under test.

A particularly concise description of the project could be:

**ISIS wishes to verify that the developing deployment system QuadPack survives the shock environments related to space travel.**

To understand what this means deeper insights on the shock phenomenon and the verification process of space equipment are required.

## 1.2 Shock

The mechanical phenomenon of shock does not have an absolute definition, much due to its complex nature. An attempt on a definition was made at the first Shock and Vibration Symposium in 1947 where mechanical shock was defined as “a sudden and violent change in the state of motion of the component parts or particles of a body or medium resulting from the sudden application of a relatively large external force, such as a blow or impact” [1]. The mechanical shock can be described as a transient loading or a violent force impulse on a mechanical system. The shock loading has a short duration, usually much shorter than the period of the fundamental frequency of the system [2], high amplitude and a high frequency on up to 1 MHz [3]. There is no easy way of directly measuring the shock loading so it is normally detected through the acceleration response of the system, see *Figure 2*.

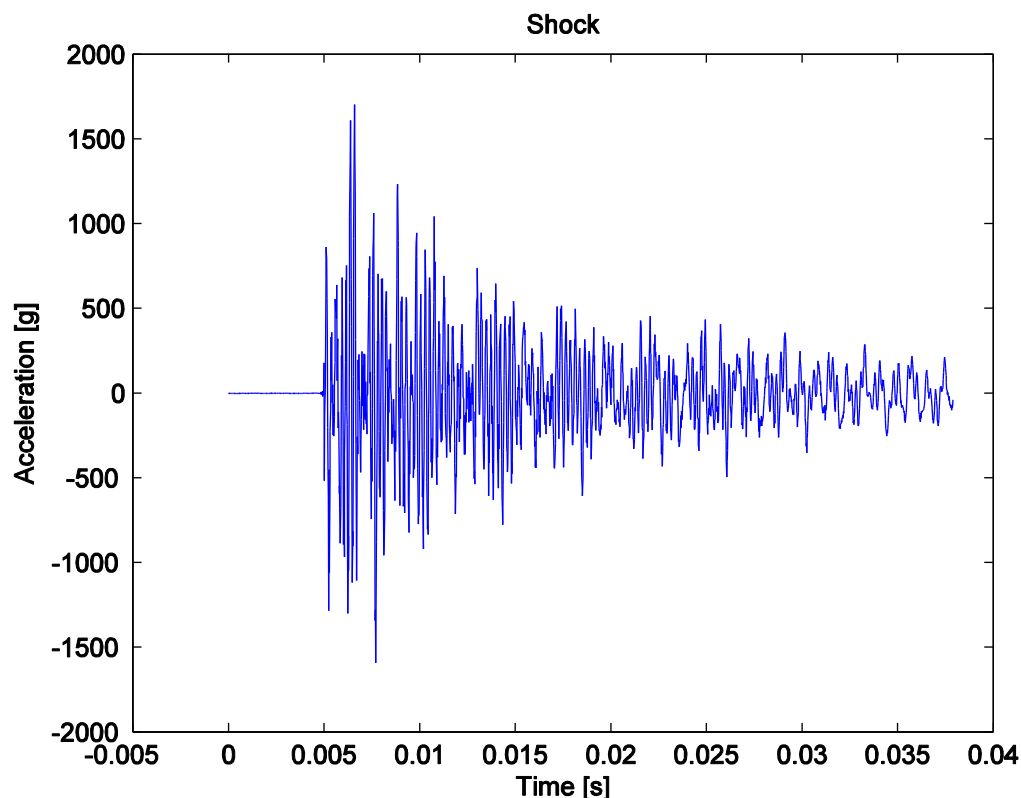


*Figure 2* Typical acceleration time history resulting from shock

The response is highly oscillatory in its nature. The positive and negative sides of the acceleration history are similar in shape and order of magnitude and their peaks trace the shape of a decreasing exponential function. It can be described as a summation of

decaying sinusoids with a rise time in the order of  $\mu\text{s}$  [4]. The acceleration response of the shock is quickly attenuated in both time and space and has usually returned to zero within 20 ms [5]. The acceleration levels can reach as high as 300 000 g but due to the short duration the rigid body velocities and displacements in the system are very small.

The response is generally better described as a stress wave propagating through the material than the ordinary standing wave response of system vibration modes. In a vibration environment the excitation time is long compared to the response time so the vibrations are considered to be forced. For the shock environment the excitation time is short compared to the response time so the system can be considered to respond freely. The shock travels with dispersive flexural waves or non-dispersive shear or tension-compression waves and whenever it hits a boundary or discontinuity, such as a hole, corner or joint reflections, dissipation and diffraction takes place in a highly complex manner [3].

## **1.3 Shock categorisation**

Shock, as described above, envelopes a large range of shock environments. They can be quite diverse when it comes to damage potential and the type of test facility used to achieve them so a categorisation is needed. How to determine the damage potential in a shock will be considered more thoroughly in Section 1.5 while different types of shock test facilities are presented in Section 1.6.

### **1.3.1 Velocity shocks**

A velocity shock is, as the name implies, a violent net change in the velocity of a system. Violent in this context means that the velocity change occurs within a timespan that is short compared to the period of the fundamental frequency of the system. These kinds of shock induce a considerable amount of energy at frequency levels around the principal natural frequency and thus hold the potential to damage structures in the system [5].

### **1.3.2 Displacement shocks**

Displacement shocks are another type of shock with the potential to damage material and structures. They are similar to velocity shocks with the difference that the event causing the velocity shock is directly repeated in the opposite direction so that the net velocity change is zero [5].

### **1.3.3 High frequency shocks**

High frequency shocks are shocks that result in no or very low net velocity change. As the name implies they are characterised by high frequency and high acceleration oscillations. The high frequencies do usually not excite the principal natural frequencies of the system and are quickly dampened in the material so these shocks do not have a considerable damage potential for structures [5]. Electronics and brittle material are, however, in the danger zone. This is the topic of Section 1.4.1

Pyroshock or pyrotechnic shock is a high frequency shock that has a pyrotechnic device as its source. Pyroshock is often interchangeable with high frequency shock in many books and articles but care should be taken since this type of environment is

also achievable with non-pyrotechnic methods such as metal-to-metal impact. It is the high frequency shocks that this text will focus on since the shock environment felt by space equipment are mainly of the pyroshock type. The shock sources in space missions are described in Section 1.4.

The high frequency oscillations are quickly attenuated with respect to distance and number of discontinuities to the source so a sub-categorisation into near-, mid- and far-field shock has become industry standard. The definitions are despite their names not firmly associated with distance but rather with the shock levels felt and the type of facility used to expose test equipment to them [2] [3] [6].

### 1.3.3.1 Near-field

In the near-field environment the shock felt is a result of direct stress wave propagation from the source of the shock. The peak accelerations reach levels above 10000 g and there is a considerable amount of energy in the spectral region over 10000 Hz. It is good aerospace engineering practice to design the spacecraft with no pyroshock sensitive equipment within the near-field environment.

### 1.3.3.2 Mid-field

In the mid-field environment the shock felt is a combination of directly propagating stress waves and resonant response in the structure. The peak acceleration amplitudes lie between 1000 g and 10000 g and the major part of the spectral energy content lies between 3000 Hz and 10000 Hz.

### 1.3.3.3 Far-field

In the far-field environment the shock is dominated by resonant response in the structure. The highest accelerations and frequencies have been attenuated so that the peak levels of the acceleration reach no more than 1000 g. The frequencies with most energy content lies beneath 3000 Hz.

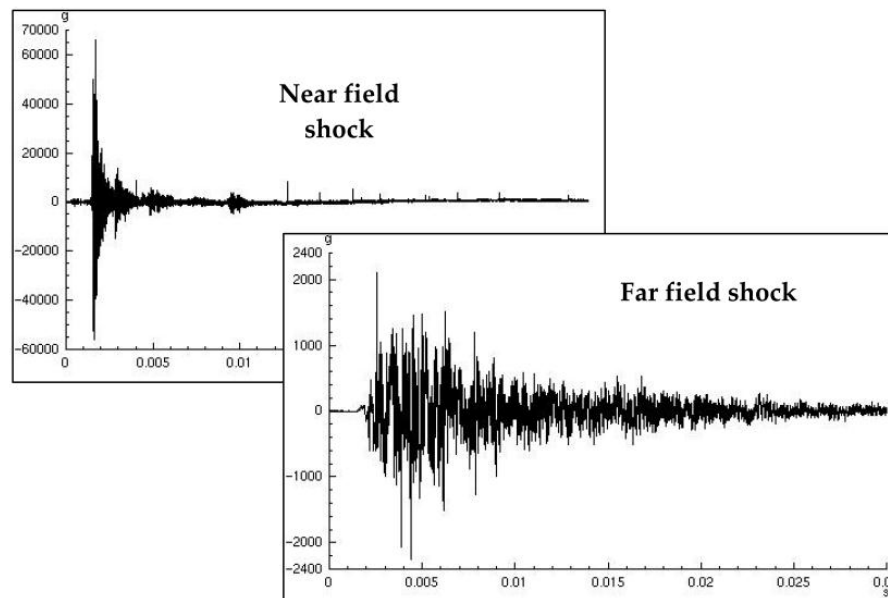


Figure 3 Difference in acceleration time history between near- and far-field shocks [3]

## 1.4 Sources of shock in space missions

The environment in space is quite hostile. There are extreme pressure and temperature differences, not to mention the excessive radiation outside the protective barriers of earth's atmosphere and magnetic field and the risk of getting struck by micrometeoroids. To reach this hostile environment a spacecraft needs to be strapped on top of a launch vehicle which in itself generates a rather unfriendly environment on its way to orbit. The spacecraft will be exposed to high accelerations, heavy vibrations due violent aerodynamic and acoustic loads and a number of different shocks. The shocks are usually due to the firing of pyrotechnic devices in the launch vehicle and the spacecraft. The pyrotechnic devices have the purpose of initiating stage separation, fairing jettisoning, spacecraft release and deployment of numerous of different mechanisms [3].

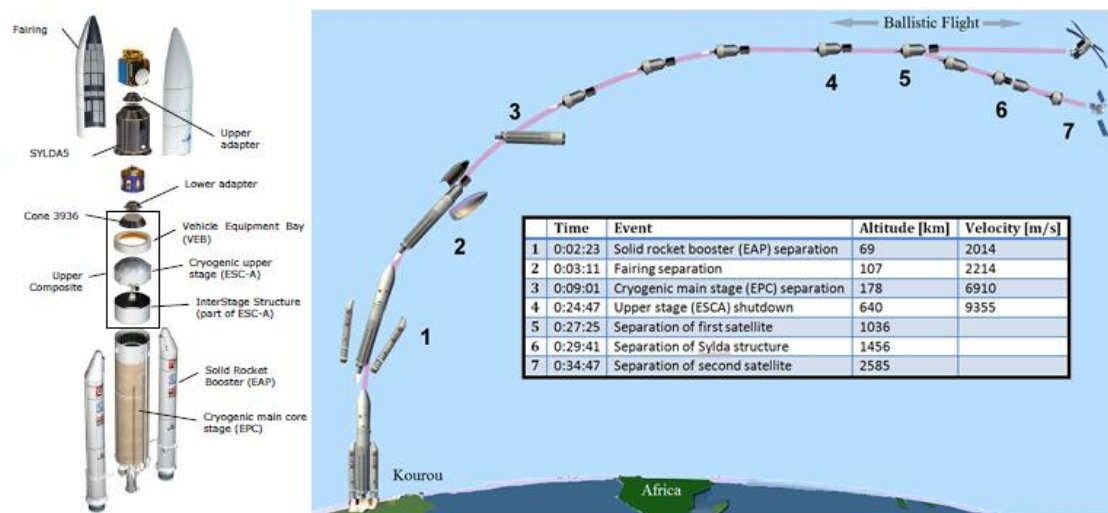
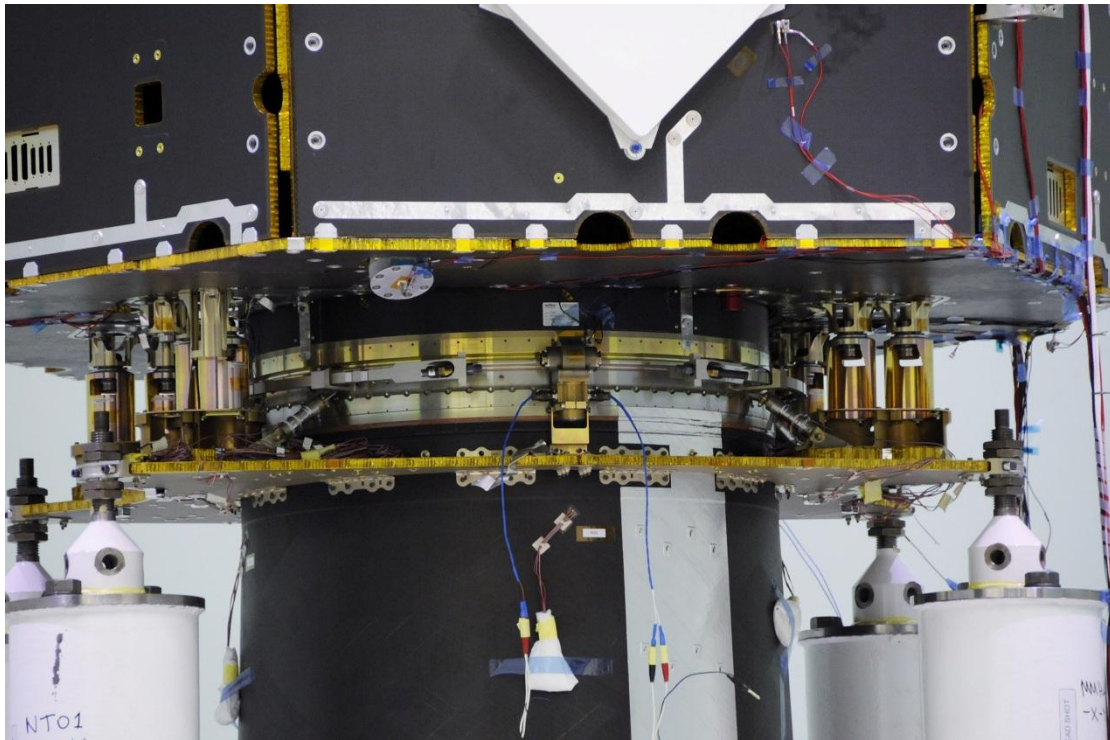


Figure 4 Typical launch sequence for Ariane 5 [7]

For every pyrotechnic device fired a shock will propagate through the launch vehicle into the spacecraft and expose its equipment to a near-, mid- or far-field environment depending on the source in question and the location of the equipment item. The high frequency content is quickly attenuated due to dissipation and diffraction effects while the low frequency content can propagate throughout the launcher and into the spacecraft. The typical launch sequence for the ESA launcher Ariane 5 can be seen in **Figure 4**. The most severe launcher induced shocks for Ariane 5 are the fairing jettisoning and the separation of the vehicle equipment bay contained in the upper stage [3]. Another shock that typically is among the most severe in a mission is the separation of the spacecraft from the launch vehicle. The interface is usually a clamp band as can be seen in **Figure 5**. When in place, the clamp band is preloaded with a tension that acts to push the spacecraft free of the launcher when a pyrotechnic device is used to release the tension. The shock that follows is an effect of both the firing of the pyrotechnic device and the sudden release of the clamp band tension.

The shocks are not over with the spacecraft leaving the launch vehicle. A typical telecom satellite uses up to 50 pyrotechnic devices over its mission life [8]. The pyrotechnic devices mentioned can for example be pyrotechnic bolt- and wire cutters, pin-pullers, explosive bolts, and pyrovalves [3]. For all the devices the general idea is to release some kind of tension or pressure to initiate a separation or a deployment.

Shocks are also generated by mechanical snap-locks and stops at the end of a deployment mechanism such as antenna or radiator deployment or solar array release but they are usually less severe.



*Figure 5 Example of a clamp band for mounting a spacecraft to a launch vehicle (Source: ESA/EADS-Astrium, used with authorisation from ESA)*

As launch vehicles and spacecraft are getting more advanced space missions include more and more pyrotechnic devices, see **Table 1**, and the shocks are getting more severe. The increase in severity is due to the fact that launcher manufacturers in their hunt for more available weight for payload are minimising the damping materials in the launchers. All of this makes shock testing a more and more important part of the qualification process of space equipment.

*Table 1 Pyrotechnic applications in space missions [9]*

<b>Program</b>	<b>Number of installed pyrotechnic devices</b>
<b>Mercury</b>	46
<b>Gemini</b>	139
<b>Saturn</b>	≈ 150
<b>Apollo</b>	249-314
<b>Shuttle</b>	> 400

### 1.4.1 Effect on equipment

Shock is known to have caused major failures resulting in total or partial loss of several space missions [3], [5]. The number of missions lost due to shock is high compared to the number of missions lost due to vibration, which might be explained by the larger understanding of vibration as phenomenon in general.

The stress waves following a pyroshock have wavelengths that correspond with the wavelengths of the natural frequencies of certain microelectronics, which puts them in harm's way. Extra prone to be damaged by shock are quartz, relays and transformers [3]. Contaminants such as solder balls are also known to dislodge and cause short circuits [2]. Materials prone to shock damage are ceramics, crystals, brittle epoxies and glass diodes which experience cracks, brittle fractures and even accelerated fatigue for repeated shocks [10]. Small bearings, gears and valves are also sensitive to the damage potential in shock.

## 1.5 Shock Response Spectrum

A shock environment is usually measured as acceleration over time but the time histories in themselves are not very useful when it comes to quantifying and managing shocks. To be able to compare the damage potential in shocks and to describe shock test specifications the SRS - Shock Response Spectrum has become the conventional tool in the aerospace and defence industry [11]. The shock is characterised by applying its acceleration time history to a standardised array of single-degree-of-freedom (SDOF) systems and calculating the output, see *Figure 6* [3].

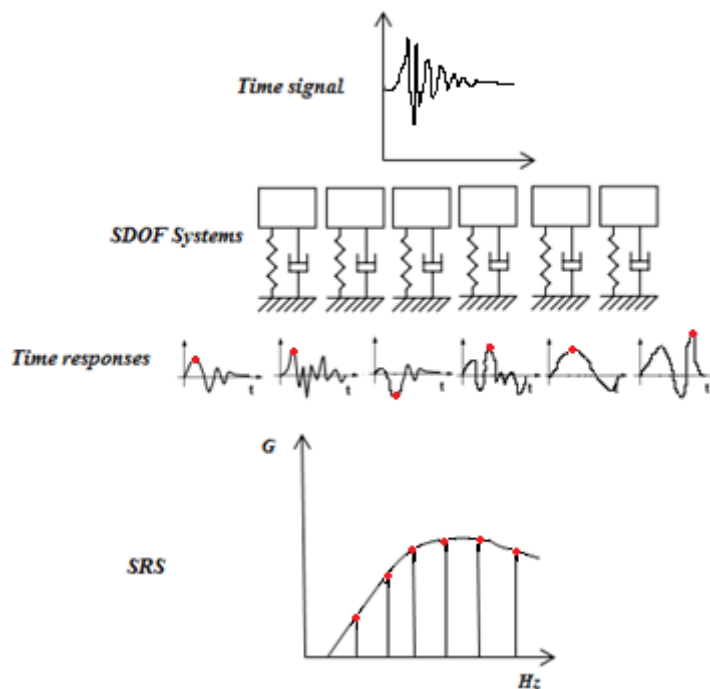


*Figure 6 Principle of shock response spectrum calculation. From acceleration time history, through maximum acceleration response of single degree of freedom systems, to shock response spectrum*

The peak accelerations for the SDOF systems are gathered in a SRS which is a log-log plot of these values over a range of natural frequencies, see *Figure 7*.

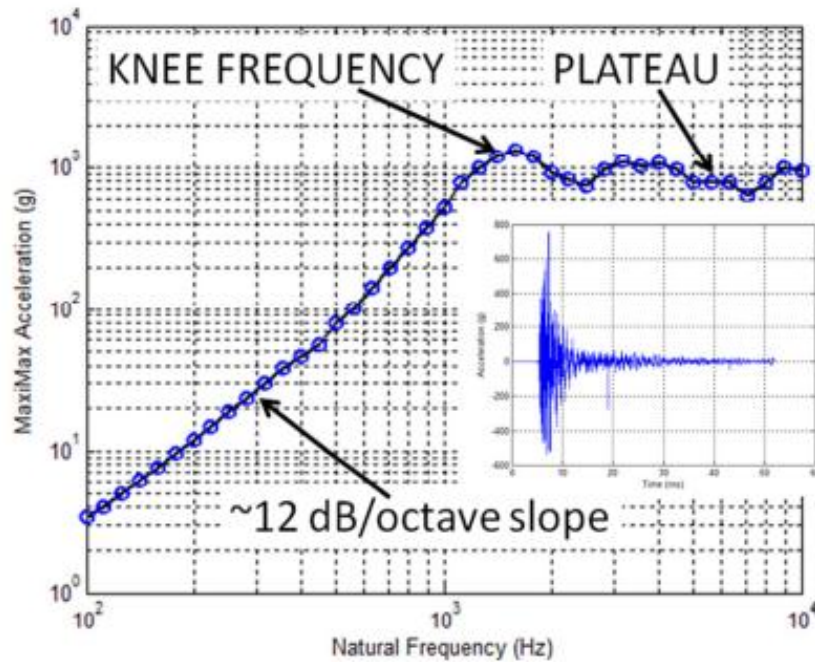


*Figure 7* Typical shock response spectrum [6]

Every SDOF system in the array represents an independent natural frequency in the SRS plot. An example is shown in *Figure 8*. The shock that is characterised is applied to the base of a SDOF system. The response acceleration of the mass is calculated to find the maximum and this value goes into the SRS, see Appendix E – Calculation of the peak acceleration of a SDOF system. For the natural frequency to be an independent variable the damping is set to a constant value of 5 %, which corresponds to a quality factor  $Q = 10$ . It can be looked upon as an average for a majority of aerospace structures [3].

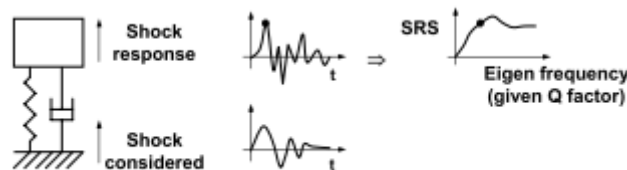


*Figure 8* From SDOF system to SRS data point [12]

This procedure gives an estimation of the damage potential in the shock for all structures, even if their resonant frequencies are unknown, since the array of SDOF systems spans over all the natural frequencies in the range of interest [13]. The range of interest is usually taken to be 100 – 10000 Hz and sometimes even higher for near-field environments. The number of unique natural frequencies used in the range is arbitrary but it is good practice to use at least a 1/24 octave resolution which means that every SDOF system in line has a natural frequency that is its forerunner's natural frequency multiplied with  $2^{1/24}$ . The rule to use the peak acceleration value without regard of its sign gives a spectrum plot called the maximax SRS. There are others but this has become the standard for shock characterisation.

The SRS seen in *Figure 7* is typical for far- and mid-field shocks in that it shows a globally increasing curve with a slope of  $\approx 12$  dB/octave up to a characteristic maximum called the knee frequency. Over this knee frequency the SRS flattens out to a plateau. All SRSs from high frequency shocks have this characteristic knee frequency although it sometimes can be difficult to define the location of it and it sometimes appears at a frequency that is over the range of interest or even over the range of the measurement equipment used [6].

SRS is the standard tool used in aerospace industry but it should be remembered that it only gives an estimate of the damage potential in a shock. The usage of SRS has its disadvantages. The reduction of a typical transient shock acceleration time history to a SRS is not bijective, which means that there is not a unique SRS for every acceleration time history and that the procedure is irreversible. Information on time parameters such as effective duration and phase is lost in the process. The knowledge of the high frequency eigenmodes of a real system is not extensive so two shocks can have similar SRSs and still have very different damage potentials. A shock can be mild in comparison with another that has a similar SRS but some frequency component close to an eigenfrequency that amplifies an eigenmode with severe consequences [3].

## 1.6 Existing shock test facilities

Shock test facilities (STFs) can be very different depending on what type of shock environment they should achieve and what type of specimen they should be able to test. Some STFs are designed to achieve a wide shock environment range for a large variety of test specimen while others are made specifically for a shock given by a certain pyrotechnic device and a certain structure. The shock test will of course be more accurate if the actual pyrotechnic device is used on structure that is similar to the flight structure, but these tests are often impossible to run due to availability, cost and insufficient information. The focus in this report is the more general STFs that can be used for many different specimens.

It should be noted that the classic free fall drop tables never should be used for high frequency shock testing. The fall and sudden stop produces a high net velocity change which gives a shock environment with a lot of energy at low frequencies. This is not representative for the high frequency shocks generally felt in space missions and usage of this kind of facility gives a high risk of over-testing the equipment [14].

### 1.6.1 Far-field shock test facilities

Another type of conventional machine are the electrodynamic shakers commonly used for vibration testing, see *Figure 9*. These facilities can reach the requirements for low far-field shock environments but they are unable to excite the required response for frequencies over 3000 Hz [6]. They are still used for far-field shock testing due to their advantages in high general availability and low operational cost.

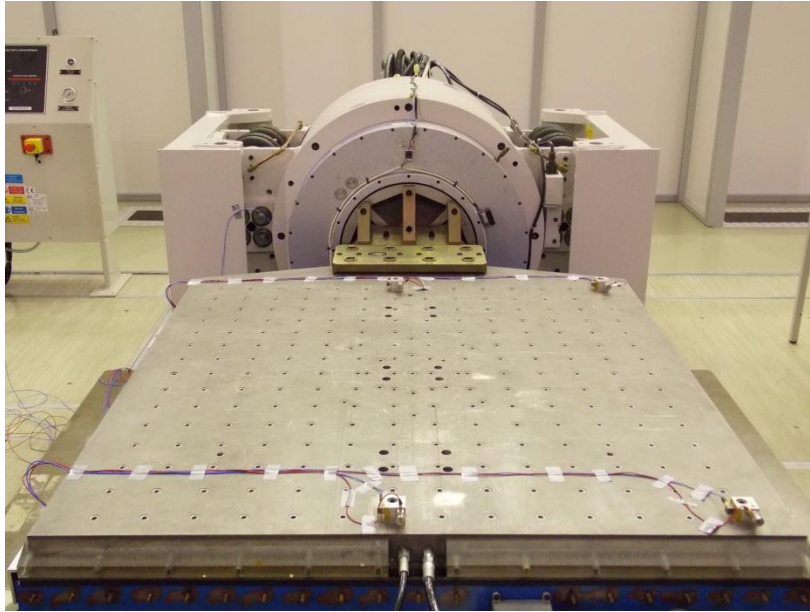


Figure 9 Electrodynamic shaker (Source: ESA, used with permission of ESA)

### 1.6.2 Mid-field shock test facilities

The mid-field environment is too violent to reach with an electrodynamic shaker but not so violent that explosives are required. Explosives can still be used but there is another method that is far simpler. A mechanical metal-to-metal impact gives a spatial uncorrelated shock excitation that is similar to a pyrotechnic shock [3]. Impact STF has been shown to produce a controllable shock environment over the whole mid-field range for specimen up to 40 kg [12], [15]. An impact STF consists of a structure that is excited into resonance by a strike from an impactor.



Figure 10 Example of metal-to-metal impact STFs a) mono-plate b) bi-plate c) tunable plate [16]

As can be seen in **Figure 10**, there are a lot of different combinations of impactor and impacted resonant structure that are used. An overview of the different types used at some aerospace companies is given in **Table 2**.

Table 2 Impact STF's in Aerospace industry [8]

Resonant structure	Impactor	Location
Resonant plate	Hammer	SSC (Sweden) ESTEC (Netherlands) Alcatel Space (France) MBDA (France) Intespace (France) RUAG Space AB (Sweden)
Resonant bi-plate	Hammer	MECANO ID (France)
Tunable plate	Air gun	Hunting Engineering (United Kingdom)
Hopkinson bar	Hammer	MECANO ID (France)
Tunable resonant beam	Air gun Hammer	SANDIA (USA) EADS-ST (France)

The Hopkinson bar is a bar which is impacted at one end and has the test specimen attached to the other end. The compression waves in the bar are used to achieve a certain shock environment depending on material, length and cross section, see *Figure 11*.

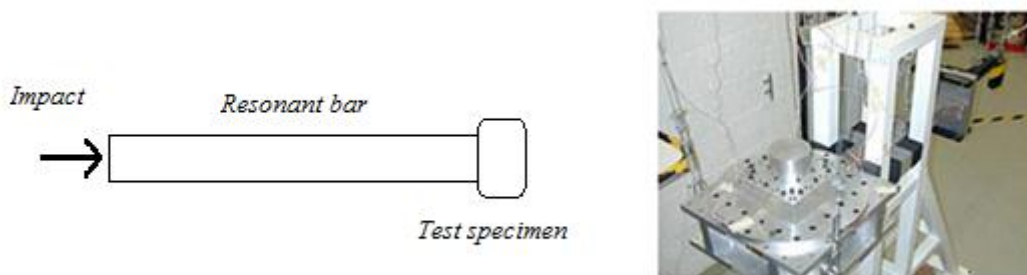


Figure 11 Resonant bar, also called Hopkinson bar [16]

A resonant beam is similar to a resonant bar with the difference that it is excited in the transverse direction and uses the flexion modes of the beam, see *Figure 12*.

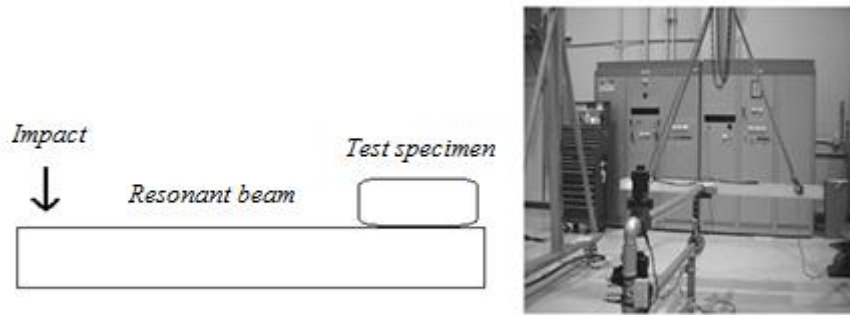


Figure 12 Resonant beam excited by a pneumatic air gun [17]

The plate is the most common resonant structure in industry [3]. The resonant plates are also called ringing plates and are usually made in aluminium or steel depending on the sought shock environment. The plate can have many different shapes but the quadratic mono-plate is most common. A bi-plate configuration is also commonly used which consist of two plates that are separated with spacers. The geometrical and material parameters of the plate together with the boundary conditions set the knee frequency of the SRS. A tunable plate is a plate which can be clamped at different locations, effectively changing its length and boundary conditions to be able to adjust the knee frequency. A tunable plate STF can be seen as picture c) in *Figure 10*.

The impactors also represent a wide array of different techniques. *Table 2* only mentions hammer and air gun but there are several different types of both and also other methods. *Figure 13* shows a STF with a plate as a resonant structure and commercial nail guns together with a normal handheld hammer as impactors.

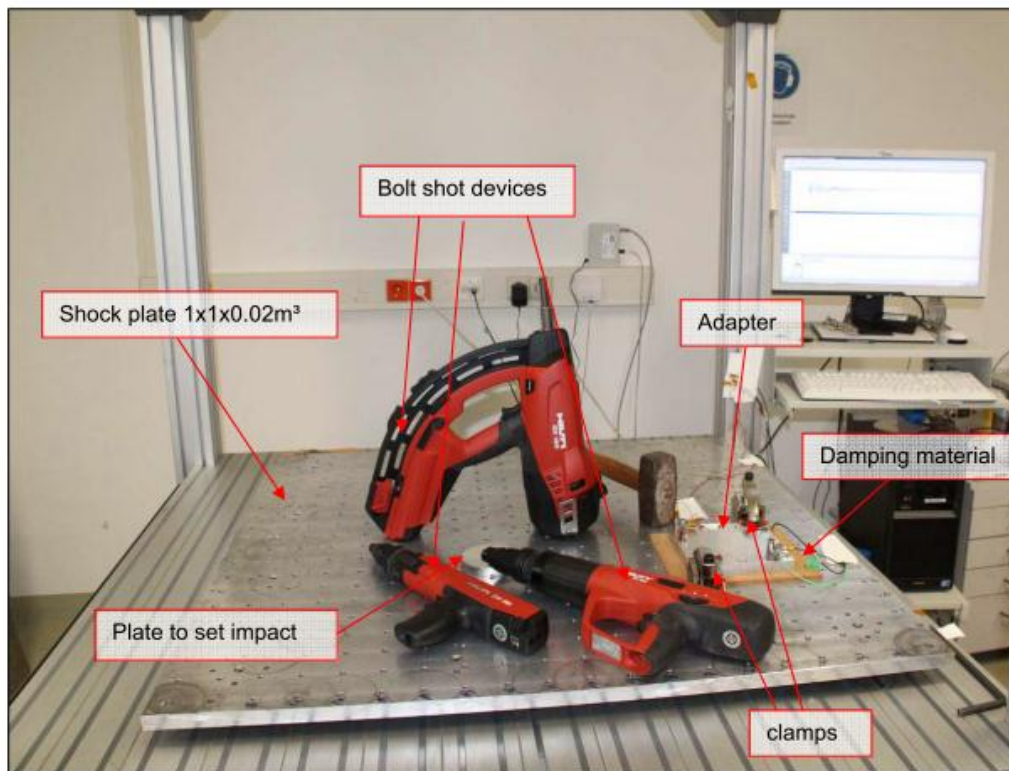


Figure 13 German Aerospace Center STF [18]

### 1.6.3 Near-field shock test facilities

The near-field shock environment is almost impossible to reach without the usage of pyrotechnic devices. Usually the test specimen is attached to a resonant plate and a certain amount of explosives attached to the opposite side or to the edge of the plate. The explosive charge is detonated which excites a near-field shock in the plate. As for the plates for mid-field STF's both mono- and bi-plate technologies are used. Some examples of commercial near-field STF's can be seen in *Figure 14*. It should be noted that most near-field STF's also can be used to produce mid- and far-field environments.



*Figure 14* Examples of pyrotechnic STF's [16]

## 1.7 Shock verification process

Dynamic tests can in general be categorised in six classes [14]:

- Development tests
- Qualification tests
- Acceptance tests
- Screening tests
- Statistical reliability tests
- Reliability growth tests

The development tests are, as the name implies, tests that are carried out in the development process to support the developer in design related questions. It is usually very specific to the issue in question and it is not typical for shock issues. Screening, statistical reliability and reliability growth tests are applicable to mass produced hardware which is usually not the case for space equipment. Space hardware is occasionally even on the other extreme of the scale where only one unique piece of equipment is available and then the qualification and acceptance tests are usually combined into a class named protoflight tests. The protoflight test criteria are usually on a somewhat lower level and/or have a shorter duration than the qualification tests to reduce the risk of wear out damage [14].

### 1.7.1 Qualification test

A qualification test is a formal test that has the purpose to demonstrate that a hardware design and manufacturing method has resulted in a piece of equipment that fulfils the requirements and can perform agreeably when and after it has been exposed to its intended environment with an appropriate margin. A qualification test is said to have failed when the tested hardware malfunctions due to a deficiency in the design. If it is apparent that a malfunction is due to a workmanship or material error, the defect should be repaired and the test should be continued [14]. The qualification tests are

usually not performed on flight hardware but instead on a prototype called QM – Qualification Model. The QM is manufactured from the same drawing, with the same materials, using the same processes and by people with the same competences [3].

### 1.7.2 Acceptance test

The acceptance test is a formal test that is carried out on flight hardware to demonstrate that it is free of workmanship errors and material defects. The purpose is to show that the flight hardware is representative of the previously qualified design. As for the protoflight tests the acceptance test levels are usually set lower or with a shorter duration not to wear out the flight hardware. An acceptance test is said to have failed if the tested equipment malfunctions due to workmanship errors or material defects. The design should already be approved from the qualification test campaign.

### 1.7.3 Test levels

The test criteria for shock testing are usually given as a qualification SRS. The levels in this SRS should be derived from the MEE – Maximum Expected Environment, sometimes also called MEFE – Maximum Expected Flight Environment. The MEE is defined as a level that the shock is guaranteed not to overpass with a certain degree of confidence. The MEE is typically not known since it varies a great deal between different locations and shock sources. The general ways of estimating this environment are [6]:

- Analytical models
- Direct measurements
- Extrapolation methods from previous measurements

For the analytical models researches are developing finite element (FE) –simulations that are constantly improved in the ability to predict the shock levels at certain locations but heuristic methods are still mainly used. Shock tests are extra difficult to replace with FE simulations since even if a very good estimation of the shock levels is found it is difficult to know how this environment propagates inside the equipment and in the next step if this shock is damaging the sensitive components.

Direct measurements are seldom taken exactly at the spot where the equipment in question is located and the measurements can differ from time to time due to other variables which are not all known. The mounting of the equipment in itself can have an attenuating or even amplifying effect on the response at different frequencies. In practice different statistical methods are used for determining the MEE from measurements [3].

When the shock level for the interesting location has been attained through measurements or appropriate analytical or numerical methods or, by all means, through all of them, SRSs are calculated. Constant slope lines are then designated in a way that they envelope all the measured/predicted SRSs and simplify them into a SRS that can be reproduced on a STF, see *Figure 15*. This procedure gives a margin for the uncertainties in the method used to estimate the MEE.

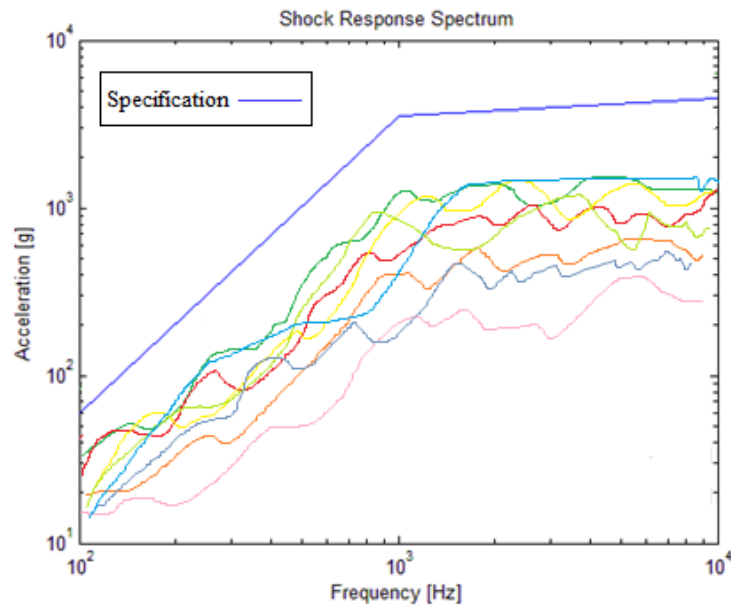


Figure 15 Example of MEE specification from measurements

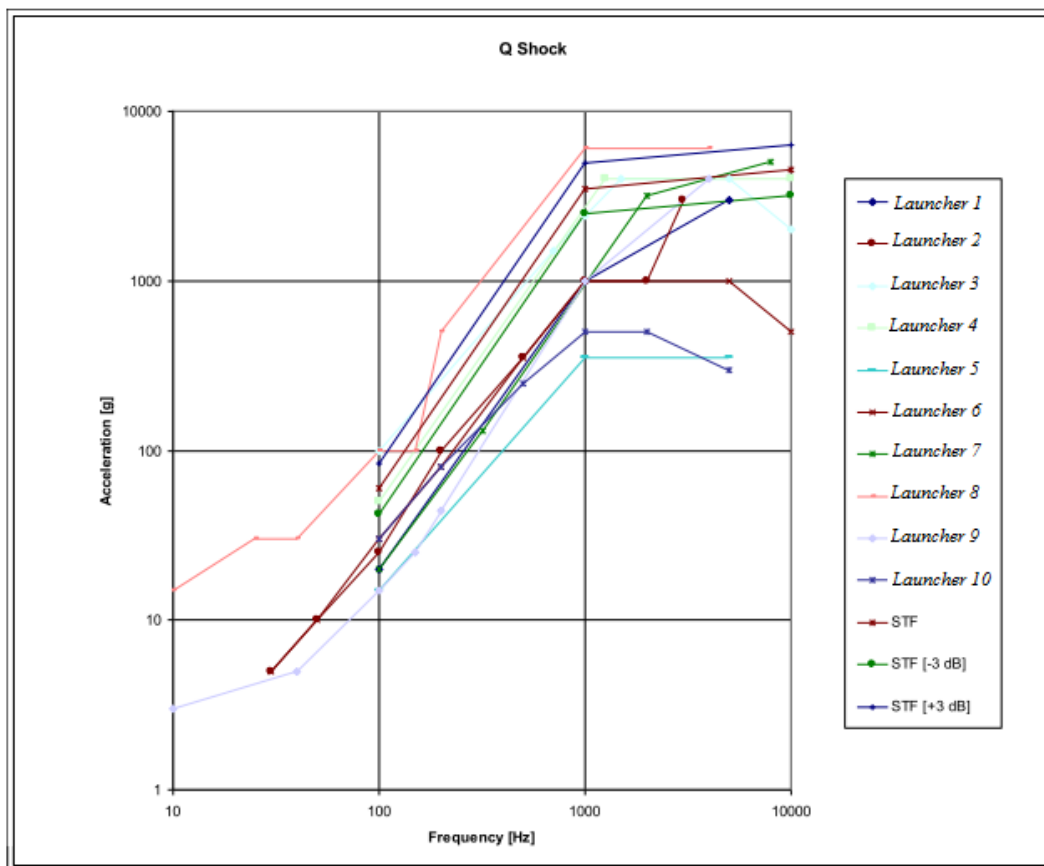
On top of the designated level a qualification margin of at least 3 dB is added to the MEE to account for the inherent randomness and variability of the shock phenomenon and for the variability in hardware strength [3]. In **Table 3** the qualification shock level SRSs are given for a number of ESA satellites.

Table 3 Shock requirements for ESA satellites [8]

ESA satellites	Equipment	Pyroshock requirements (SRS)	
	Mass/Footprint		
ATV(Valve)	0.2 kg/40x60 mm	200 Hz	250 g
		1000 Hz	4000 g
		1.2 kHz – 10 kHz	5000 g
SMART 1	3 kg/400x200 mm	100 Hz	20 g
		300 Hz	500 g
		600 Hz – 10 kHz	1500 g
GOCE	<50 g/20x20 mm	100 Hz	150 g
		300 Hz	200 g
		1.5 kHz – 10 kHz	3000 g
GALILEO	3 kg/400x200 mm	100 Hz	20 g
		1 kHz – 10 kHz	3000 g
TEAMSAT (Camera)	n/a	300 Hz	600 g
		600 Hz	4000 g
		1000 Hz	4750 g
		1500 Hz	5446 g
		2 kHz – 10 kHz	6000 g
ARTEMIS	n/a	650 Hz	2000 g
		2 kHz – 10 kHz	2500 g
HERSCHEL PLANCK	19 kg/800x700 mm	100 Hz	30 g
		1.5 kHz – 10 kHz	1500 g

The footprint of the QuadPack is about 300x400 mm, its test weight is 17 kg and the qualification SRS for the QuadPack can be described as [100Hz, 1000Hz, 10000Hz], [60g, 3500g, 4500g], see **Figure 16 - Figure 18**.

The qualification SRS for the ISIS QuadPack has been produced as an envelope containing the MEE for several launch vehicles that has the potential for future launches of the system. It is not uncommon for this type of development project of space equipment that not only the location in the launcher but also the launch vehicle in itself is unknown beforehand. In **Figure 16** the qualification SRS levels from several Russian launch vehicles, such as Dnepr, Proton and Soyuz, are shown together with the requirement SRS for the STF. The requirement levels can vary between launchers themselves and also between different mounting locations in the same launcher which is the case for the converted submarine-launched ballistic missile Shtil. An exposed payload mounting location close to the third stage rocket nozzle is subject to a very high shock environment while a more friendly position in the upgraded model Shtil 2.1 has lower levels. In **Figure 17** the qualification SRS levels for eight different non-Russian launch vehicles, such as the European Vega, the American Falcon 9 and the Indian PSLV, are shown in a similar way. For clarity the qualification SRS for the QuadPack is given alone in **Figure 18**.



**Figure 16** Qualification SRSs for Russian launch vehicles compared to the STF SRS requirement

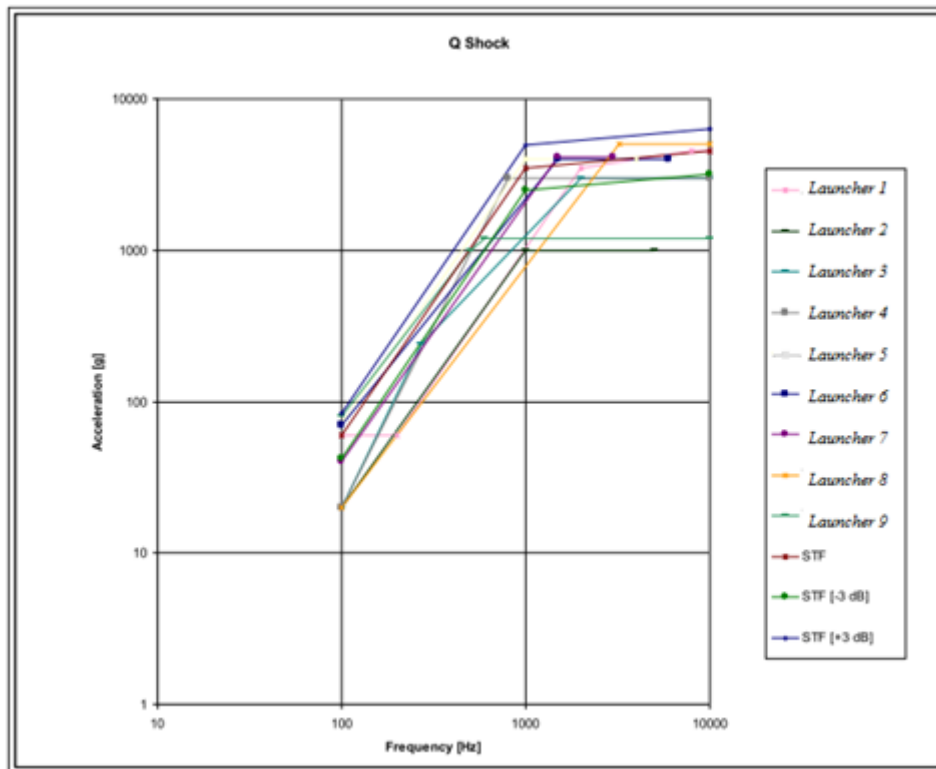


Figure 17 Qualification SRSs for non-Russian launch vehicles compared to STF SRS requirement

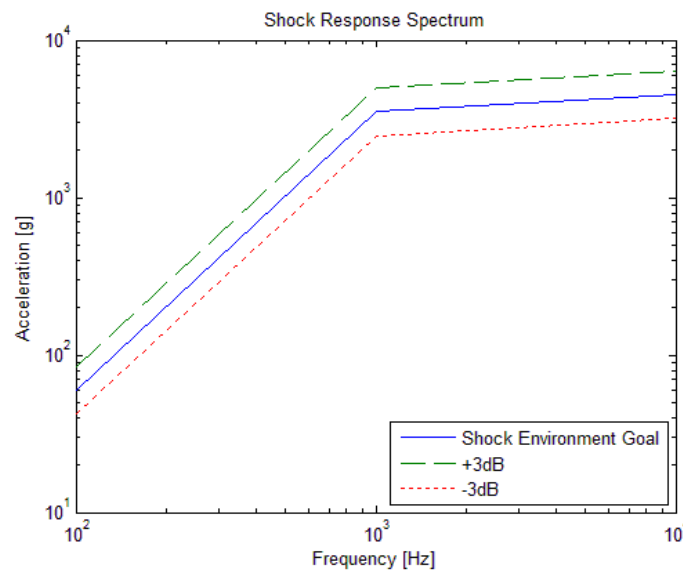


Figure 18 Qualification SRS described by [100Hz, 1000Hz, 10000Hz], [60g, 3500g, 4500g]

This is the level that the QuadPack needs to be exposed to by the new STF to verify that it can survive the shock environments related to space travel. The new STF can hence be realised as a mid-field STF. Tolerances of  $\pm 3$  dB have been added to the plot, however, the tolerances are not univocal in the standards and handbooks, see **Table 4** and **Figure 19**.

Table 4 Shock test tolerances of the SRS [3], [6] and [19]

Organisation	Tolerances	Additional criterion
MIL	[ -3, +6 ] dB for 100 – 10000 Hz	90 % of all data points shall lie within this range
	[ -6, +9 ] dB for 100 – 10000 Hz	10 % of the data points may lie within this range
		50 % of the data points shall lie over the reference level
NASA	[ -6, +6 ] dB under 3000 Hz	50 % of the data points shall lie over the reference level
	[ -6, +9 ] dB over 3000 Hz	
ESA	[ -0, +6 ] dB under 1000 Hz (knee frequency)	The results shall be taken at two places and the difference shall be less than 6 dB
	[ -3, +6 ] dB over 1000 Hz (knee frequency)	

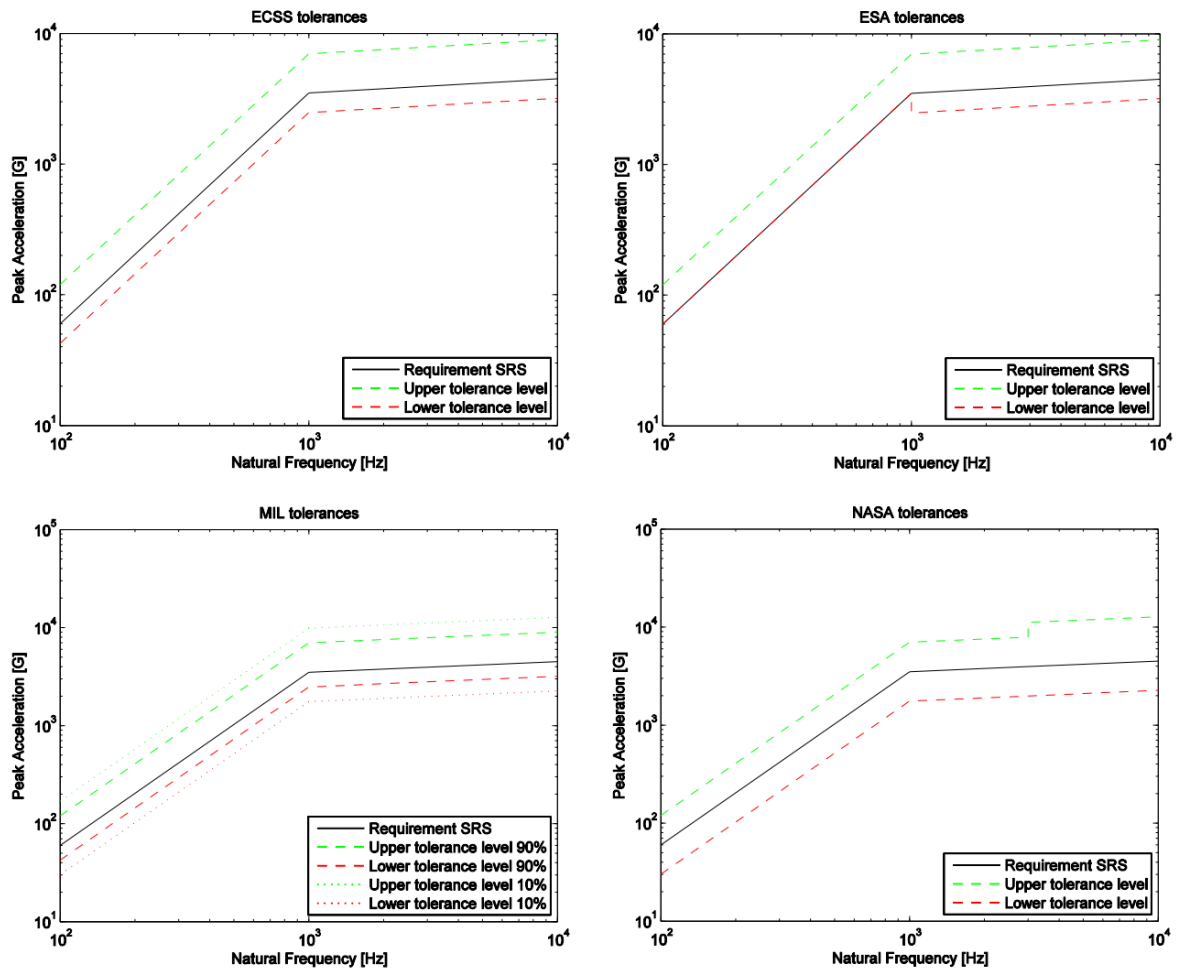


Figure 19 Shock test tolerances from different sources a) ECSS b) ESA c) MIL d) NASA

## 2 System Engineering

The journey from mission statement to goal is far from straightforward. Akin's third law of spacecraft design captures this well: *“Design is an iterative process. The necessary number of iterations is one more than the number you have currently done. This is true at any point in time”*. The work needs to be structured into steps and goals need to be defined so that the steps can be taken in the right direction.

ECSS concisely defines system engineering as the interdisciplinary approach governing the total technical effort required to transform a requirement into a system solution [20]. ECSS gives one way of visualising system engineering through dividing it into the five functions:

- Requirement engineering
- Analysis
- Design and configuration
- Verification
- System engineering integration and control

Where the system engineering function has boundaries to Management, Production, Operations, Logistics and Product assurance, see **Figure 20**.

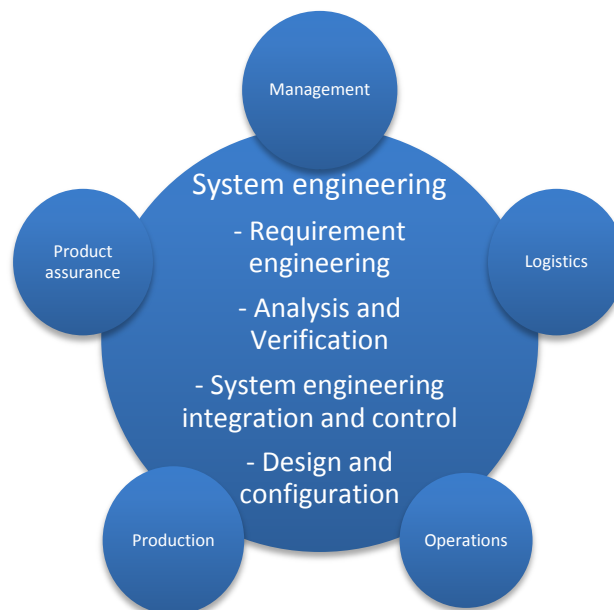


*Figure 20 System Engineering functions and boundaries*

Another similar view of system engineering is NASA's where it is defined as a logical way of thinking. The system engineer is the engineer that maintains a holistic view of the project and balances it between the different engineering disciplines in a chain of phases that defines the total lifecycle of the project [21]. In the same way as a system can achieve things that the separate components of the system cannot accomplish

alone, system engineering is a discipline that allows better achievements than what the separate engineering disciplines can reach by themselves.

The phases of a development project are [21]:

- Pre-Phase A: Concept Studies
- Phase A: Concept and Technology Development
  - Define the project
  - Identify and initiate necessary technology
- Phase B: Preliminary Design and Technology Completion
  - Establish preliminary design and develop necessary technology
- Phase C: Final Design and Fabrication
  - Complete system design
  - Build components
  - Code components
- Phase D: System Assembly, Integration and Test, Launch
  - Integrate components
  - Verify the system
  - Prepare for operations
  - Launch
- Phase E: Operations and Sustainment
  - Operate and maintain the system
- Phase F: Closeout
  - Disposal of systems
  - Analysis of data

These phases are not independent since, as mentioned earlier, this is an iterative process. This means that even though this project will not include the operation and closeout of the system the processes in Phase E and F still need to be considered to get a good result.

## 2.1 Goals with project

To be able to get a good start of the project, clear goals are required. The goals for this project were derived from the mission statement and the good practises of system engineering as:

- Research the field and define requirements for a new STF
- Develop STF concepts based on the found requirements and the QuadPack
- Get data from simulations based on the requirements and concepts
- Hold elimination process and trade-off studies based on requirements, simulation results and input from experts to select final concept
- Design the concept details to a level where the STF can be manufactured
- Test the STF to verify that it gives predicted results

## 2.2 Requirements specification

As mentioned earlier, requirement engineering is one of the functions of system engineering. Design should always be driven by requirements. The requirements are the foundation of the project and the requirements specification functions as an agreement between the different stakeholders and the project team on how they want the final system to work. The requirement engineering process spans over four main activities, namely, requirement capture, requirement allocation, requirement analysis and validation and, last but not least, requirement maintenance [20].

### 2.2.1 Requirement capture

An extensive requirements specification was made for this project. The first step in defining these requirements was to analyse the mission statement and the goals to make it clear what was expected of the system, see *Figure 21* and [21].

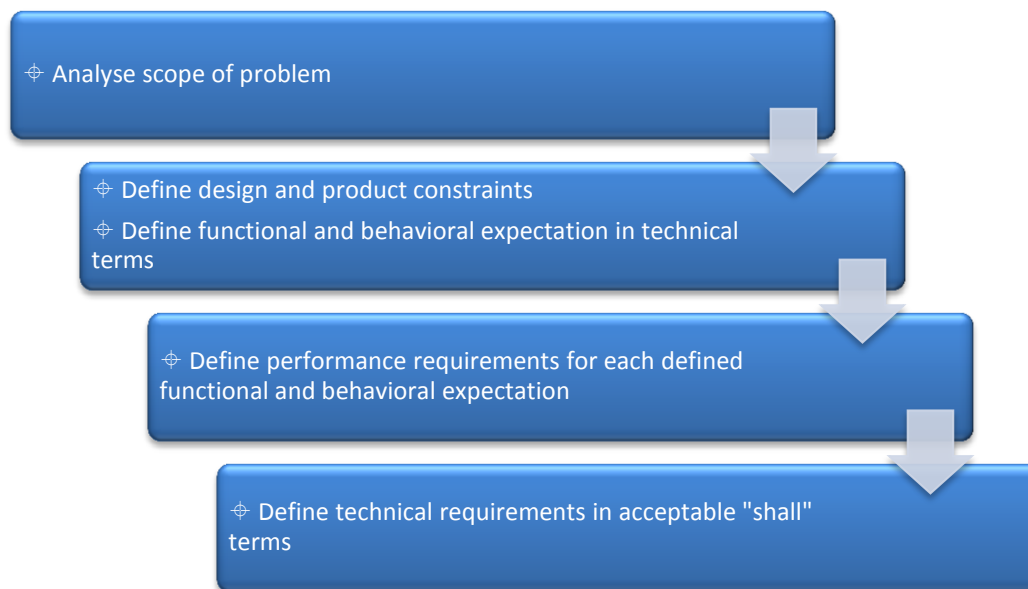


*Figure 21 Requirement capture*

The top level functional requirements are usually not difficult to define but most requirements are not apparent at the first glance. Requirements were also captured from shock-, testing- and space environment handbooks and standards [2], [3], [4], [5], [6], [13], [14] and [22], interviews with shock experts [23], [24], [25] and [26] and good requirement engineering practices [20] and [21].

### 2.2.2 Requirement allocation

The requirements specification must be as enveloping as possible. If the system complies with all the requirements it should deliver everything that all the stakeholders request. A STF that fulfils all requirements is a good facility. To not oversee any class of requirements they are allocated to different classes, see the space system requirement types in *Table 5* and [20]. Care must also be taken so that the requirements are unique and do not contradict each other. If a requirement is complex and spans over a large system it should be broken up and allocated to appropriate levels and classes. A good requirement should only handle one parameter.

Table 5 *Space system requirement classes*

Requirement class	Explanation	Typical requirements
<b>Functional</b>	What the system shall perform to satisfy the objective	Need or Mission statement
<b>Mission</b>	What the system shall do to perform the functional requirement	System modes System states System functions System functional relations Hardware functions Hardware performance Software performance
<b>Interfaces</b>	Which interfaces the system shall have towards external world and between internal modules	Launcher GPS Crew Between modules GSE
<b>Environmental</b>	The conditions under which the system shall perform the work	Contamination Fungus Humidity Meteoroids Plasma Precipitation Pressure Radiation Shock Space debris Vibration
<b>Physical</b>	The boundary conditions for which the system shall ensure physical compatibility	Mass Materials MOI Shape Size Volume
<b>Operational</b>	How the operability of the system shall be	Autonomy Control Failure management
<b>Human factor</b>	Which human capabilities the system shall comply with	Ergonomics Perception
<b>Logistic support</b>	The logistic constraints the system shall comply with	Maintenance Personal Packaging Supply Transportation
<b>Product assurance</b>	The product assurance constraints the system shall comply with	Availability Correctness Efficiency Integrity Flexibility Life Maintainability Manufacturing processes Radiation System safety Effectiveness Testability Transportability Usability
<b>Configuration</b>	The configuration constraints the system shall comply with	Compositional Major components
<b>Design</b>	The design constraints the system shall comply with	Imposed design Margins Interchangeability
<b>Verification</b>	The verification constraints the system shall comply with	Inspection Simulation Review of design Analysis Test

### 2.2.3 Requirement analysis and validation

All requirements shall have a reason for existing and a way of verifying their fulfilment. A rationale should be given if the requirement is not self-explanatory. The general verification methods are test, simulation, analysis, review of design and inspection [27].

A requirement review meeting was held at ISIS to validate the requirements specification which led to the discovery of some masked requirements and definition of some additional constraints. One important example was that no explosives were to be used which left metal-to-metal impact as excitation method to reach mid-field shock levels.

### 2.2.4 Requirement maintenance

One of the most important points to make when it comes to the requirements specification is that it is a living document. It needs to undergo several turns of evolution under the whole lifecycle of the project, from kick off to final shut down. Each requirement shall be the subject of communication and iteration with the stakeholders to ensure a mutual understanding [21].

## 2.3 Concept generation

The idea of concept generation is to find every thinkable solution so that no range of solutions is overlooked and the best possible concept can be found. During the process of generating concepts and finding the best one, the system will be more and more defined and more will be known about it. At the same time new data and new limitations can emerge. With this information the requirements can be updated which changes the baseline of the concept generation and a new iteration in the design loop is introduced. One visualisation of the nested design loop is given in *Figure 22*.

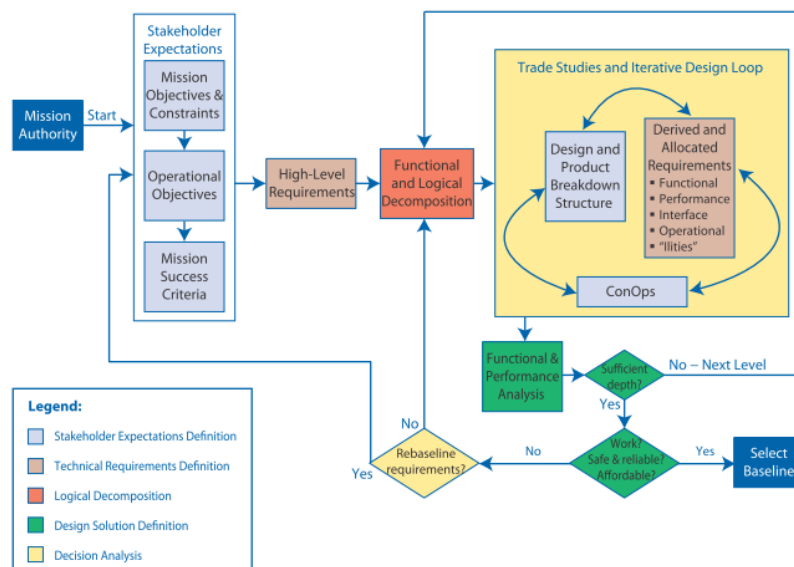


*Figure 22 Development chain from mission start to design concept (This figure is taken from NASA/SP-2007-6105 Rev1, NASA Systems Engineering Handbook, and used with permission of NASA) [21]*

Another way of visualising the concept generation process is as a list of possible solutions that grows larger as more solutions are found and diminishes as solutions are eliminated. The number of solutions are getting larger for example when brainstorming sessions are held, when solutions are broken up into sub-solutions and fused in new ways or when a constraint is found to be redundant. An example is given in *Figure 23* where **A** is the baseline requirements specification. A brainstorming session is held to find concept solutions and the list is big at **B**. Some solutions are found unfeasible and the list becomes smaller at **C**. The solutions are broken down into sub-solutions and united in new ways together with sub-solutions already found from existing solutions in the market. This makes the list larger again at **D**. Before **E** simulations are made which shows that some of the solutions could not comply with all the requirements and were therefore eliminated. The simulations also showed that another requirement could lower its value which allows for some more solutions at **F**. Trade-off studies are held and a final concept is found in **G** but at the final concept review meeting new input is attained which makes two alternations of the concept more attractive at **H**. Finally one of the alternations is found to not be compatible for some reason and a final concept is selected at **I**.

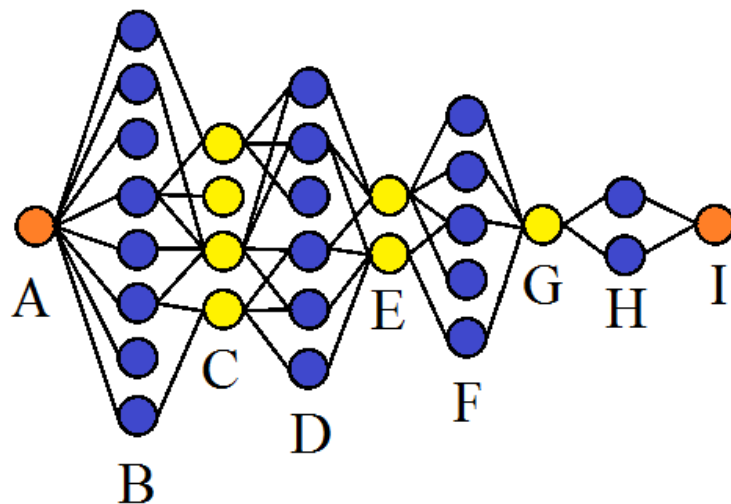


*Figure 23* Concept generation process as growing/diminishing list of concepts

The development process of the STF has been comparable to the example given above but the requirements specification was not the only foundation for the brainstorming sessions.

### 2.3.1 Functional analysis

The functional analysis of a system is partly made to help with the identification and definition of functional requirements and to allocate these to appropriate sub-function requirement levels [20]. The main reasons are, however, [21]:

- To translate the top level requirements into functions of the system
- To divide these top level functions into sub-functions in an iterative process
- To identify the interface between the sub-functions

The easiest way to shock the QuadPack would be to give it some altitude and drop it to the floor. The surface, angle of impact and height could be altered to tune the required shock. This would, however, not give the shock environment sought after since it is not the QuadPack itself that gets an impact in the setting that is being

simulated. In the launch vehicle it is the fastening elements of the QuadPack that receives the prescribed shock and it is through them that the shock propagates. The main function of the STF is therefore to put a required shock into the fastening elements of the QuadPack. To do this there are three major sub-functions that need to be realised. The QuadPack needs to be fastened using its normal fastening elements to something that will be called “holder”, this holder needs to be connected to the ambient environment and finally this holder must be forced to propagate a shock into the QuadPack. The sub-functions are shown in *Figure 24*.

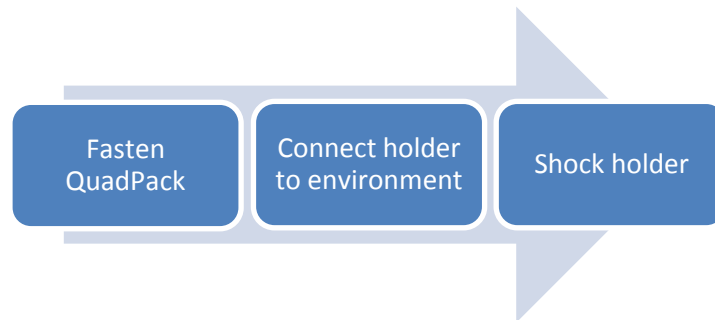


*Figure 24* STF sub-functions

Again it would still be simpler to cut out the middle function and just drop the QuadPack and the holder into the floor but then the person doing this can be defined as a solution to the sub-function *Connect holder to environment* and the division is still valid. *Shock holder* is still a substantial function that should be divided further. The “shocker” needs to store energy and then transform this energy to a shock in the holder. A function tree can be seen in *Figure 25*.

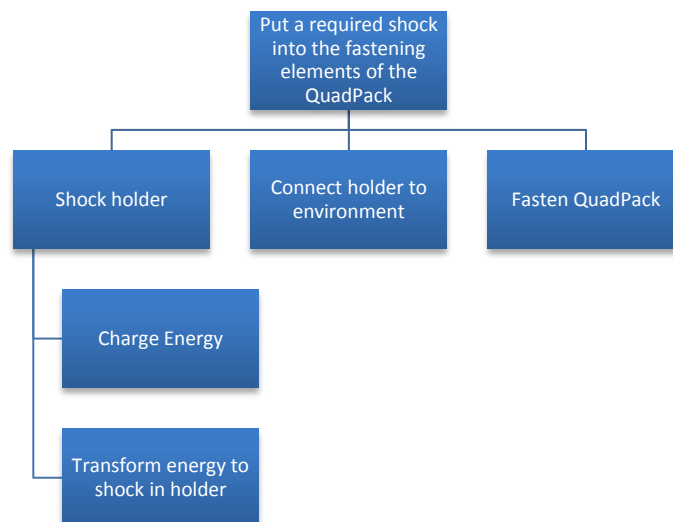


*Figure 25* STF function tree

As mentioned earlier the STF had to be able to produce a mid-field shock environment without using explosives. Explosives can be dangerous to handle and they require specific licences and facilities. This left mechanical metal-to-metal impact as the method to achieve the sub-function *Transform energy to shock in holder*. To realise a mechanical impact, stored energy will be transformed into kinetic energy of a mass that will strike a surface and thereby excite the required shock. This means that an “Impactor” and a “Receiver” of the impact are needed.

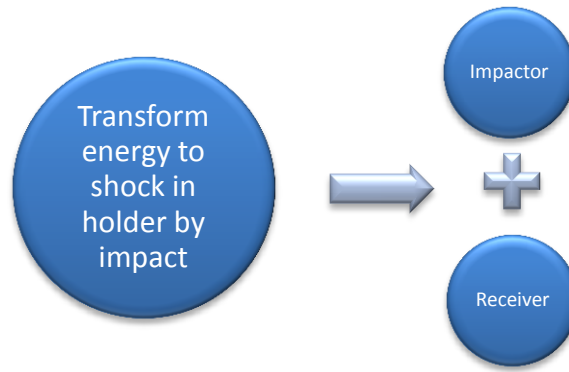


Figure 26 Mechanical impact

This last division is more a constraint that leads to class of solutions than a sub-function division but the end result is still five sub-functions that needs to be fulfilled:

- Impactor
- Receiver
- Charge energy
- Fasten QuadPack/Test specimen
- Connect holder to environment

### 2.3.2 A more systematic look on existing mid-field STF

In section 1.6.2 several different mid-field STF's excited by means of impact were discussed. Two other examples are given in *Figure 27* and *Figure 28*.

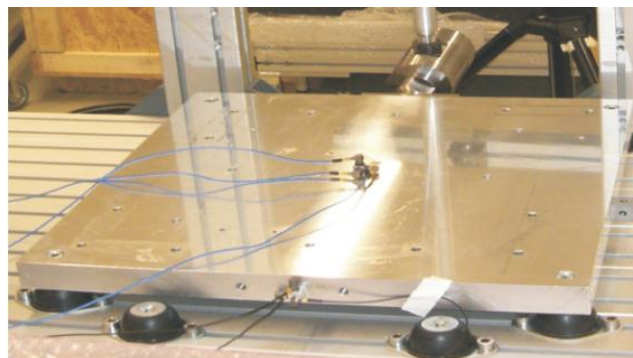


Figure 27 Shock test setup with resonant plate and pendulum hammer [28]

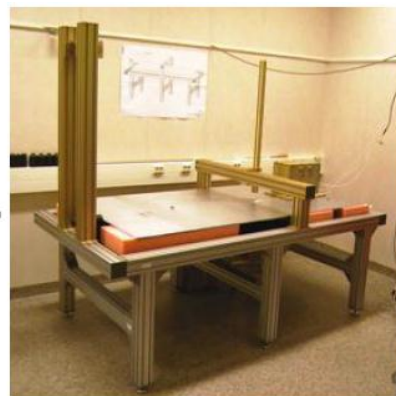
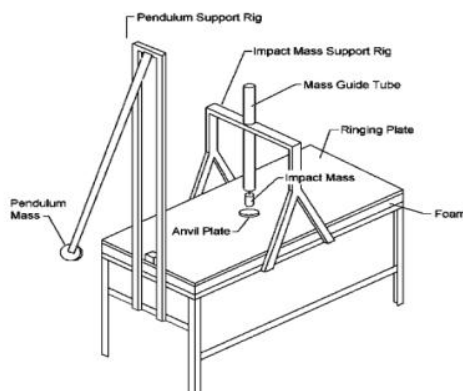


Figure 28 RUAG Space AB STF [23]

All the existing impact STFs found were analysed on how they solve the five identified sub-functions. The results can be seen in **Table 6**.

*Table 6 Sub-function solutions of existing STFs*

<b>Impactor</b>	<b>Receiver</b>	<b>Charge energy</b>	<b>Fasten specimen</b>	<b>Connect holder to environment</b>
Drop hammer	Anvil (usually mounted on the following devices)	Height (Potential energy)	Directly on resonant structure, same side as impact	Guide rails that are mounted to floor and steers the motion
Pendulum hammer	Resonant plate	Air/Gas /Pneumatic pressure	Directly on resonant structure, other side than impact side	Resting on foam pad on table
Ram hammer	Resonant beam	Muscle power	Inside of compounded resonant structure	Adaptable clamping plates for tunable knee frequency mounted on concrete base
Pneumatic gun	Resonant bar	Gunpowder	On bi-plate	Bolts with springs
Pneumatic piston	Fastener/Resonant structure in one		Anvil/Resonant Structure /Fastener in one	Hanging in ropes
Regular hammer	Resonant bi-plate		On fixture/bracket /fastening adaptor which in turn is mounted on resonant structure	Hanging in chains
Nail gun	Tunable resonant plate			Resonant structure on wheels
Drop table	Tunable resonant beam			Hanging in bungee cords
	Tunable resonant bar			
	Compounded structure from above parts			
	Plate with elastomeric pads between hammer/anvil			

Different combinations of these sub-solutions compose all the existing STF's for mid-field shock that have been examined. The next step was to fill up the table with every thinkable sub-solution.

### 2.3.3 Brain storming and initial elimination

Brainstorming sessions were held for each of the sub-functions and a large number of sub-solutions were created; see Appendix A – Brainstorming Results. During the sessions strong connections between some of the sub-functions were exposed and it would not be correct to call them independent. The *Impactor* is closely linked to the *Charge energy* sub-function and the *Receiver* is closely linked to the *Fasten specimen* sub-function. A drop hammer as *Impactor* implies the usage of the potential energy in drop height as *Charge energy* function. The *Fasten specimen* function is reduced to the question if the specimen will be fastened directly on the *Receiver* or with some sort of adaptor or bracket.

A concept is created by following the algorithm in *Figure 29*. Even with the identified dependencies between the sub-functions the total number of permutations, and thereby the number of concepts, reached an amount with five digits. To find the best concept among these an elimination process was initiated.

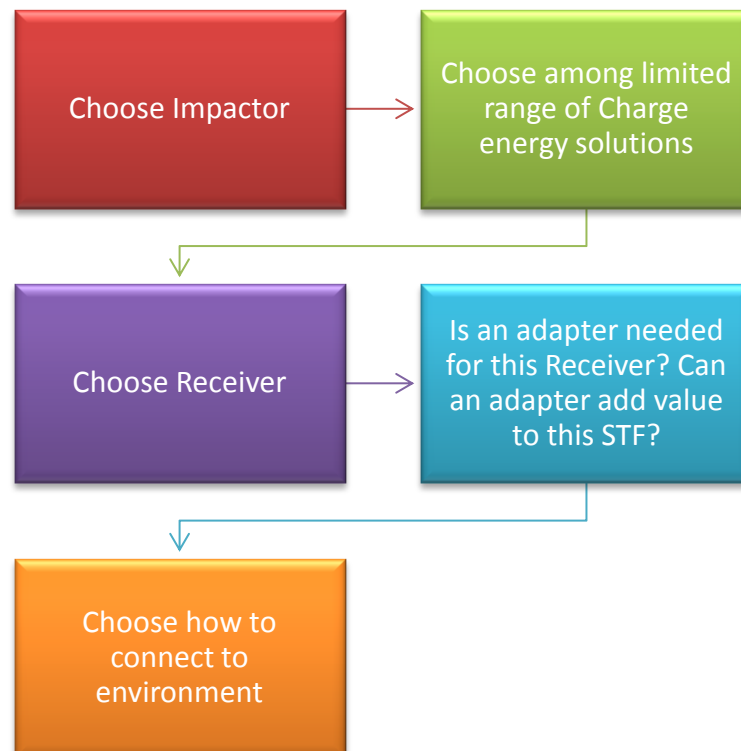


Figure 29 From sub-solutions to concept

### 2.3.4 Trade-off studies

There are three levels of trade-off studies [20]:

- Mental
- Informal
- Formal

The mental trade-off is based on the judgement of the system engineer and used when the outcome is obvious or when the consequences are not too important. The informal trade-off study follows the same procedure as the formal one but without the formal need of documentation and review.

The first step is to use mental trade-off to eliminate non-feasible sub-solutions and obvious losers. The requirements specification was used to define arguments for why a sub-solution was better than another to make sure good solutions were not eliminated for the wrong reasons. A list of eight requirements that were good to “over-do” and goals in the form “The more/less, the better” were selected:

- Repeatable
- Discrete, documentable and adjustable parameters
- Sustainable, as small impact on the environment as possible
- Minimise time for one test cycle
- Easy and safe to operate
- Enable future development
- Achieve shock in a simple way
- As cheap as possible

At this stage no formal verification of the arguments were made but solutions that did not impress on any of these points were deemed as bad and were eliminated together with the ones for which no implementation could be found. After a couple of iterations of mental trade-off elimination the number of concepts had been reduced to 392. The surviving sub-solutions can be seen in **Figure 30**.

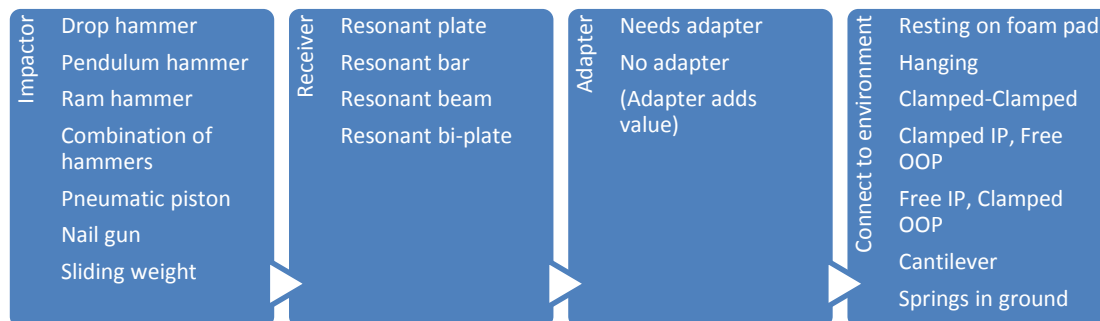


**Figure 30** Surviving sub-solutions

During this process additional constraints were also defined for the concepts which meant that not all permutations were feasible. For example when the drop hammer is selected as *Impactor* the STF can only impact the *Receiver* from above so the rest of the system must ensure that the specimen can be tested in all directions. Another example is that when a resonant beam or bar is used as *Receiver* an adaptor must be used since the beam would otherwise need to be huge in order to fit the QuadPack. After these constraints had been implemented the number of concepts was boiled down to 115. See **Figure 31** where the surviving concepts are shown as a tree where each of the outermost branches represents a concept.



Figure 31 STF concept tree showing the 115 surviving concepts

As mentioned earlier the selection of one sub-solution can put additional constraints on the rest of the STF but a unique sub-solution does not always have to be selected. An example to prove this point is the Alcatel ETCA (now Thales Alenia Space ETCA) STF that can be seen in **Figure 32**. This STF consist of a versatile scaffold in which all of the surviving receivers could be hung and for which they can use several different impactors such as ram hammer, pneumatic gun and even explosives.

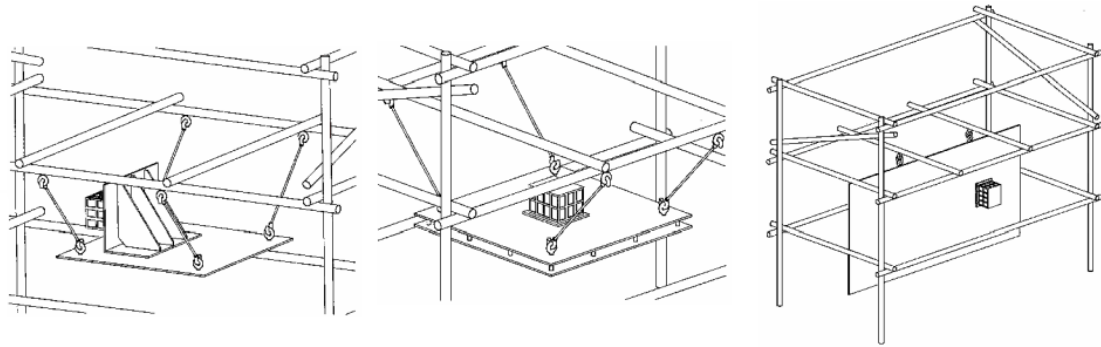


Figure 32 Thales Alenia Space ETCA shock test facility [26]

To be able to narrow the list of concepts further a new approach was required. Instead of looking on mid-field impact STF's generally, the specific requirements in this case were used together with a closer look on the capabilities of the different sub-solution techniques. Shock experts all over Europe were contacted to gain knowledge on the practical usage of the different methods. Resonant bars and beams are usually not designed for specimen of the QuadPack size and are therefore not the best option [26]. Moreover, the bi-plate technology is not used to reach high shock levels in the in-plane (IP) direction [26] so the resonant plate was selected as the final sub-solution for the *Receiver* sub-function.

The development of an adaptor is not required if the STF can test the specimen in all directions without it and since that is the case for the resonant plate technology [26] [29] the concepts with the adaptor sub-solution were eliminated. Regarding the *Impactor* pneumatic pistons have been known to give problems with repeatability [23] and reaching the high required levels [26] and were therefore eliminated. The nail gun is relatively cheap and can be added as a future improvement of any STF, although it does spread too much particles to be applicable in a clean room environment. The nail gun was thus considered as a potential future development. The sliding weight was also eliminated in this process since the velocities required can be reached with the simpler gravity charged hammers.

The concept tree was now significantly smaller and easier to overview, see **Figure 33**, but a few more eliminations were made before the finalist concepts were selected.

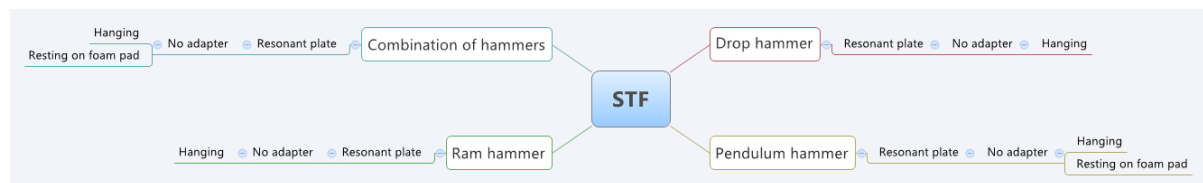


Figure 33 Concept tree after additional trade-off iterations

The ram hammer was considered to be weaker than the other solutions. The pendulum hammer can be charged to at least twice the height for the same length of attaching string/rod and the repeatability of the ram hammer at the max level of charge is questionable. For the same height the ram hammer would take a lot more space, see **Figure 34**. Because of this the ram hammer was eliminated.

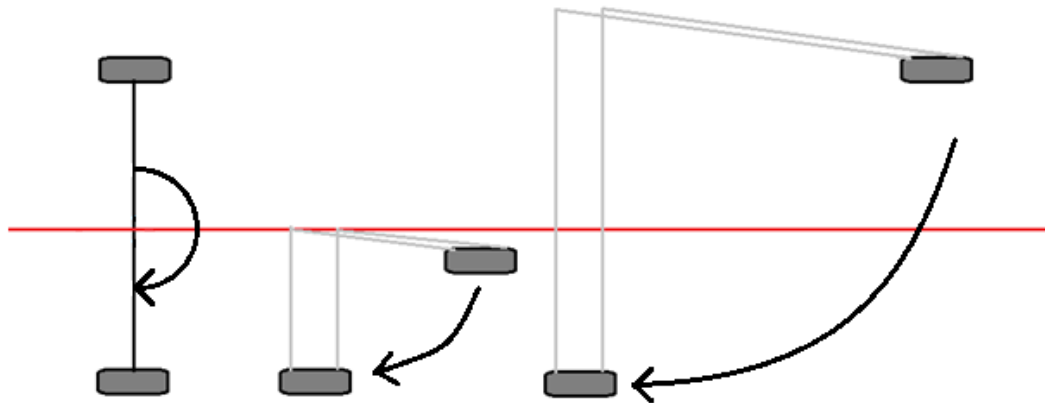


Figure 34 Comparison between pendulum and ram hammer

The drop hammer can only strike the plate vertically from above which means that it is incompatible with hanging solutions which are mainly designed to be impacted horizontally or from below. Therefore were the drop hammer and the hanging combination of hammers eliminated. This left three finalist concepts that were developed further. The finalists can be seen in **Figure 35** and were named:

- Hanging pendulum
- Foam pad pendulum
- Hammer combination

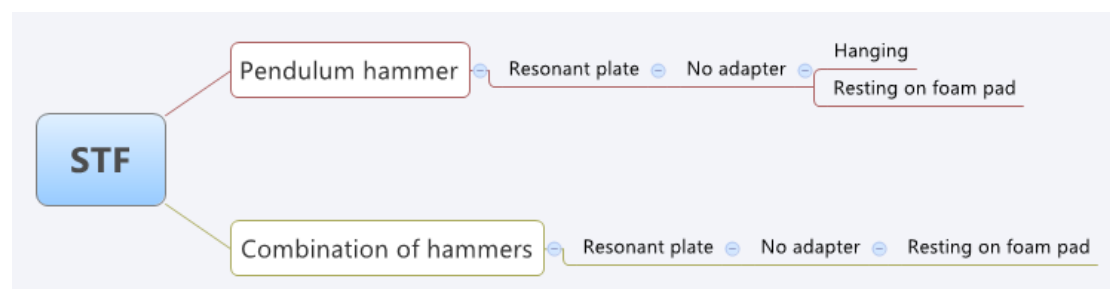


Figure 35 Concept tree with the three finalist concepts

To enable further development more knowledge was required on the dimensions of the STF.

## 2.4 Simulation and analysis

To acquire more information on the dimensions of the STF FE simulations were made with Abaqus Explicit. Explicit methods have an advantage over implicit methods when the simulated phenomenon is highly dynamic, has a short duration or is dominated by wave propagation. All of these can be used to describe the shock phenomenon and therefore explicit methods are recommended for shock simulation [3].

An apprehensible way of describing the difference between explicit and implicit methods is the way the FE model is updated between  $t$  and  $t + \Delta t$ . For implicit

methods the state in  $t + \Delta t$  is determined from information of the system at time  $t + \Delta t$ . For explicit methods the state at time  $t + \Delta t$  is instead determined from information at time  $t$  [30]. It is possible to take larger time steps with the implicit solution method, as it can be formulated to be unconditionally stable, while each step is computationally more expensive. For every time step the global stiffness matrix  $\mathbf{K}$  has to be formulated and inverted in an iterative process until a convergence criterion is met. For explicit solution methods the only matrix that is inverted per time step is the lumped mass matrix  $\mathbf{M}$ . Since it is diagonal its inversion is trivial and the computational cost is low [30]. The explicit solution method is, however, not unconditionally stable. There is a maximum length of the time step defined as:

$$\Delta t \leq \frac{2}{\omega_{\max}} \quad (1)$$

where  $\omega_{\max}$  is the highest frequency of the system.

This is the largest drawback with the explicit methods so when the time step for physical reasons needs to be short, as is the case for shock simulations, this problem is diminished. The advantage that implicit methods have in a longer time step cannot be used so explicit methods are favourable.

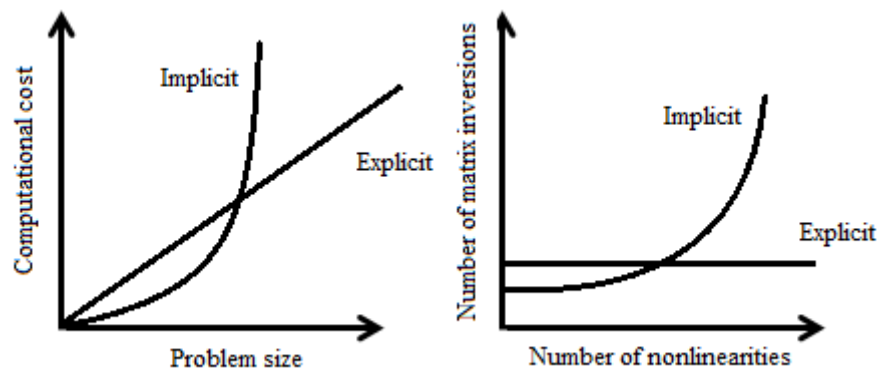


Figure 36 Comparison between explicit and implicit solution methods, based on [31]

Simulation and analysis are iterative processes. A feature is analysed with FEM which gives information on its design parameters which in turn can be used to alter the feature. A new simulation could be done and this process could be iterated in order to optimise the feature's parameters. At the same time new information is attained as the system moves forward in the development chain which could also influence the parameters of the feature in question, see *Figure 37* and [32].

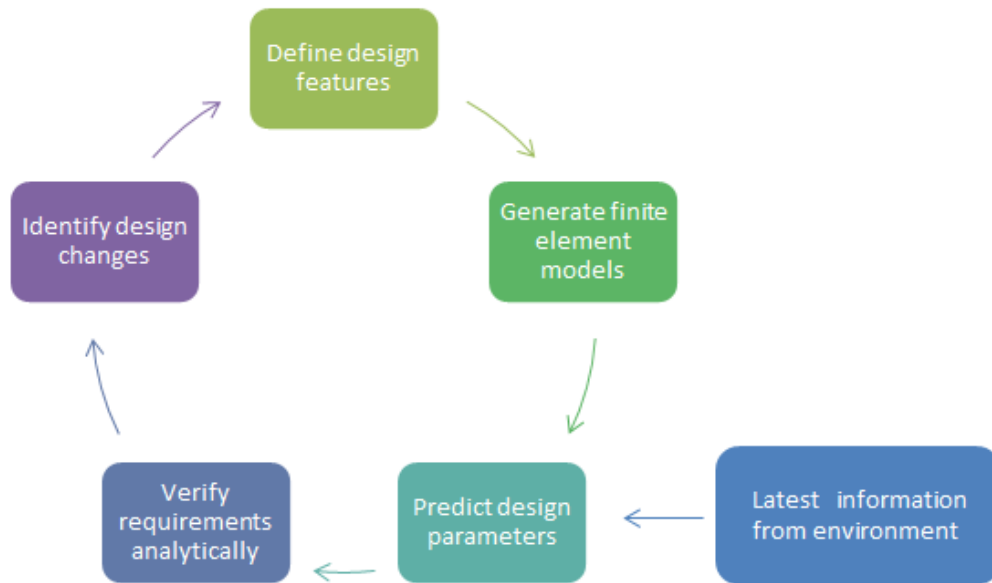


Figure 37 Simulation cycle

This cycle is nestled in an even larger loop where the FE models can be improved by investigating and implementing the parameters of the actual STF after manufacturing. With the STF available the FEA results can be validated but that is not the case for the initial simulations. It is important not to put too much confidence in FEA results that have not yet been validated, especially in this case since shock is known to be difficult to simulate [3] and [32]. It is still, however, a strong tool for designing purposes. Even if it cannot be stated with confidence that the results are at the exact right level they can be used for comparison purposes. A parameter can, for example, be shown to have a larger impact on the SRS than another and the effect on the SRS of tuning a parameter can be investigated. Before the simulations could be commenced a starting point model and the parameters to investigate had to be determined.

#### 2.4.1 Selection of parameters and starting point model

A STF needs to be able to tune the shock environment it produces depending on the specimen and on the SRS requirement. There are numerous ways of altering the SRS in an impact STF. Examples of parameters that can be modified are:

- Impact velocity
- Receiver shape
- Receiver material
- Receiver dimensions
- Impact location
- Specimen location
- Receiver boundary conditions
- Extra masses added to receiver
- Impact surface shape
- Impactor material
- Anvil material
- Specimen mounting method
- Mechanical filters between impactor and receiver

These parameters can be combined in an unlimited number of ways. Designing a STF can be seen as the process of selecting which of these parameters to keep constant and which to use as variables to tune the result. Some parameters are more straightforward to alter and some have a larger impact than others. Once the STF is manufactured it is difficult to alter the material of the different parts while it is quite simple to change the impact velocity or adding mechanical filters. The material and shape can be altered by having several versions of key parts but this can be expensive, especially for big or complex parts.

It always takes a considerable amount of trial and error to tune the SRS to a certain requirement. This procedure can, however, be minimised by gaining knowledge on how the parameters influence the SRS. Seven parameters were identified as key parameters [15], [26], [29], [33], [34] and [35] and their influences on the SRS were examined. The parameters were:

- Resonant plate dimensions
- Measurement location
- Impact location
- Impact velocity
- Anvil material
- Hammer mass
- Hammer impact surface radius of curvature

At the time the only things known about the STF were that it would use a resonant plate and a hammer to achieve an impact which should produce the proper SRS and allow adequate control. Two independent experts [26] and [35] gave the advice to use a 1 x 1 m aluminium plate which was selected as an initial assumption for the simulations. All in all the starting points for the simulations were:

- Resonant plate dimensions: 1000 x 1000 x 30 mm Aluminium
- Impact velocity: 1 m/s
- Hammer impact surface radius of curvature: 200 mm
- Hammer mass: 5 kg
- Impact location: Dead centre
- Measurement location: 300 mm to the side of the impact location
- No anvil

The simulations were first carried out without the influence of an anvil, damping and test specimen. Modal damping is usually recommended for shock analysis [3] but for explicit codes the modes are not directly available so it cannot be used. There are, however, several other ways of including damping in the model. With damping the maximum time step in Abaqus becomes:

$$\Delta t \leq \frac{2}{\omega_{\max}} (\sqrt{1 + \xi_{\max}^2} - \xi_{\max}) \quad (2)$$

where  $\xi$  is the fraction of critical damping in the highest frequency mode. This means that including damping shortens the time step which can be contradictory to intuition [36]. Including damping can even shorten the stable time step to a point where it is not feasible to run the simulation [37]. On the short time scales of shock, however, the damping has a negligible effect [35]. Realistic results have been acquired without the inclusion of damping and it was therefore selected to not include the damping in the simulations. More detailed information on the analysis can be found in Appendix B – Analysis information.

## 2.4.2 Parameter simulations

To see how a parameter affects the SRS, the parameter was adjusted while everything else was kept constant. First of all, however, the starting point model was simulated, see *Figure 38*.

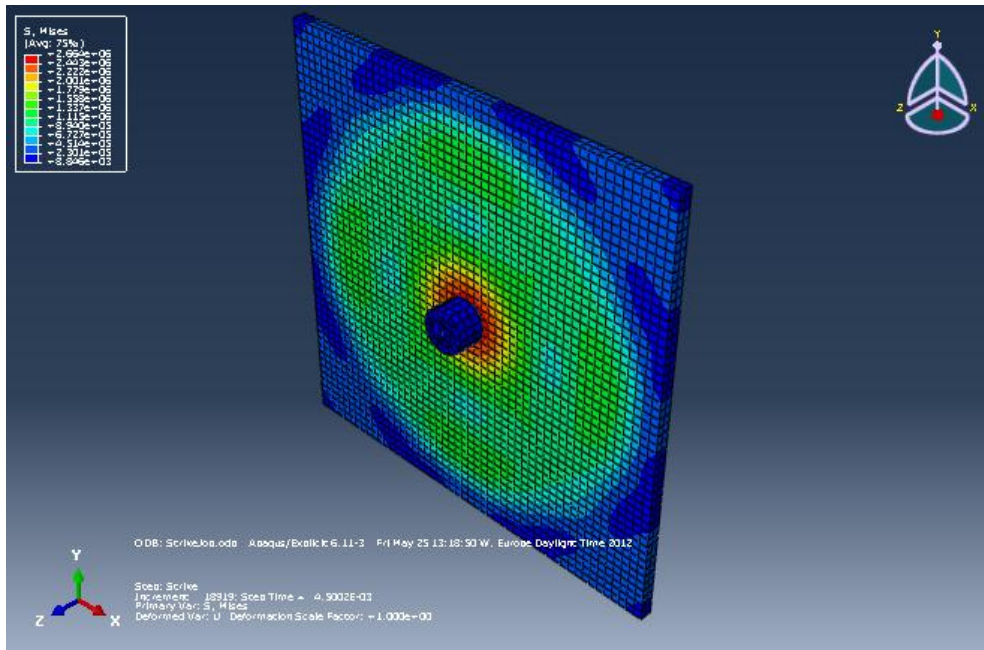


*Figure 38* Von Mises stress levels [Pa] captured milliseconds after impact

The acceleration time histories were exported to Matlab where the Smallwood algorithm [38] was used to calculate the SRS. There are several different algorithms to calculate the SRS but the Smallwood algorithm has been shown to be the most representative one [19].

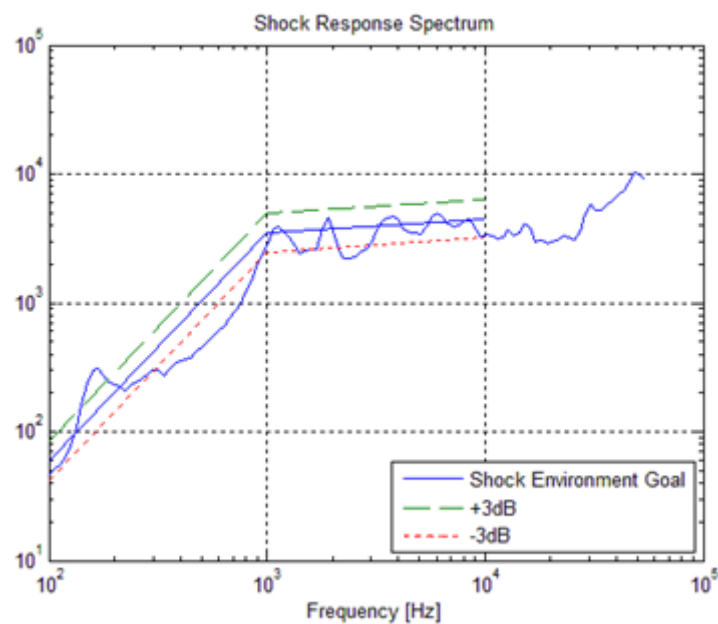


*Figure 39* Starting point simulation SRS. It compares quite well to the requirement SRS also plotted

A mesh sensitivity study was performed with the SRS results in order to give confidence to the point that the results were independent of the mesh. The starting point was modified somewhat by lowering the impact velocity to 0.7 m/s to make it compare better to the STF requirement levels, see *Figure 39*, but more on the influence of impact velocity in Section 2.4.2.4.

### 2.4.2.1 Plate dimensions

The size, shape and material of the resonant plate affect the SRS strongly. To uphold some structure in the simulation campaign the shape was limited to be rectangular. Triangular plates and other forms are also present in industry but usage of such plates is here looked upon as a potential future development. Firstly, the influence of the thickness of the plate was examined.

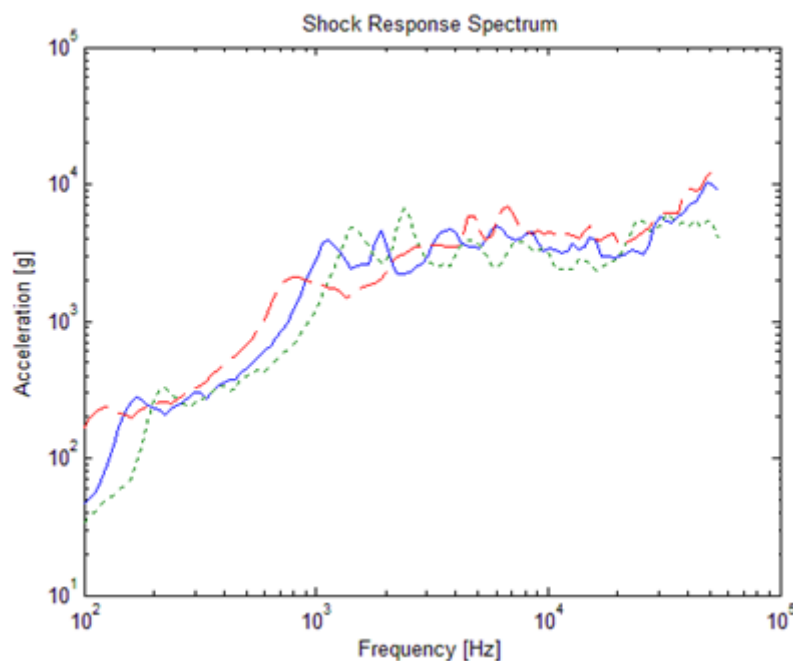


*Figure 40* Influence of plate thickness on SRS

As can be seen in *Figure 40*, adjusting the thickness of the plate, and keeping everything else constant, results in a shift of the knee frequency of the SRS. Several different plates could be used but since the plate stands for a considerable cost this option is also considered to be a potential future development. The requirement on the shape of the SRS defined the knee frequency to lie at 1 000 Hz and have a magnitude of 3500 g. The simulations made confirm that 30 mm is a reasonable choice of thickness since it puts the knee frequency spot on at the required 1 000 Hz. Using a thicker plate pushes the knee frequency to higher levels while a thinner plate pushes it to lower frequencies.

Secondly, the effects on the SRS of the side lengths of the plate were investigated. In *Figure 41* the effect on the SRS of making the sides shorter are shown.

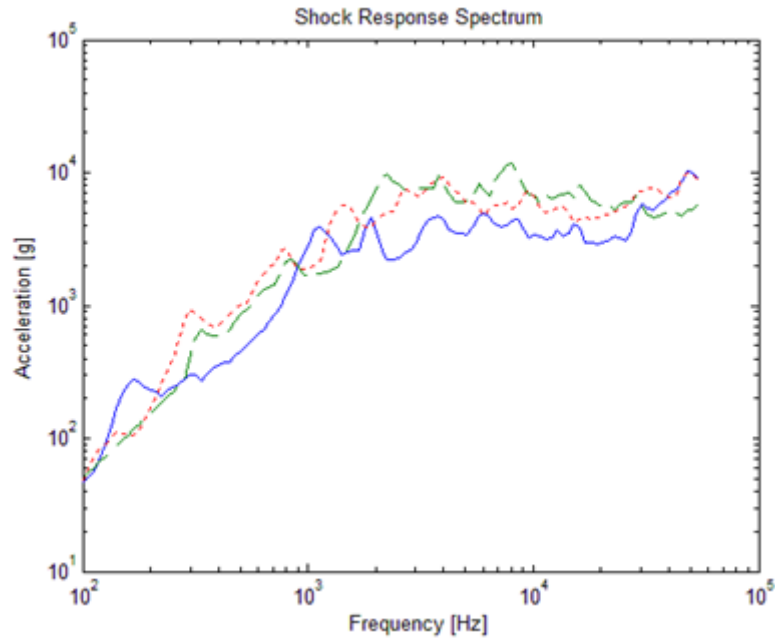


Figure 41 Influence on SRS when shortening the plate

The knee frequency was pushed up and away from the requirement on 1000 Hz and the overall SRS levels were increased. Another strong downside with making the plate smaller is that it would be difficult to fit the test specimen on it. The QuadPack has a significant footprint of around 300 x 400 mm.

The plate is also used for the IP shock direction so it was important to verify that the required shock level could be acquired also with this configuration, see **Figure 42**. This arrangement is used at many places in industry with successful results [26] and [24]. The IP and OOP shocks usually look different both in the time and frequency domain but it can be tuned to fall within the requirements [23].

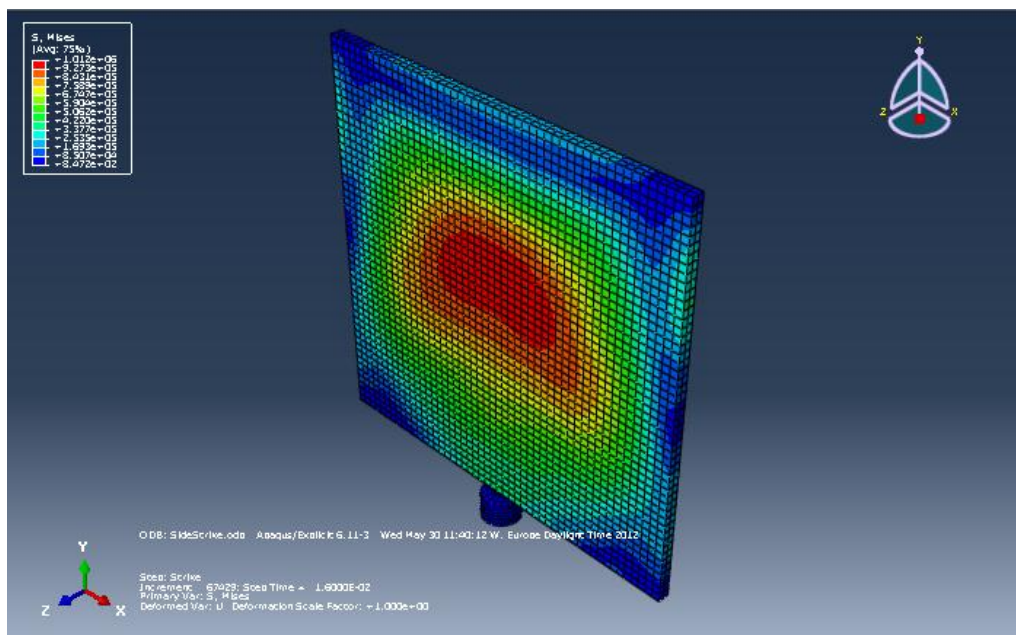
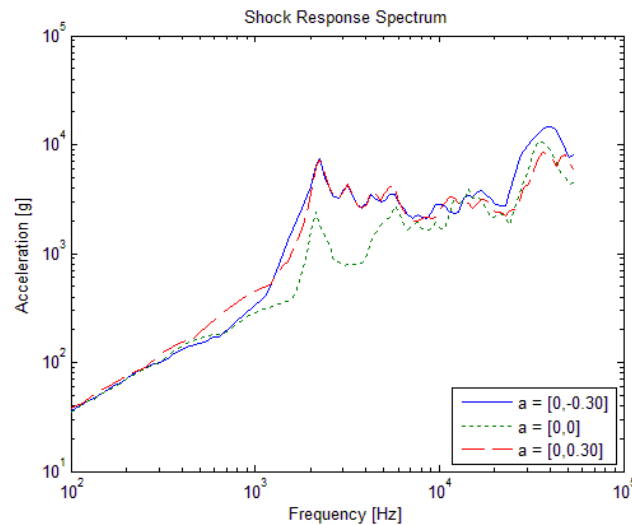


Figure 42 In plane impact. Von Mises stress [Pa] captured milliseconds after impact.

The simulated shock level was measured at three locations; at the centre of the plate ([0,0]) and 30 cm closer respectively farther away from the impact location. The results can be seen in **Figure 43**.



*Figure 43 SRS for side impact with three measurement locations. Note that it is the IP acceleration that has been plotted.*

For the same impact velocity the shock environment reaches the same magnitudes of acceleration but the knee frequency is shifted to a higher level. This makes sense since the longitudinal compression waves, that are more substantial in this configuration, are always faster than the transversal waves in the same material. A rule of thumb for the knee frequency tuning of a resonant bar that is excited in the longitudinal direction is given [5]:

Introducing the length of the bar  $l$ , the wave speed in the material  $c$ , the sought knee frequency  $f$ , the density of the material  $\rho$  and the material's Young's modulus  $E$ .

The length of the bar can be described as

$$l = \frac{c}{2f} \quad (3)$$

And the longitudinal wave speed in the material can be simplified to

$$c = \sqrt{\frac{E}{\rho}} \quad (4)$$

For aluminium with  $E = 71.1$  GPa and  $\rho = 2650$  kg/m<sup>3</sup> the length of the bar for  $f = 1\,000$  Hz becomes  $l = 2.59$  m

It was not feasible to make the plate this long but simulations were made with a 1 x 2 m plate to see its effect. The IP results did indeed show a knee frequency shift towards the sought 1 000 Hz but the overall acceleration levels were also lowered. To see if it could be beneficial to lengthen one of the sides of the plate slightly, the IP impact was also simulated for a 1.3 m long plate with results shown in **Figure 44**.

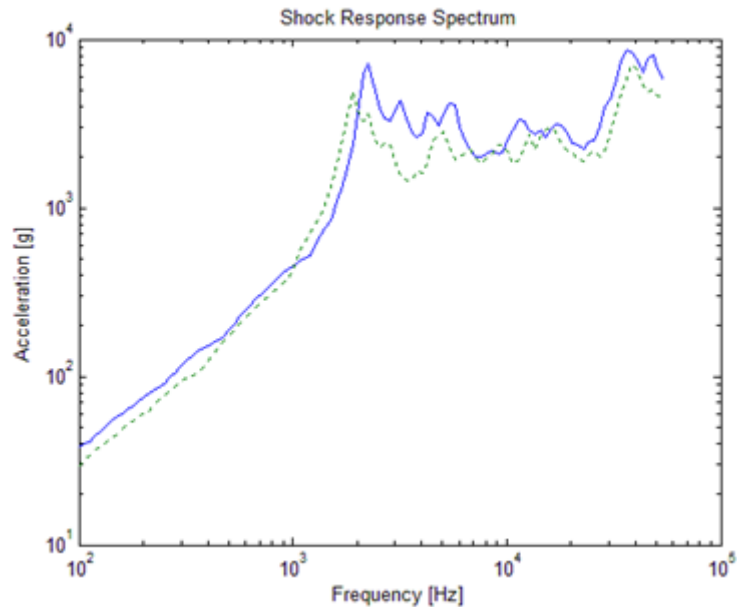


Figure 44 SRS effect of the length of the plate

The same tendencies can be seen here as for the 2 m plate. The shift in knee frequency was, however, not significant enough to make it worth implementing an extension of the plate with the extra cost and weight it would induce.

It should be noted that the simulations were carried out without the influence of a test specimen. Adding the extra mass on the plate should not induce a significant change on the overall acceleration levels but it should shift the SRS curve to the left [35]. This effect could be used to help push the knee frequency to within the tolerances.

The dimensions of the plate were thus selected to be 1 x 1 x 0.03 m.

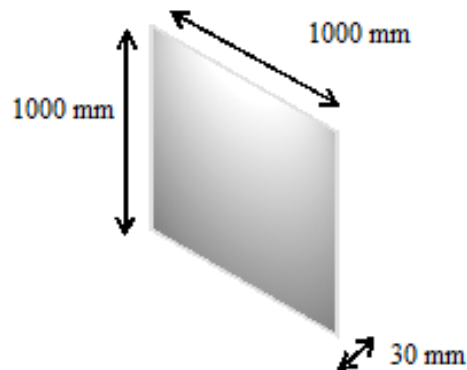


Figure 45 Resonant plate dimensions

#### 2.4.2.2 Measurement location

The test specimen can be mounted on different locations on the plate and the measurement location is therefore moved accordingly. The location of measurement does alter the SRS but the results do not change in an easily predictable way. Simulations were made with measurement locations at the positions shown in **Figure 46**.

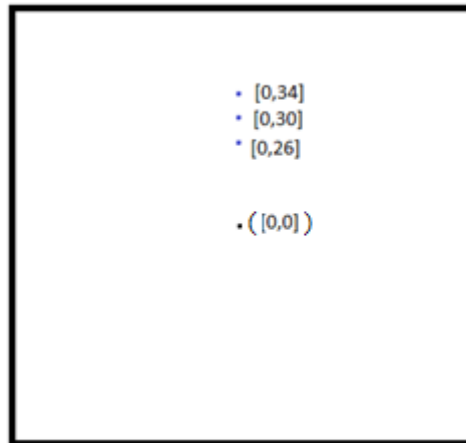


Figure 46 Measurement locations (and impact location in brackets)

The resulting SRS at the different locations can be seen in **Figure 47**. They differ somewhat but it is difficult to see a pattern. All of the three curves are at certain frequencies the lowest and at other frequencies the highest in magnitude and they have similar characteristic features.

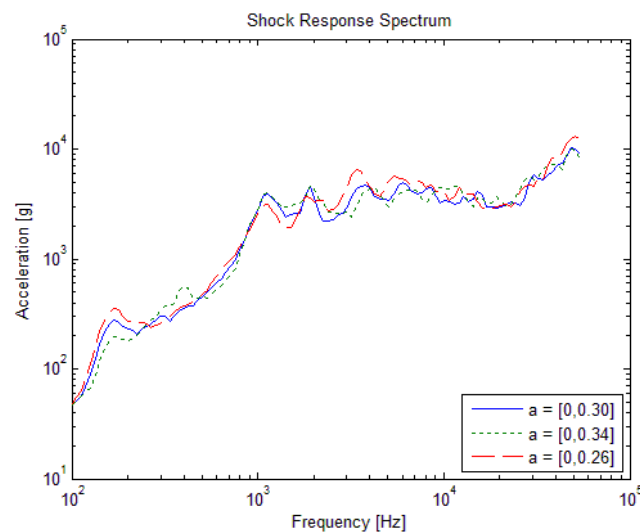


Figure 47 Influence of measurement location as can be seen in the former Figure

From this analysis it is difficult to see exactly how this parameter can be used to tune the SRS and it can be argued that all the three measurement locations lie on a line that could have similar characteristics for many modes. Because of this a more thorough simulation was made to map the behaviour at different locations, see **Figure 48**.

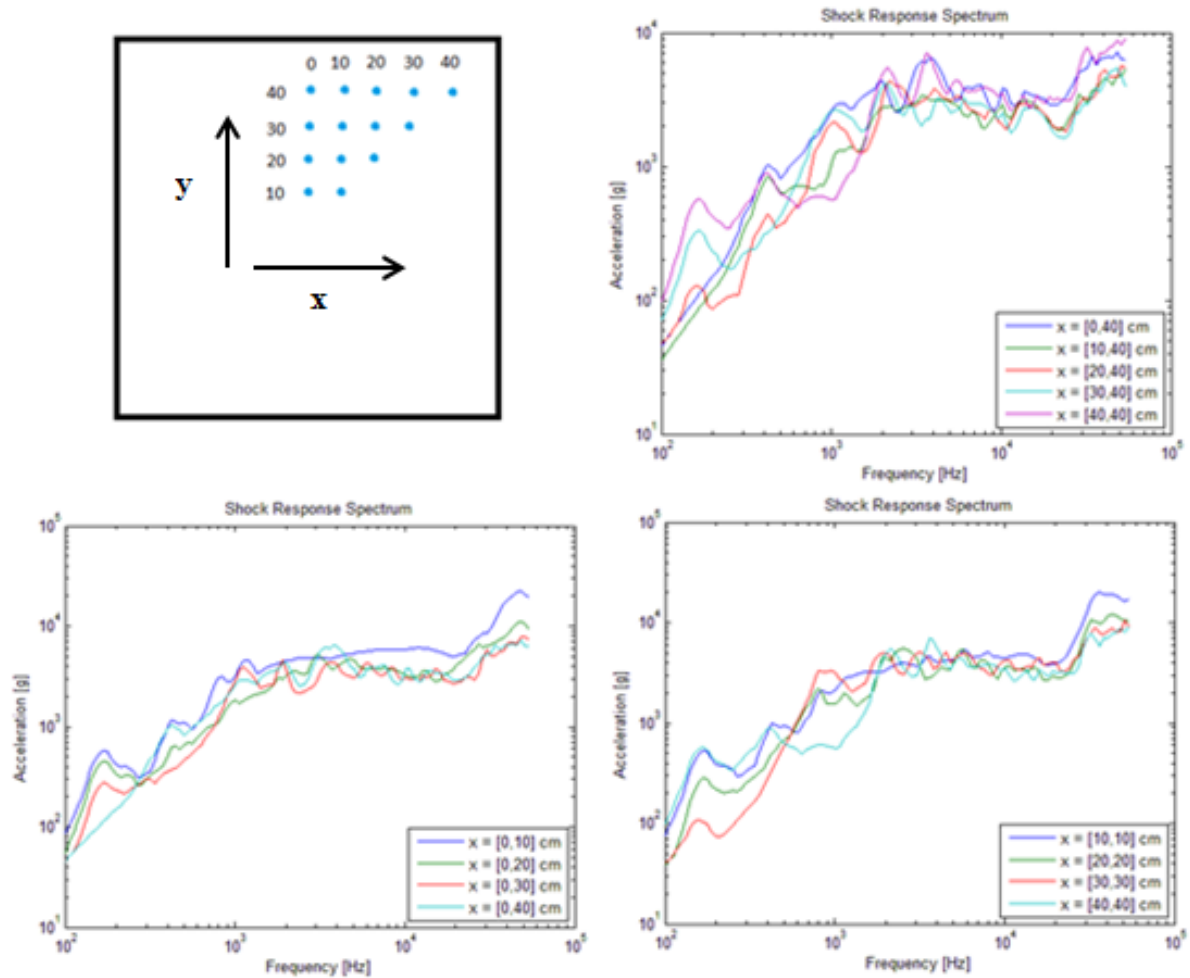


Figure 48 Examination of different measurement locations

No consistent patterns could be found in the simulations and since every different mounting location of the specimen requires a substantial amount of holes the mounting location was selected to be kept constant in the STF initially. To be able to use the location as a tunable parameter, good knowledge of the STF is required and this type of knowledge can usually only be attained by a good characterisation test campaign [39].

### 2.4.2.3 Impact location

As for the measurement location, the location of impact also has an influence on the SRS. It is, however, equally difficult to define exactly how the parameter alters the SRS. The impact locations in the simulations and the results are shown in **Figure 49**.

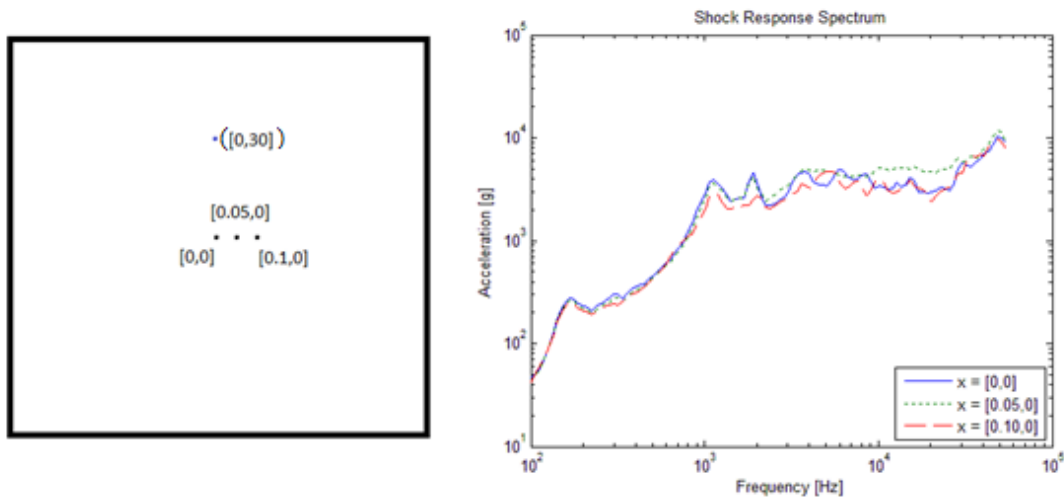


Figure 49 Different impact locations (and measurement location in brackets) and SRS results for these configurations

It can be seen that the influence is larger for frequencies over the knee frequency but since the changes are inconsistent no conclusions can be drawn on exactly how the SRS is affected. Different impact locations are, however, easy to implement in a STF so it was allowed to be a variable in the STF.

#### 2.4.2.4 Impact velocity

The impact velocity is the main tuning parameter of the STF. A higher velocity gives higher accelerations over the whole frequency spectrum. Results from the simulations can be seen in **Figure 50**.

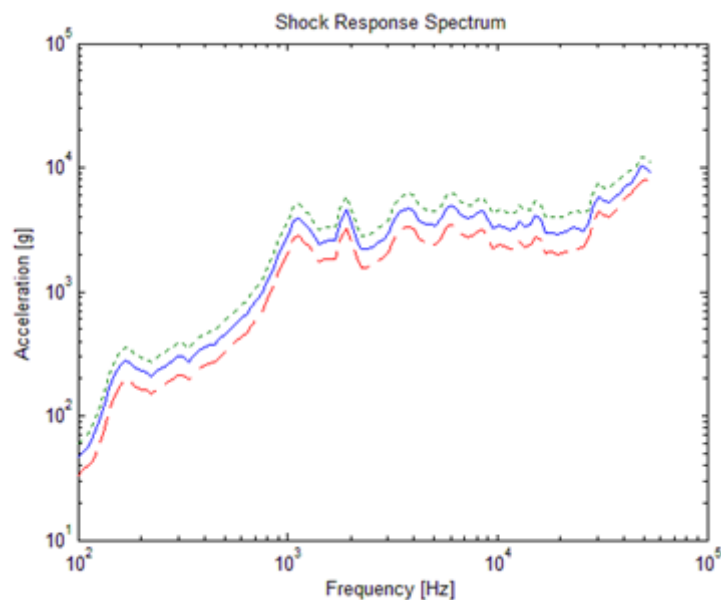


Figure 50 Influence of impact velocity on SRS

Note how the shape of the SRSs are constant and how the magnitude is shifted a constant distance over the whole spectrum. The impact velocity can be continuously altered in a range that is set by the design of the STF. In the simulations, impact velocities of below 1 m/s were sufficient to reach the required levels but that was

unexpected. Experts have suggested that 3 m/s should be enough for the required shock levels [35] while others thought a somewhat higher level was required [26]. Increasing the maximum impact velocity does not change the STF's potential at lower values. The range was therefore selected to the double suggested value which meant 0 – 6 m/s. This implies a maximum charge height of around 1.8 m. This potential should be more than enough for the required levels

#### 2.4.2.5 Anvil material

To prolong the lifetime and assure the repeatability of the STF, plastic deformation of the resonant plate is unwanted. The immediate impact is therefore given to a small sacrificial anvil plate. The material of this plate together with the material of the hammer defines the duration of the impact and influences the SRS mainly for the higher frequencies, see *Figure 51*.

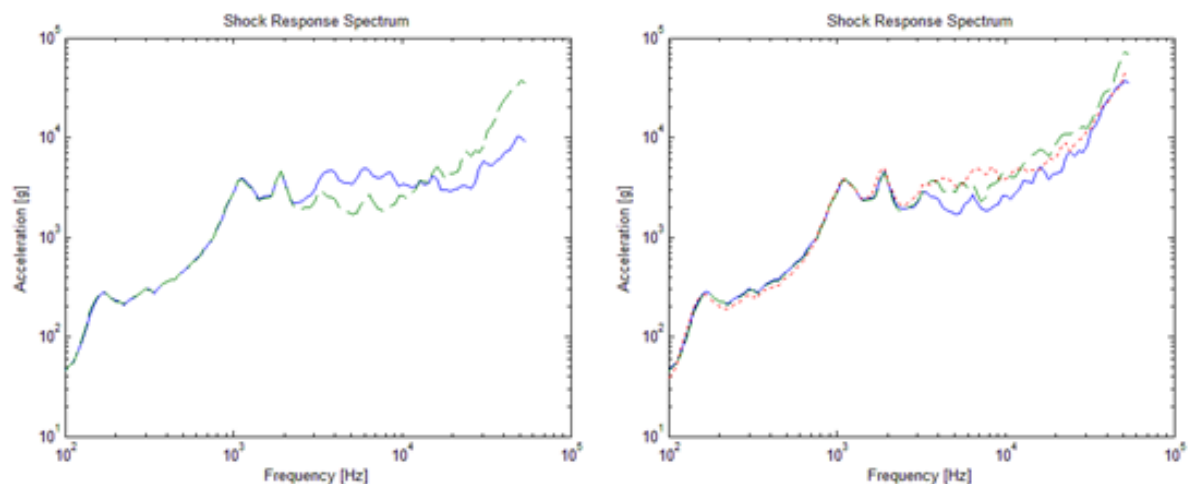


*Figure 51* Influence of anvil on SRS

The usage of different anvil plates was selected to be one of the variables in the STF. It is important to make sure that the anvil materials are softer than the material in the hammerheads so that the impact surface on the hammerhead does not lose its radius of curvature.

As can be seen in *Figure 51* the anvil introduces an overshoot in the high frequencies. This overshoot is typical for impact STF's and should be able to be attenuated with the usage of mechanical filters, such as a paper between the impacting surfaces [24].

#### 2.4.2.6 Hammer mass

The influence of the mass of the hammer is not as large as can be expected. It is only in the frequency domain under the knee frequency that the influence is substantial. The results from simulations can be seen in *Figure 52*. The results are higher for the low frequencies with a heavier hammer.

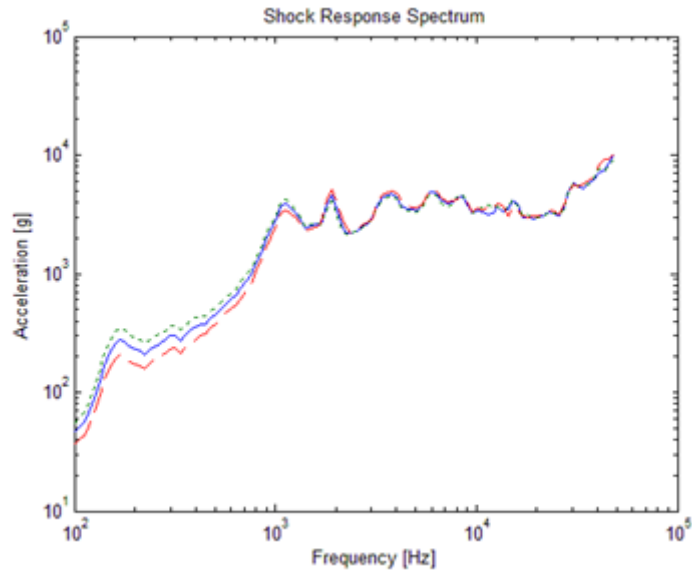


Figure 52 Influence of hammer mass on SRS

This is the main parameter for tuning of the slope of the SRS in the lower frequencies. A water tank could realise the mass tuning in a continuous way but the hammer needs to be robust and it needs to be adjusted in a simple manner to fulfil the requirement of repeatability. The STF was therefore realised with hammer mass as a variable. The range goes from “0” to around 10 kg where “0” means without any add-on mass. The exact weights of the add-ons are not that important as long as they span the range in a documentable way.

#### 2.4.2.7 Hammer radius of curvature

The hammer radius of curvature is the radius of curvature of the impacting surface of the hammer. If a flat surface impacts another flat surface a small misalignment causes the contact zones to differ greatly. This is disadvantageous for the repeatability of the STF. To have the impact surface of the hammer curved gives some alignment tolerance since a small misalignment will not change the contact zone, see *Figure 53*.

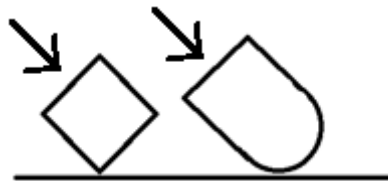


Figure 53 Curved surface vs. flat surface of misaligned hammer

The SRS is influenced by the hammer radius of curvature mainly in the higher frequencies over the knee frequency. The larger the radius is the higher the acceleration becomes, see *Figure 54*.

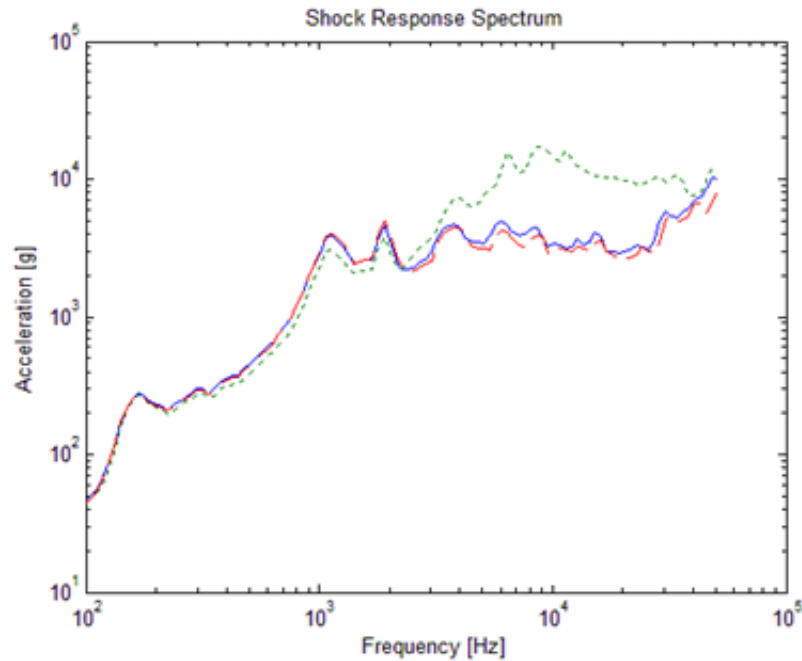


Figure 54 Influence of hammer radius of curvature from simulations

Together with the anvil material this is a method of tuning the SRS in the high frequency domain. After a review meeting with an expert [24] the hammer radius of curvature was selected to be kept constant. From experience the influence of radius changes was small in comparison to that of changing the material of the hammerhead. The material of the hammerhead was selected to use as a variable instead and the radius of curvature was selected to be kept constant at 10 cm.

#### 2.4.2.8 Parameter conclusions

After input from experts [23], [24], [25], [26] and [35] and the parameter simulation campaign the parameter ranges and plate dimensions that were to be implemented in the STF were selected. They can be found in **Table 7**.

Table 7 Parameter and dimension specification for STF

Parameter	Constant	Continuous variable	Discrete variable	Value/Range
Plate dimensions	X			1 x 1 x 0.03 m
Specimen location	X			Decided by design
Impact location			X	Limited by design
Impact velocity		X		0 – 6 m/s (≈ 1.8 m drop )
Anvil material			X	3 different materials
Hammer mass			X	0 – 10 kg, steps of 2 kg
Hammer radius of curvature	X			10 cm
Hammerhead material			X	2 different materials

## 2.5 Selection of the final concept

With the new information attained from simulations and experts it was possible to develop the finalist concepts to a level where a rational selection of the final concept could be made. To get an idea of the concepts and make sure that they were developed to a somewhat equal level a number of questions that the three concepts had to answer were defined.

1. How will the concept implement the connection to the environment?
2. How will the concept allow for the impact location to be adjusted?
3. How will the concept implement both the IP and OOP impact?
4. How will the test specimen be mounted on the concept?
5. How will the concept ensure that the setup is aligned?

### 2.5.1 Hanging pendulum

The hanging pendulum is a concept that uses a pendulum hammer and a plate hanging in a scaffold.



Figure 55 The hanging pendulum concept

1. In **Figure 56** a first suggestion of the scaffold used to connect the plate and the pendulum hammer to the environment can be seen. The cables are not illustrated but the idea is that there would be one cable per corner of the plate that connects to respective corner of the highest rectangle of the scaffold.
2. The cables earlier mentioned can have their connection point on the scaffold moveable which allows for impact location adjustment.
3. The cables need to allow the plate to be hoisted. The leftmost of the pictures of **Figure 56** shows the IP configuration and the other two the OOP configuration. To alter between the two the cables closest to the hammer needs to be shortened while the other two needs to be lengthened.
4. Since the plate is hanging it is straightforward to reach the underside of the plate to mount the specimen.
5. The scaffold is designed so that gravity will hold the plate against the two vertical beams on the sides of the hammer and this is the aligned position.

Table 8 Apparent advantages and disadvantages

Advantages	Disadvantages
+ Only one hammer design	- Have to hoist up/down plate for IP/OOP configuration
+ Mounting of test specimen is not a problem	- Alignment might be a hard nut to crack

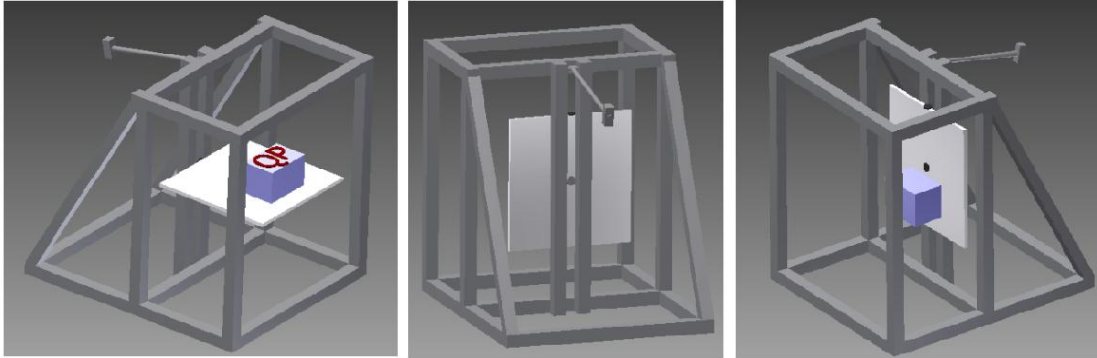


Figure 56 Hanging pendulum concept, a) In plane configuration and b) c) Out of plane configuration

### 2.5.2 Foam pad pendulum

The foam pad pendulum concept also uses a pendulum hammer but instead of hanging the plate is resting on a foam pad.



Figure 57 The foam pad pendulum concept

1. The resonant plate is resting on a foam pad on a table. As can be seen in **Figure 58** an edge or side rail goes all around the table and on this adjustable rubber blocks will be inserted. The rubber blocks can if necessary “clamp” the rigid body movement of the plate.
2. The side rails will give the plate enough margins to move so that the impact location can be adjusted.
3. There are two different configurations of the pendulum hammer that allows the concept to use both IP and OOP excitation. For the IP configuration the pendulum hammer is mounted at the top of the vertical beams and for the OOP configuration it is mounted at the bottom. Note that only half the charge height of the IP configuration can be reached in the OOP configuration.
4. Since the QuadPack needs to be fastened from the opposite side of which it is mounted this is a problem for the foam pad resting solutions. The plate either needs to be lifted up or the table plate needs to be opened to allow access.

- Before every excitation the plate is pushed towards the formerly mentioned rubber blocks that will assure that the setup is aligned as required. If the rubber blocks are used to “clamp” the plate no re-alignment is required between excitations.

Table 9 Apparent advantages and disadvantages

Advantages	Disadvantages
+ Can be “clamped”	- Configuration change between IP and OOP
+ Only one hammer design	- Requires solution/configuration for mounting specimen
	- OOP configuration can only reach half the height of the IP configuration

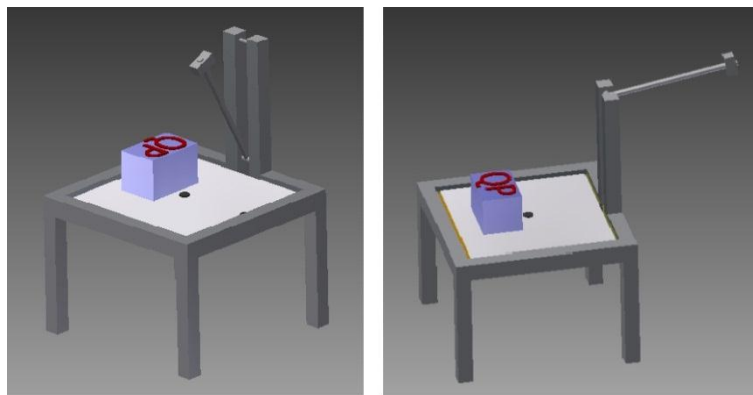


Figure 58 Foam pad pendulum concept a) OOP configuration b) IP configuration

### 2.5.3 Hammer combination

The hammer combination concept is similar to the foam pad pendulum but uses a pendulum hammer for the IP excitation and a drop hammer for the OOP excitation.

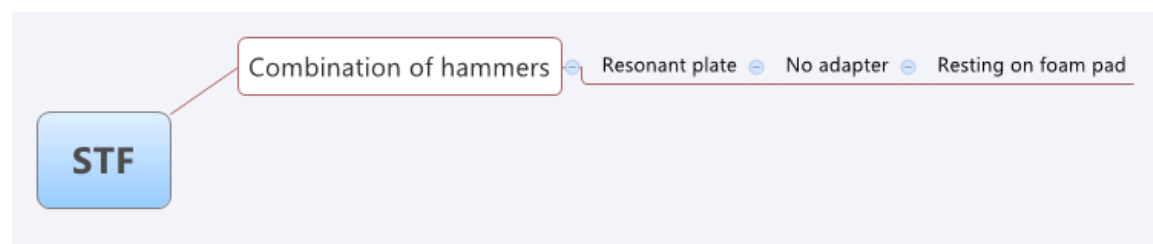


Figure 59 The hammer combination concept

- As for the former concept the resonant plate is resting on a foam pad on a table. The same type of side rail goes all around the table and also has the adjustable rubber blocks. The rubber blocks can if necessary “clamp” the rigid body movement of the plate.
- The side rails will give the plate enough margins to move so that the impact location can be adjusted.

3. No configuration change is required. For IP impact the pendulum hammer is used and for OOP impact the drop hammer is used. To make the STF cost efficient it would be best if it is possible to use the same hammerheads and interchangeable masses for both hammers so the requirements on them will be more extensive.
4. The same problem as for the foam plate pendulum is present here but since the drop hammer obstructs the possibility to lift the plate there must be a hole in the table or a mechanism to open it downwards.
5. It will be solved in the same way as for the foam pad pendulum. Before every excitation the plate is pushed towards the rubber blocks that will assure that the setup is aligned as required. If the rubber blocks are used to “clamp” the plate no re-alignment is required between excitations.

Table 10 Apparent advantages and disadvantages

Advantages	Disadvantages
+ Can be “clamped”	- Needs two hammers
+ Only one setup, no configuration change between IP and OOP	- Requires solution/configuration for mounting specimen

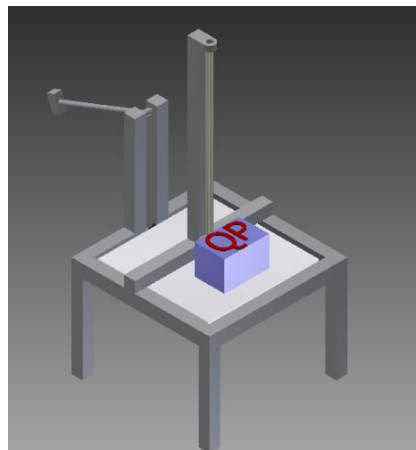


Figure 60 Hammer combination concept

#### 2.5.4 Numerical trade-off and the final concept

A finalist concept review meeting was held with various people at ISIS to select the final concept. The concepts advantages and disadvantages were discussed and the criteria for the trade of process were determined. A numerical trade off method was used to give some guidance but care should always be taken when using such methods. The incentive is to get an unbiased result but the risk is that it becomes a way of covering up a subjective view in numbers. Reason and sound logic should always stand behind the decisions.

A list of possible requirements and arguments that could distinguish between the three concepts was suggested. Some requirements and arguments were eliminated and split up and the survivors were used as criteria. These criteria were discussed and given a weight depending on their importance. The concepts were given scores depending on how well they were believed to implement the criteria in comparison to each other. The result of the numerical trade of process can be seen in **Table 11**.

Table 11 Results from numerical trade-off

Requirement/ Argument	Weight 1 – 5	Hanging Pendulum	Hanging Score	Foam Pad Pendulum	Foam Pad Score	Hammer Combination	Combination Score
Repeatable	5	1	5	2	10	2	10
Documentable and adjustable parameters	4	2	8	1	4	2	8
Sustainable	2	2	4	2	4	2	4
Short time for one test cycle	3	1	3	2	6	3	9
Enable future development	3	1	3	2	6	2	6
Low life-cycle cost	5	2	10	2	10	2	10
Simple configuration change	4	1	4	2	8	3	12
Easy to mount specimen	3	2	6	2	6	2	6
Easy to assemble/disas semble	1	1	1	3	3	2	2
Easy to manufacture	2	1	2	2	4	1	2
<b>Total</b>			46		61		69

Based on these results the Hanging pendulum concept was selected to be deleted. For every criterion one of the other concepts were believed to implement it better or just as good.

The Hammer combination scored higher than the Foam pad pendulum in the trade off table but not enough to make the decision indisputable. The two last concepts are similar in their design since the resonant plate is resting on the same type of table. The differences are that the Foam pad pendulum has a moveable pendulum hammer, i.e. with two attachment locations (for IP and OOP), and the Hammer combination has an additional drop hammer. With this in mind the Foam pad pendulum could easily be developed into the Hammer combination with the addition of a drop hammer in the future. For this reason the Foam pad pendulum was selected as the concept that was to be developed further as the final concept and the Hammer combination was to be put aside as a potential for future development.

The final concept Foam pad pendulum can be seen in *Figure 58*. As the name implies it uses a pendulum hammer as an impactor both for the IP and OOP configuration and the plate is resting on a foam pad. Some of the important design features were the implementation of the mounting of the hammer on the rig and the flexibility of the hammer itself, but more on that in the next section.

## 2.6 Design process

The design process is the process of developing the final concept into a system detailed out to a level where it can be manufactured and where it can be said with confidence that the STF can implement the parameters from *Table 7*.

The design process is iterative. The different parts are dependent on each other, on the general knowledge of the STF and on the requirements. As these evolve the design will also evolve. The evolutions of the different parts are shown in this section. Throughout the design process Autodesk Inventor has been used as CAD software to bring the ideas from mind and paper to virtual prototypes.

### 2.6.1 Plate

The specimen location on the plate was selected to be kept constant while the impact location was selected to be variable. In the first round the plate was designed with 28 holes for the different mounting patterns of the QuadPack at the specimen location and two holes per impact location for fastening of the anvil plate. The anvil plate was later updated to a design with four holes which meant two more holes per impact location. Another mounting pattern was added for the specimen location.

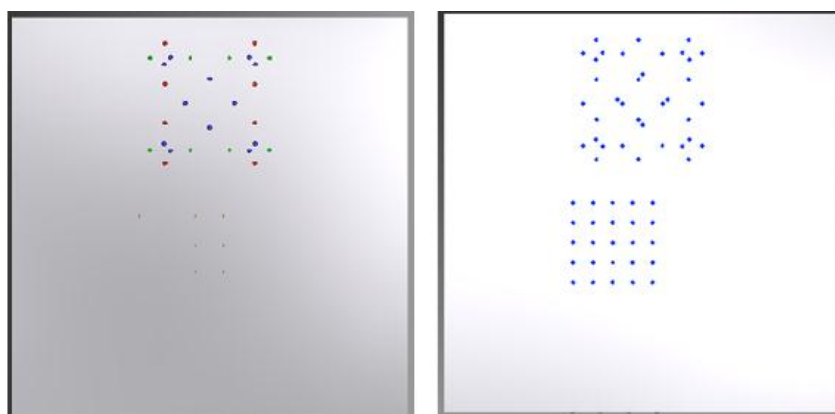


Figure 61 Plate with holes for assembly a) Design 1 b) Design 2

### 2.6.2 Anvil plate

The anvil is the sacrificial part that will take that direct impact of the hammer. The first design was of a small 7 x 7 x 1 cm metal plate that was to be fastened with two fasteners on either the big side of the resonant plate or on the edge for the IP impact. It was after a review meeting updated to a version with four holes, see *Figure 62*.

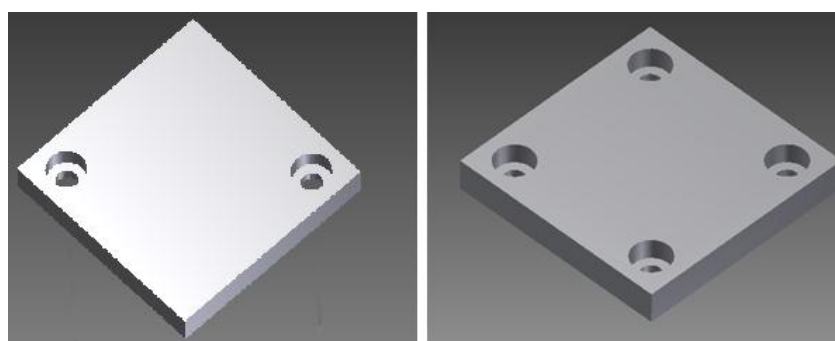


Figure 62 Anvil plate a) Design 1 b) Design 2

### 2.6.3 Hammerheads

The hammerheads are the realisation of the interchangeable impact surface. The first design was made with threaded pins for fastening on the rest of the hammer but this was later revised to make the hammerhead easier to manufacture. The second design had holes and used standard fasteners so no weldment were required, see *Figure 63*.

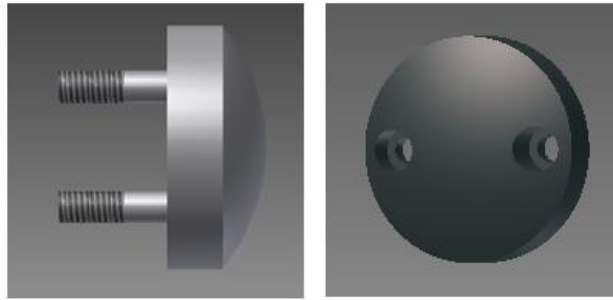


Figure 63 Hammerhead a) Design 1 b) Design 2

#### 2.6.4 Hammer masses

The interchangeable hammer masses were in the first idea made as four cylinders weighing 1, 2, 3 and 4 kg respectively. This could span 0 – 10 kg in steps of 1 kg by adding the masses in different combinations. The hammer masses were thought to be cheap so when the requirements were updated the first design that reached assembly was another. It consisted of five different masses as cylinders with different diameters that could be attached to the rest of the hammer. With this setup all the masses had the same required length of fastener. To push the price of manufacturing down the design was later updated to five 2 kg masses that can be added to the hammer in steps.

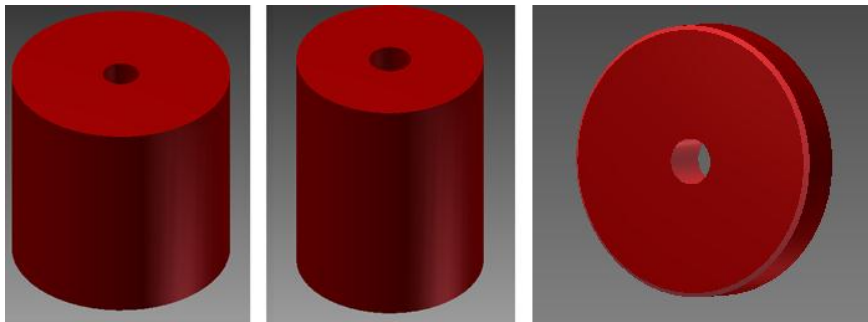


Figure 64 Hammer masses ab) Design 1 c) Design 2

#### 2.6.5 Hammer arm and connector

The hammer arm and the connector are the parts that have had the longest evolution chain. The first design was an integrated arm and connector that connected the hammerhead, the mass and the rest of the rig, see *Figure 65*. This part was later split up into hammer arm, hammer connector and bearing solution.

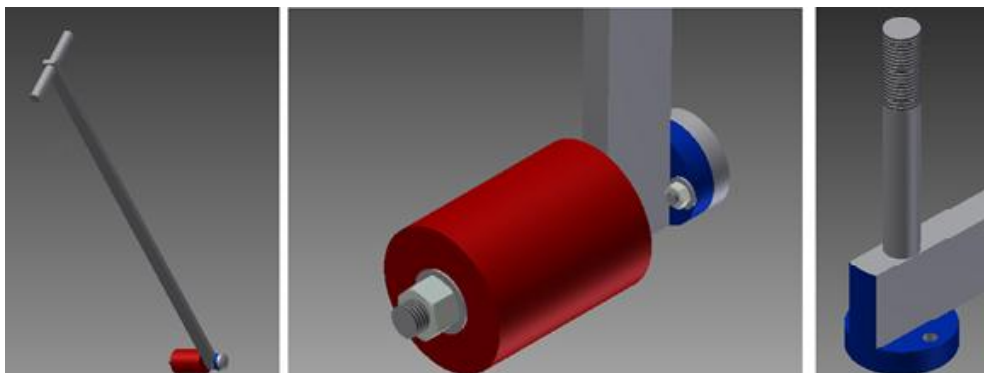


Figure 65 Hammer arm and connector, design 1

### 2.6.5.1 Hammer arm

The length of the hammer is the parameter that limits the impact velocity of the STF. The initial plan was to have a 90 cm long arm but since the charging height in the Foam pad pendulum only reaches half the height potential of the IP configuration in the OOP configuration it was decided that the arm should be longer. 150 cm was selected which limits the maximum impact velocity to 5.4 m/s OOP. It does thus not reach the initially sought 6 m/s but it should still more than enough [24].

Making the hammer arm longer will also make it more pliant. Plastic deformation can be a problem in the long run but with the short scope there are additional hurdles. The arm should transport as much of the kinetic energy in the hammer as possible to the resonant plate but if the arm is too weak energy is wasted in exciting the bending modes of the arm. Thin walled beams have very high bending stiffness to cross-section area ratio and they are generally available at manufacturers. The second design of the hammer arm was made with thin walled beams with circular cross-section.

Another update to the hammer arm was that the shaft that connects the arm to the rest of the rig was made longer. If the bearings have a small misalignment on the rig then the influence of it on the arms movement will be smaller the longer this shaft is. The longer shaft also allows for two extra beams to be attached to the arm to stiffen the design. The second arm design can be seen in *Figure 66*.



Figure 66 Hammer arm, design 2

### 2.6.5.2 Hammer connector

The first separate design of the hammer connector can be seen in *Figure 67*.

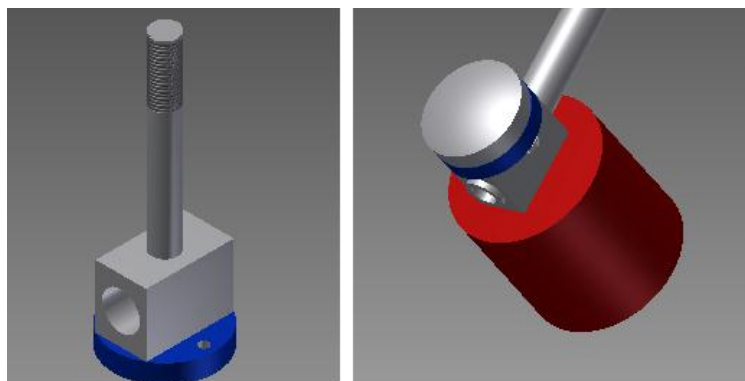


Figure 67 a) Hammer connector, design 2 b) Hammer assembly, design 2

This was, however, an unnecessarily complex solution to manufacture so the design was updated to a design that required no weldments. The hammerhead and the hammer masses are here fastened with standard fasteners instead of attached pins. The third hammer connector design can be seen in *Figure 68*.

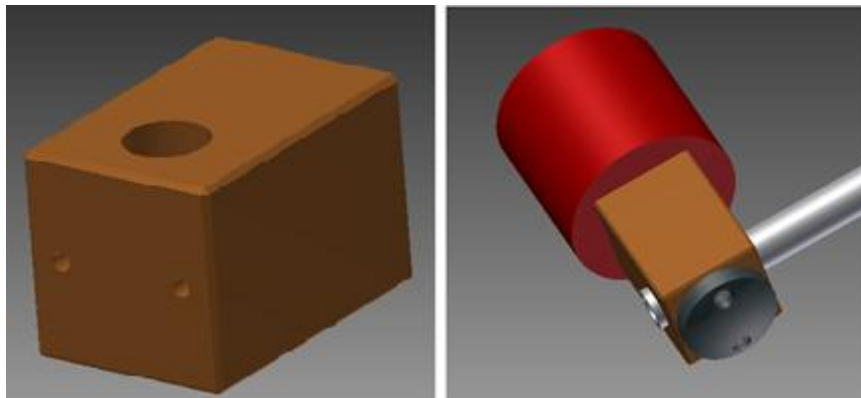


Figure 68 a) Hammer connector, design 3 b) Hammer assembly, design 3

### 2.6.5.3 Bearing solution

To connect the hammer arm to the rest of the rig a bearing solution was designed. It is this part that allows the hammer to be moved between the IP and OOP configuration without resetting the arm in the bearings. Ball bearings are used and a plate where the angle of the hammer can be seen was added. This plate is used to make sure that the same height can be reached for consecutive shocks which provides repeatability.

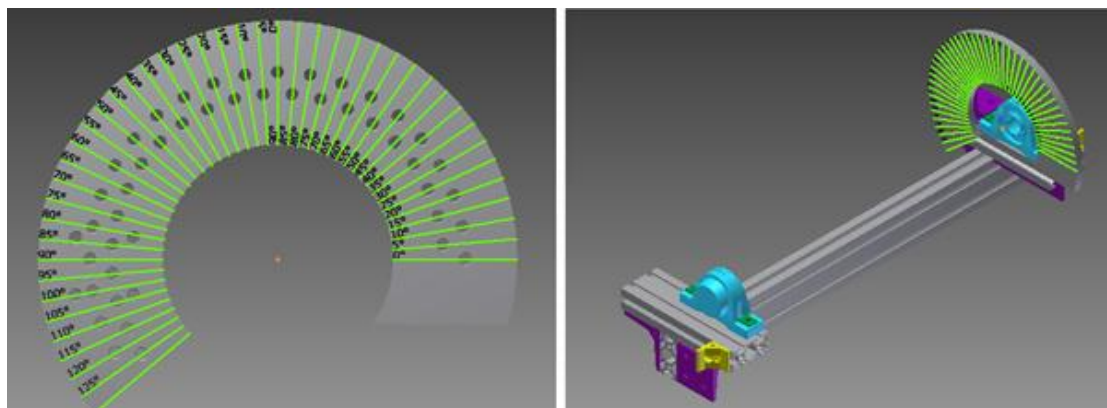


Figure 69 a) Charge angle plate to provide repeatability b) Bearing solution

Note the type of beam used for the bearing solution in *Figure 69* b). This is an extruded aluminium profile called MK-profile which has been used for the main structure of the STF called the rig.

### 2.6.6 Rig

The rig is the structure that will support the plate and hammer and allow the function of the shock test facility. It has been designed with MK-profile which makes it easy to assemble, gives it a short lead time and allows it to be developed further indefinitely. The structure can be adjusted to meet future needs and gives high flexibility.

Before implementing the MK parts, however, a sketch was made to check the dimensions, see *Figure 70*.

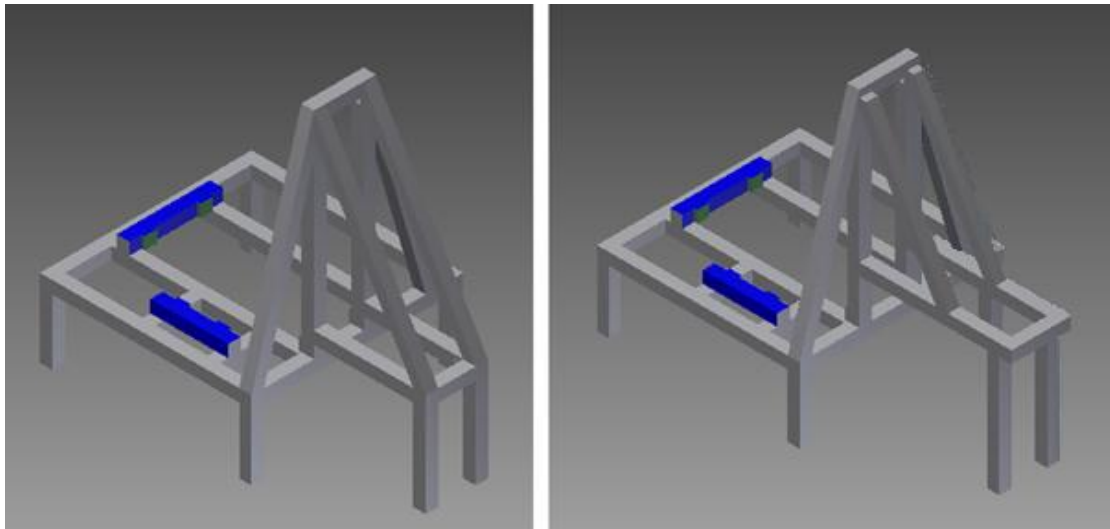


Figure 70 a) Table sketch 1 b) Table sketch 2

After a test assembly of the first table sketch it was selected that the hammer should be attached to vertical beams. This so that its vertical position can be easily adjusted which makes the characteristics of the foam that the plate rests on less crucial. A new sketch was made and the dimensions and interferences were examined. In the MK catalogue the angles available between beams are 30, 45, 60 and 90 degrees. The fastenings between the MK beams are done with special nuts that make them rigid. The rig converted to MK parts can be seen in **Figure 71**. The horizontal beams of the table that the plate will rest on are positioned such that the holes in the plate can be reached from below.

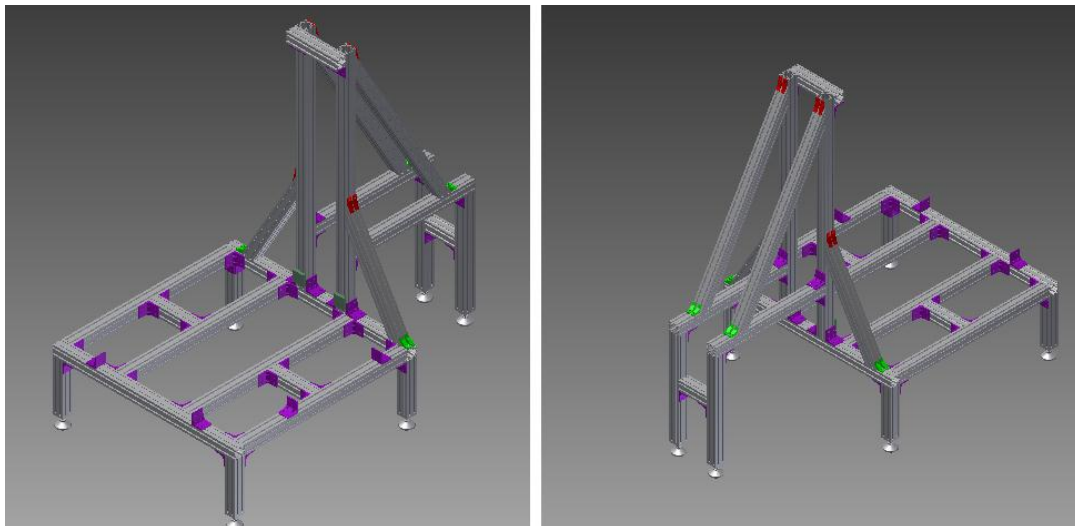


Figure 71 MK table rig, design 1

When the design changes were implemented in the other parts an update was also required on the rig. More space was required between the high vertical beams and thus the stabilising side beams had to be moved to the inside of the vertical beams, see **Figure 72**. A permanent corner into which the plate can be pushed to ensure alignment was also added.

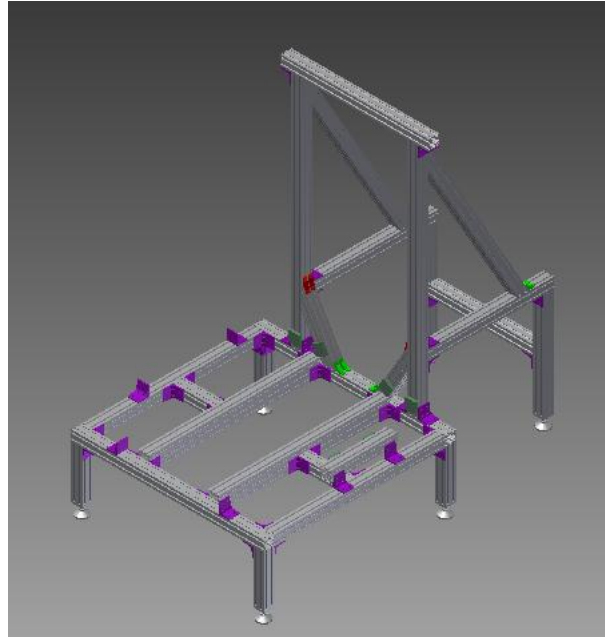


Figure 72 MK rig, design 2

### 2.6.7 Assembly

The assembly for both the IP and OOP configurations can be seen in *Figure 73*. The blue beam's positions are adjustable and they set the alignment position of the plate when it is not in the default position which is the opposite corner to the one the blue beams define. The foam pads that sit between the plate and the beams cannot be seen in the figure. The characteristics of the foam are important since they constitute the boundary conditions of the plate and could have an effect on the results. It was, however, not used as a design parameter where the characteristics were simulated to find an optimum from which perfect foam was manufactured. Foam is cheap so different types were purchased and their influence tested. This could subsequently be used as a tuning parameter.

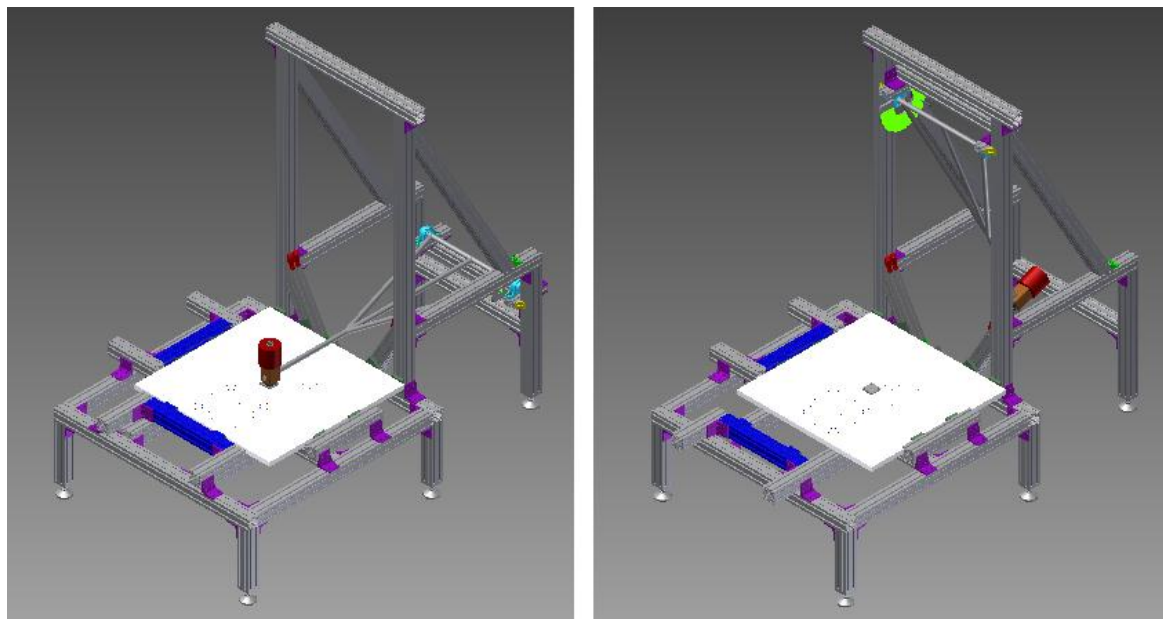


Figure 73 Final design STF a) OOP configuration b) IP configuration

### 3 Research and Development Process Results

This chapter concludes the research and development phase of the project and introduces the characterisation test campaign of the actual STF. It also brings up the data acquisition chain that is an important part of any STF.

#### 3.1 Final design, parameters and range

The final design of the STF can be seen in *Figure 73*. The materials of the different parts were selected from the simulated characteristics together with the availability of the materials at the manufacturers. The final STF parameters and their implemented ranges can be seen in *Table 12*.

Table 12 Final parameters and their range

Parameter	Constant	Continuous variable	Discrete variable	Value/Range
Plate dimensions	X			1 x 1 x 0.03 m Al6082
Specimen location	X			See <i>Figure 61</i>
Impact location			X	See <i>Figure 61</i>
Impact velocity		X		0 – 5.4 m/s OOP 0 – 7 m/s IP (1.5 m arm)
Anvil material			X	Al6082, Al7075, SS304
Hammer mass			X	0 – 10 kg, steps of 2 kg
Foam type			X	Three types of different composition (material, stiffness, thickness )
Hammerhead material			X	SS303, SS630
Boundary conditions			X	Clamped or free

#### 3.2 Expected results

From the simulations of the shock and from the research process there were certain performances that were predicted to be seen for the actual STF in the characterisation test campaign.

As shown in Section 2.4 there are some characteristic behaviours that can be controlled in different ways. The knee frequency, see the plus sign in *Figure 74*, is set by the plate dimensions and was therefore predicted to remain constant when most of the other parameters were altered. The parameters excepted from this rule were predicted to be a shift between the IP and OOP configuration, exchange of foam pads and clamping/unclamping of the plate. This is because these parameters alter the boundary conditions of or the dominating wave type in the plate.

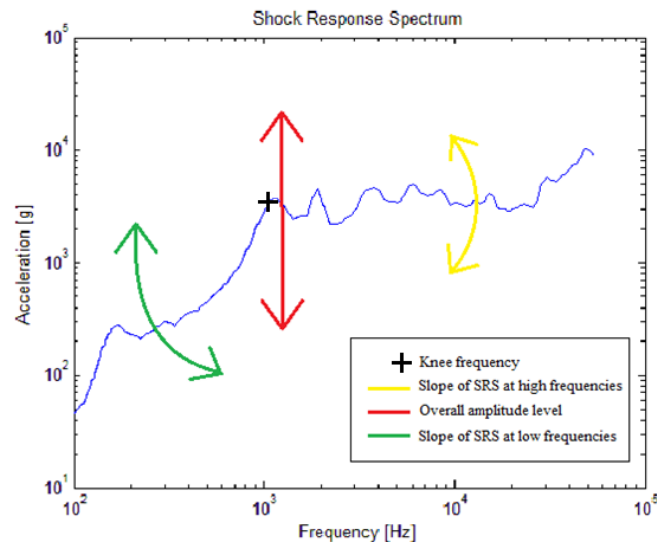


Figure 74 Predicted behaviour of STF. The slope over and under the knee frequency as well, as the overall amplitude level, are expected to be controlled by different parameters

The overall amplitude of the SRS was predicted to be controlled by the impact velocity which in turn is set by the height of the hammer when it is released. The higher the impact velocity the higher the amplitude levels will be.

With the accurate knee frequency set and the accurate overall amplitude level reached the SRS has two more features that can to be adjusted, namely the slope of the SRS curve for the high frequencies over the knee frequency and the low frequencies under the knee frequency respectively. The simulations showed that the slope of the curve for the lower frequencies could be adjusted by altering the weight of the hammer. A heavier hammer gives a SRS with higher shock levels at the lower frequencies. For the higher frequencies on the other hand it was the material of the hammerhead and the anvil that were predicted to influence the slope of the SRS. The simulations gave results indicating that using a stiffer anvil material gave higher amplitude levels for the high frequencies.

For the impact location no consistent rule could be defined for the behaviour so the testing for this parameter was more of an experimental nature than verification testing. The same was true for the testing of the different foam pads and the different ways of clamping the plate.

It was predicted that it would be more difficult to reach all requirements in the IP configuration but that it should be possible to tune the results within the tolerances. The results from the characterisation test campaign can be found in Section 4.2.

### 3.3 Data acquisition chain

The DAQ chain consists of:

- Shock sensor
- DAQ hardware
- DAQ software

- Data handling system

The DAQ system is an important part of the STF. If the physical STF is the body and the muscles, the DAQ chain is the brain and the senses. A STF is not useful if it is not possible to measure the shock environment it produces.

One of the requirements on the STF was that the data handling system shall be a standard laptop which was implemented without issues. The other parts of the DAQ chain are described below.

### 3.3.1 Sensor

The selection of the sensor is very important for the DAQ chain to function properly. Accelerometers are most common in industry for shock measurements [3] but other methods, such as Laser Doppler Velocimeters, are also used.

A known problem in high shock measurement is zershift, see *Figure 75*. Care should always be taken to minimise the presence of this phenomenon.

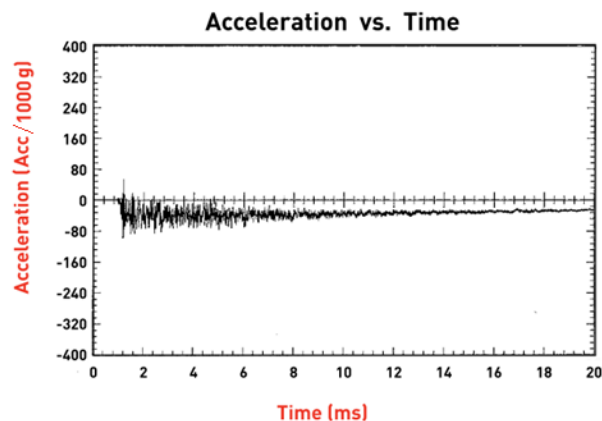


*Figure 75* Zershift of shock signal [40]

The zershift is a shift of the mean acceleration from zero. It can be both positive and negative and of an unpredictable amplitude. Six causes of zershift have been identified [41]:

- Overstressing of sensing elements
- Physical movement of sensor part
- Cable noise
- Base strain induced errors
- Inadequate low frequency response
- Overloading of signal conditioner

If zershift is identified in the measurement the data should not be used and the source should be identified. If the zershift cannot be seen in the acceleration time history it can still be identified as an erroneous slope of the SRS curve in the low frequency region [3] or as a significant difference between the positive and the negative SRS [9].

The best method to minimise zershift is prevention and the best prevention is to use a high quality accelerometer. What type of accelerometer that is suitable depends on the shock environment that it is supposed to capture. For mid-field shock levels, piezoelectric accelerometers with integrated electronics are suitable [3]. These accelerometers are called IEPE accelerometers and have built-in signal conditioning circuits.

The accelerometer that was selected for the STF was a PCB 350C02. It is an IEPE (ICP for PCB accelerometers) sensor that is designed to measure shock up to 50000g. It has a built-in mechanical filter which makes it practically impossible to excite its resonance frequency, something that otherwise can be a considerable problem. It was compatible with both the DAQ software and the DAQ hardware. The PCB 350C02 is used for shock measurements throughout industry [23] and [24] and has been called the best one that exist at the moment [26].

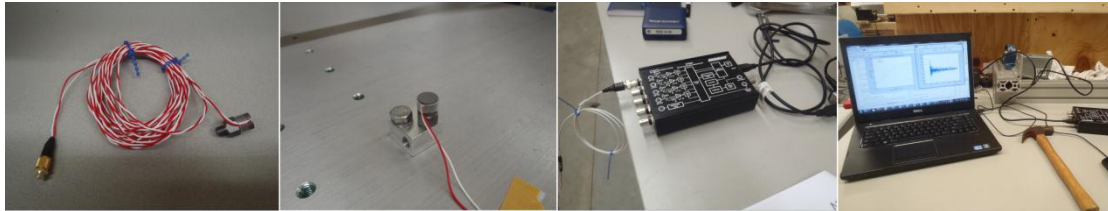


Figure 76 a) Sensor b) Sensor cube c) DAQ-module d) Initial software tests

### 3.3.2 DAQ hardware

With the DAQ hardware it is important to make sure that it is compatible with the sensor and that it can sample at a rate that is high enough to capture the high frequency behaviour of the shock. The sampling rate should be at least seven times higher than the highest frequency of interest in the SRS but it is recommended to use a sampling rate that is ten times higher. The highest frequency of interest in the SRS for a mid-field environment is 10 000 Hz which puts the recommended sampling frequency at 100 000 Hz [3].

The DAQ hardware selected for the STF is the Data Translation signal acquisition module DT9837. The module is adapted for IEPE accelerometers and its only power source is a USB connection to a computer. DT9837B can sample at 105 400 Hz which is more than enough for mid-field shock measurement. As a first step a DT9837 module was used. Its maximum sampling rate is 52 700 Hz so it does not reach the recommended values for the frequencies over 7000 Hz. It does, however, show the compatibility of the system and how a data acquisition chain can be accomplished without expensive modules and software.

### 3.3.3 DAQ software

Another reason for selecting the DT9837 module was that Data Translation has a free to download adaptor for Matlab that works together with Matlab's Data Acquisition Toolbox. Matlab and the DAQ Toolbox can together with the adaptor control and acquire information from the DT9837 and the sensor. With this information the full power of Matlab can be used to post-process the results such as plot graphs and calculate the SRS.

A Matlab program was written that saves the acceleration and time data when a shock occurs and automatically plots the acceleration time history and calculates and plots the SRS. In addition to the maximax SRS, the positive and negative SRS are also plotted. This is to make sure that the measurement did not see any zershift and that the requirement that the positive and negative SRS should lie within 3 dB of each other is fulfilled. Another program was written to simplify the characterisation test campaign by making comparison between shock results or between a shock result and requirements fast and easy.

## 4 Shock Test Facility Results

A characterisation test campaign was held to examine the actual performance of the STF and establish its capacity. To do this, however, the STF first had to be assembled.

### 4.1 Actual shock test facility

The STF was assembled in steps since the parts were manufactured at different firms and had different delivery dates. The standardised MK parts were delivered first and required the longest assembly time. No major issues were met during the assembly process of the MK parts. The custom made parts also required some assembly since the hammer arm had to be attached to the rig with the bearing solution. The custom parts were manufactured according to the drawings and everything fitted well together. Some pictures from the assembly process can be seen in Appendix F – Assembly of STF.

The fully assembled STF can be seen in *Figure 77*. The alignment and motion of the hammer was good and the impact location adjustable. See *Figure 73* to compare the actual assembled STF with the final design.

The STF was named THOR, Testing Hammer for extraOrdinary Rough environments.

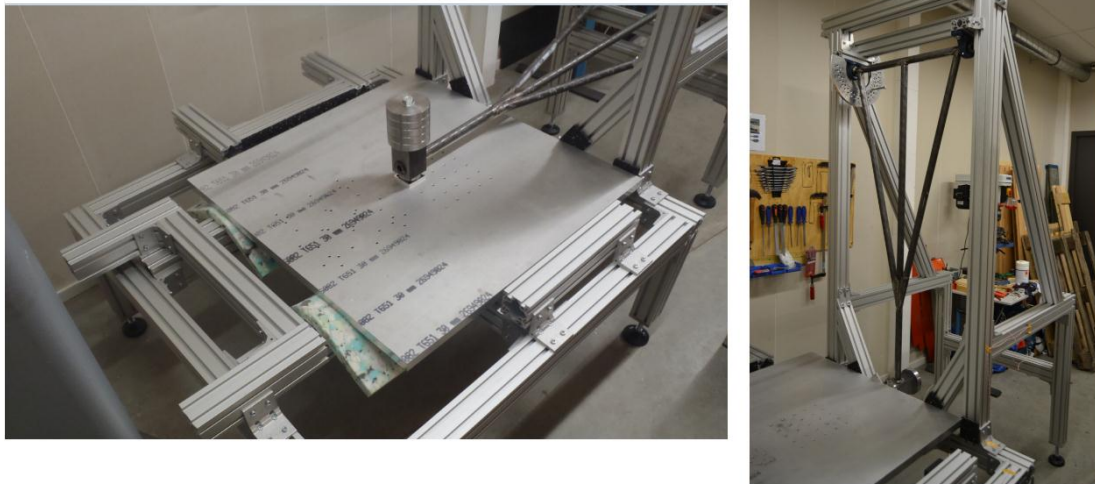


*Figure 77* Fully assembled STF in a) OOP configuration b) IP configuration

### 4.2 Characterisation test campaign

In section 3.2 the expected results of the characterisation test campaign were reviewed. With the actual STF in operation it was time to see how well it could perform. The characterisation test campaign is one of the most important phases in the development of a STF. The true influences of the parameters were measured and experience was gained on how to use them to tune the SRS.

One of the first lessons learned were that screws that are not fastened tight will come loose from the shock. This applies to the anvil, the hammerhead, the hammer masses, the test specimen and even the sensor so it is important to double check that nothing is loose over time. Another issue is the sound level of the STF. Hearing protection must be used and if possible testing should be done outside office hours.

Before starting to test the parameters the repeatability of the STF had to be asserted.

### 4.2.1 Repeatability

For the STF to be repeatable it needs to give identical results for consecutive shocks with the same initial settings. Identical in this sense means that the SRSs shall lie within 1 dB of each other. The repeatability of the STF is a very important parameter. If the facility is not repeatable no other result is reliable. It becomes practically impossible to know if an effect shown for a parameter change is truly caused by the parameter change or just by the inherent variability of the setup. The first tests were therefore carried out with the same settings on all parameters. This configuration was named the benchmark (BM) configuration.

Parameter	Benchmark configuration
Impact velocity	15°
Hammer mass	0 kg add-on
Anvil material	Medium, Al7075
Hammerhead material	Soft, SS303
Impact location	Centre
Foam type	Soft
Boundary conditions	Free
Mass dummy	No dummy
Impact direction	OOP

The results of the repeatability tests can be seen in *Figure 78*. The results were very positive with very small discrepancies between the consecutive shocks well within the required 1 dB.

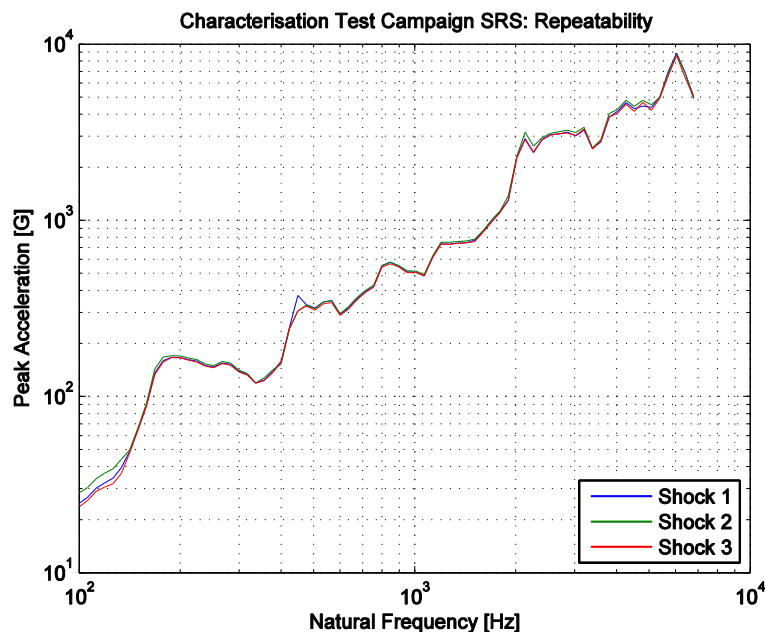


Figure 78 Repeatability of three consecutive shocks

There was no apparent knee frequency in the SRS but before addressing this issue the test campaign was carried on since the answer was thought to be found in some of the several parameters and this would most effectively be examined by continued testing.

Knowing that the STF gives repeatable results it was possible to continue with the characterisation testing of all the other parameters.

The parameters whose influences were tested were:

- Impact velocity
- Hammer mass
- Anvil material
- Hammerhead material
- Impact location
- Foam type
- Boundary conditions of resonant plate

In addition to these parameters the STF was also be tested for:

- Influence of mass dummy
- OOP/IP shift in impact direction
- Influence of mechanical filters

With all these parameters it would take more than 90 000 shocks to test all configurations. It was not feasible to do that many tests so to bring the number down the benchmark was used and the influence of the different parameters were tested by altering them one by one. The influence the parameter change had on the SRS was found and this behaviour was assumed to be present for all other configurations. There were a few exceptions from this rule, namely the IP and OOP configuration shift and the usage of a mass dummy. The shift between IP and OOP configuration was expected to alter the SRS significantly so the STF was tested for both configurations thoroughly. The behaviour of the STF when using a test specimen mass dummy was also thoroughly examined.

#### **4.2.2 Impact velocity**

The impact velocity is a continuously variable parameter but to impose some structure on the testing it was tested in discrete steps. The impact velocity is controlled by the drop height of the hammer. The maximum height is around 1.5 m in the OOP configuration and around 3 m in the IP configuration. The BM was in the OOP configuration so it was in this configuration that the initial tests were held.

The STF is equipped with a system to ensure that the same drop height can be used for consecutive shocks. It is, however, not graded as height in meters but instead as the angle of the pendulum hammer arm, see *Figure 79*.



Figure 79 Charge angle plate in a) OOP configuration b) IP configuration

The BM for the impact velocity was a charge angle of  $15^\circ$ . In this test round the levels tested were:  $15^\circ$ ,  $30^\circ$ ,  $45^\circ$ ,  $65^\circ$  and  $75^\circ$  ( $\approx 1.7$  m/s, 3.4 m/s, 4.2 m/s, 4.9 m/s and 5.3 m).

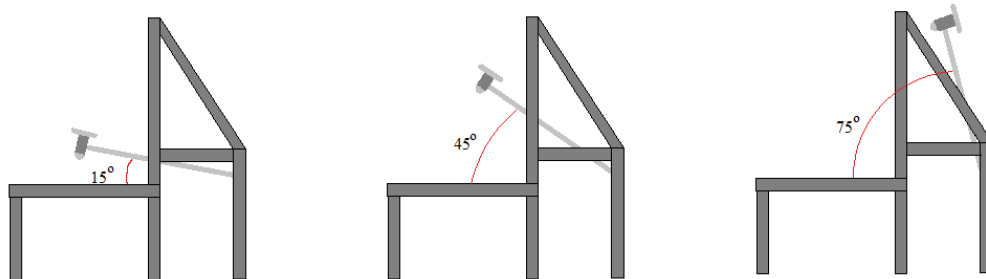


Figure 80 STF with different charge heights  $\rightarrow$  different impact velocities

The expected results were that the shape of the SRS would stay constant while the overall shock level would rise when the drop height was increased. This was confirmed by the results, see **Figure 81**. The step in the SRS was much larger for  $15^\circ \rightarrow 30^\circ$  than for  $60^\circ \rightarrow 75^\circ$ . The reason for this is partly the logarithmic scale and partly the circular trajectory of the hammer. The step  $15^\circ \rightarrow 30^\circ$  is larger in height difference than  $60^\circ \rightarrow 75^\circ$  and the difference in impact velocity is therefore naturally larger.

In general the shock levels were achieved at higher velocities than in the simulations. This was expected since the impact velocities in the simulations were surprisingly low. To go for extra potential in the drop height was a good decision.

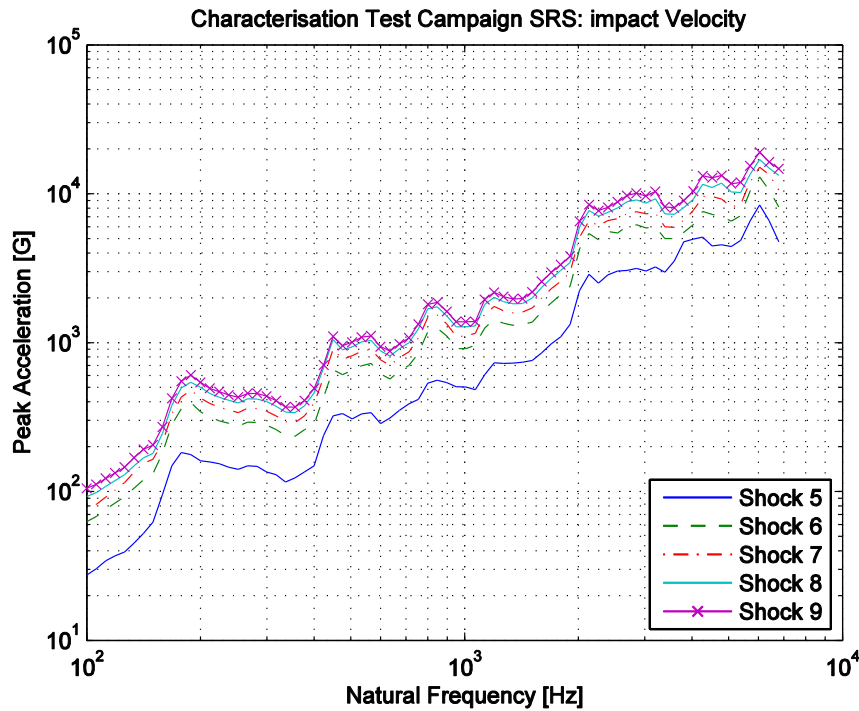


Figure 81 Influence of Impact velocity

### 4.2.3 Hammer mass

The hammer has a “naked” mass which is the minimum mass it has without any add-on masses. There are five add-ons each weighing 2 kg which can be added in steps. The BM was without any add-on masses. The configurations tested were: 0 kg, 2 kg, 4 kg, 6 kg, 8 kg and 10 kg.

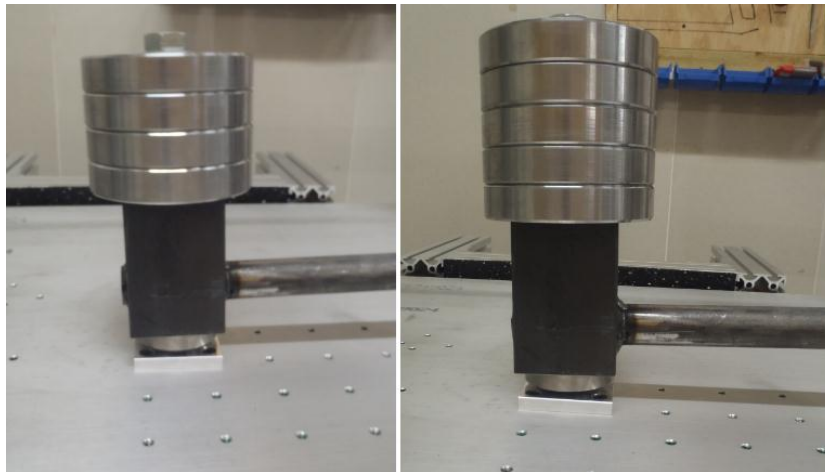


Figure 82 Hammer with attached extra mass a) 8 kg b) 10 kg

The expected result was that an increase in hammer mass would have an effect on the frequencies under the knee frequency in the SRS. With a heavier hammer the shock levels should get higher for the lower frequencies which in effect straightens out the SRS curve.

This effect was confirmed by the results as can be seen in *Figure 83*.

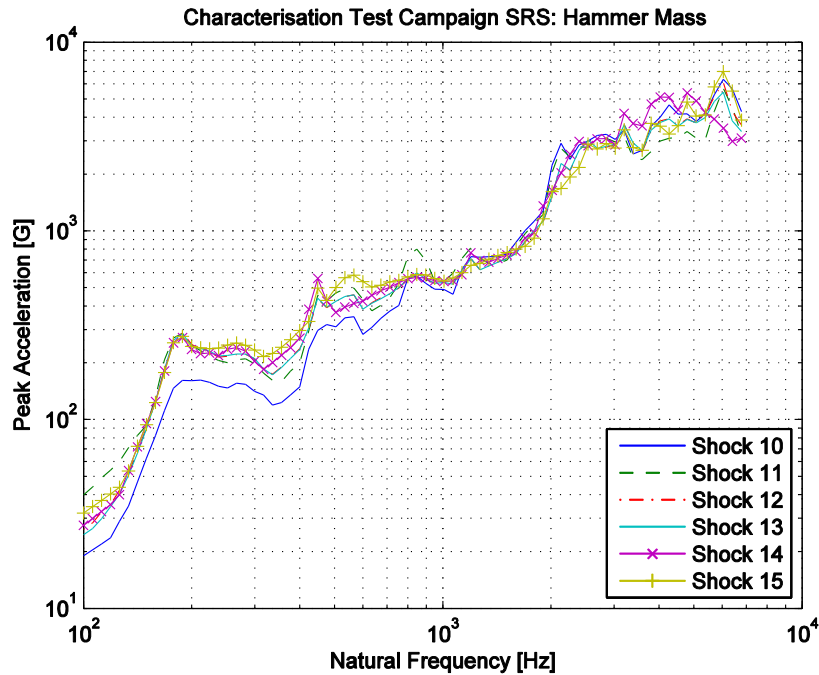


Figure 83 Effect of increasing hammer mass

The effect was also here much more evident for the initial step 0 kg→2 kg than for the subsequent steps. For the last two steps, 6 kg→8 kg and 8 kg→10 kg, this difference was not apparent at all. The difference was here rather that the heavier hammers excite a mode at around 550 HZ more and had lower shock levels for the highest frequencies in the SRS. Another trend picked up was that the difference between the positive and the negative SRS was growing with the hammer mass. This is an unwanted behaviour since there is a requirement on the similarity of the two curves.

#### 4.2.4 Anvil material

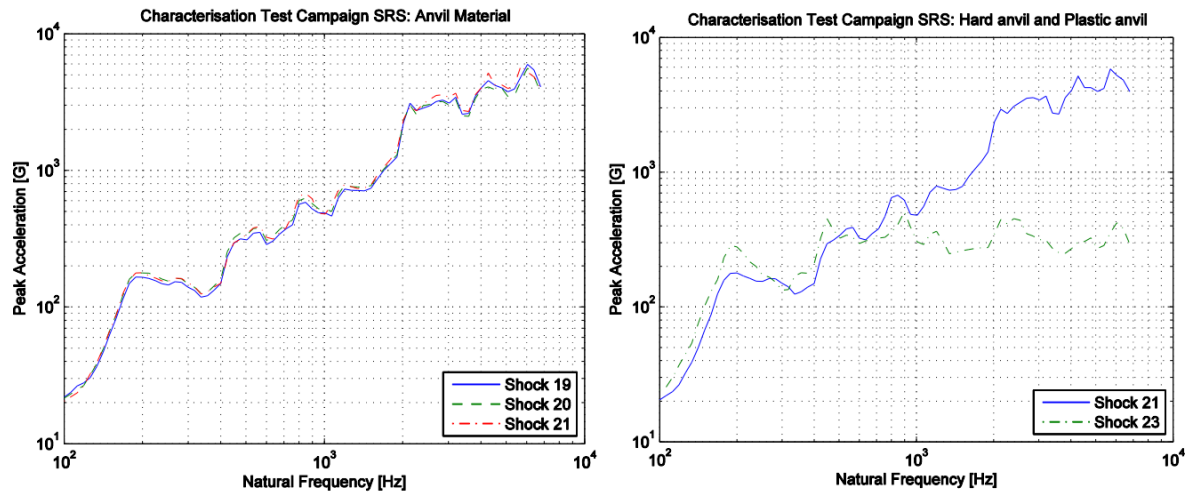
The anvil plate was manufactured in three different materials. They range from the “Soft” Al6082, over the “Medium” Al7075, to the “Hard” stainless steel SS304. The medium anvil Al7075 was selected for the BM configuration instead of the softest one since it got more shocks than the other two and a softer anvil is more prone to deformation. All the three anvils were tested: Medium, Soft and Hard.



Figure 84 Anvil plates in three different materials

The expected result was that the anvil material would influence the SRS for the frequencies over the knee frequency. The shock levels were expected to be higher for the harder anvil and lower for the softer material. The results were somewhat disappointing since the results for the two aluminium plates were almost identical and only marginally higher for the stainless steel anvil, see **Figure 85 a)**.

One reason for the unexpected result could be that the anvil materials are too similar. Larger extremes should give larger differences. An anvil in a hard polymeric material was manufactured and tested to strengthen this point, see **Figure 85 b)** for the results. The shock levels were higher for the lowest frequencies but the impact could not excite levels over 500 g even for the highest frequencies.



**Figure 85** a) Influence of anvil material b) Influence of anvil in plastic material

Another way of altering the impacted surface is by adding mechanical filters, such as papers or foam, to the anvil. The effect of adding a pile of 9 papers to the anvil as a mechanical filter can be seen in **Figure 86**. The shock levels were lower overall but the difference is more significant for the higher frequencies.

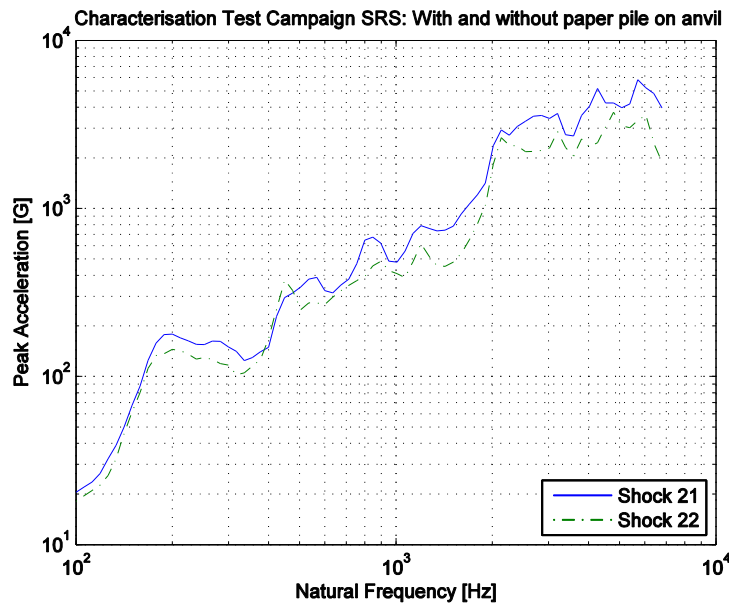


**Figure 86** Influence of mechanical filter on anvil

## 4.2.5 Hammerhead material

The hammerheads were manufactured in two materials, the “Soft” SS303 and the “Hard” SS630 which was treated with a hardening process. The softer hammerhead was used in the BM. Both hammerheads were tested: Soft and Hard.

The expected results were similar to those for the anvil plate. The harder hammerhead was expected to give a SRS that has higher levels for the frequencies over the knee frequency.

The results, that can be seen in **Figure 88**, were not as significant as expected. There is a deviation for the very lowest frequencies but the most surprising thing was that for some reason the harder hammerhead gave slightly lower shock levels for the highest frequencies.



*Figure 87* The two different hammerheads. The hammerhead on the left is the hardened one

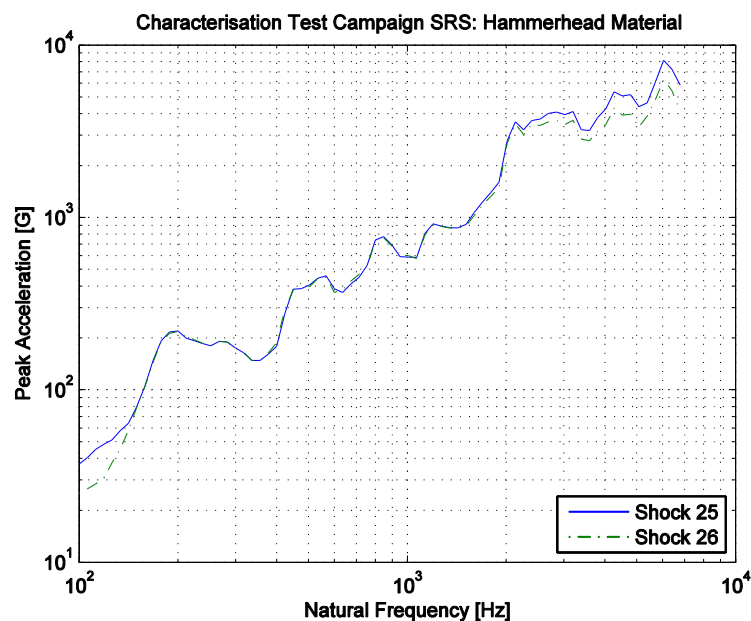


*Figure 88* Influence of hammerhead

Since neither the hammerheads nor the anvils were as influential as expected further tests were made with mechanical filters. This parameter was also added to the list of key parameters. **Figure 89** shows the influence of a soft and thin foam pad on the anvil plate. The levels are lower with the foam on the anvil and the difference increases with frequency.

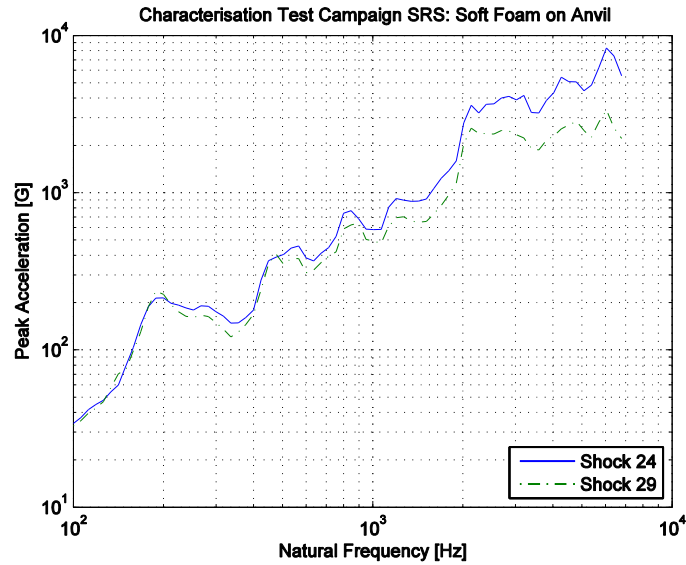


Figure 89 Influence of soft foam on anvil

#### 4.2.6 Impact location

There are 16 different impact locations for the OOP impact direction which was the BM configuration. The BM for the impact location was the dead centre of the square plate. In the simulations no consistent rule could be found for the behaviour of the SRS when the impact location was altered so the testing was of an experimental nature. Ten different locations were tested, see *Figure 90*.

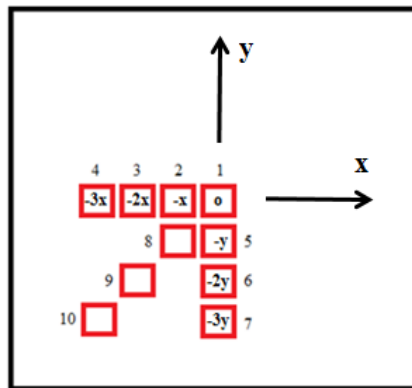


Figure 90 Impact locations of resonant plate

The impact locations tested were hence: Centre,  $-x$ ,  $-2x$ ,  $-3x$ ,  $-y$ ,  $-2y$ ,  $-3y$ ,  $-x-y$ ,  $-2x-2y$  and  $-3x-3y$ .



Figure 91 Impact location shift between  $-2y$  and  $-3y$

At this point a small dent was barely visible on the medium anvil. The long term repeatability of the STF can be seen in **Figure 92**. Shock 24 and shock 30 are identical while they both are slightly higher than Shock 4 for the mid frequencies. This could be because of the dent or some other settling factor. Consecutive shocks were still identical for the same settings, however, and the parameter influences were always measured against the latest BM shock.

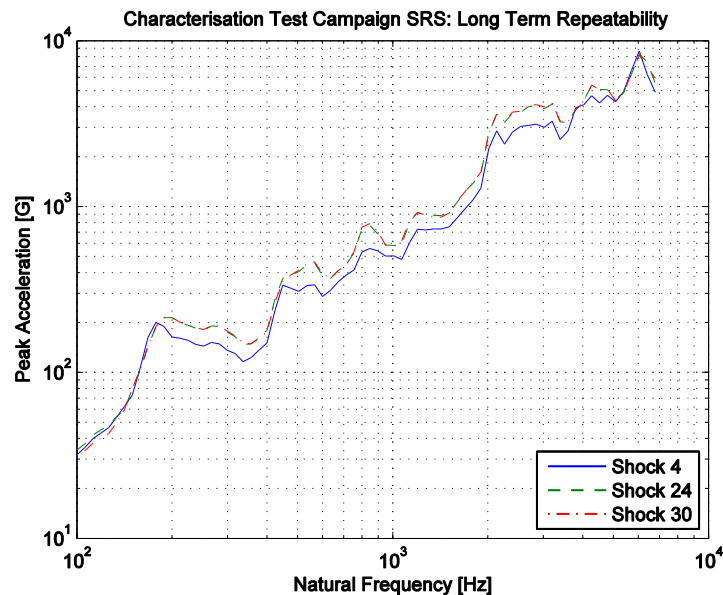


*Figure 92 Long term repeatability*

The results of the impact location shift in the  $x$ -direction can be seen in **Figure 93**. The impact location seems to affect how much certain modes are amplified or attenuated. The exact modes are different for each location but overall a shift of the impact location in the  $x$ -direction has the tendency to attenuate the low frequency modes and amplify the mid frequency modes.

For the shift in the  $y$ -direction it can be argued that the exact same behaviours should be evident because of symmetry but the measurement location is not on a symmetrical location in relationship to the  $x$ - and  $y$ -direction and the introduction of a mass dummy would also add to the dissymmetry.

The results for the  $y$ -direction shift can be seen in **Figure 94**. They are similar to the results in the  $x$ -direction in that the different impact locations attenuate or amplify certain modes but an effect that was not present in the  $x$ -direction was that the SRS was smoothed for the lower frequencies. Particularly the mode at 158 Hz is attenuated but more about that in Section 5.2.

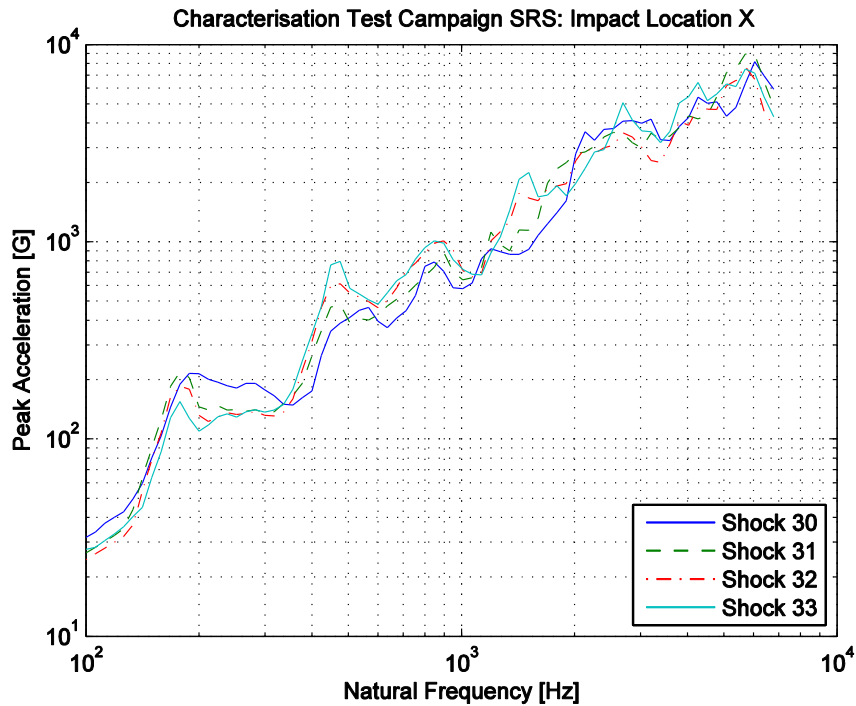


Figure 93 Influence of impact location shift in the  $x$ -direction

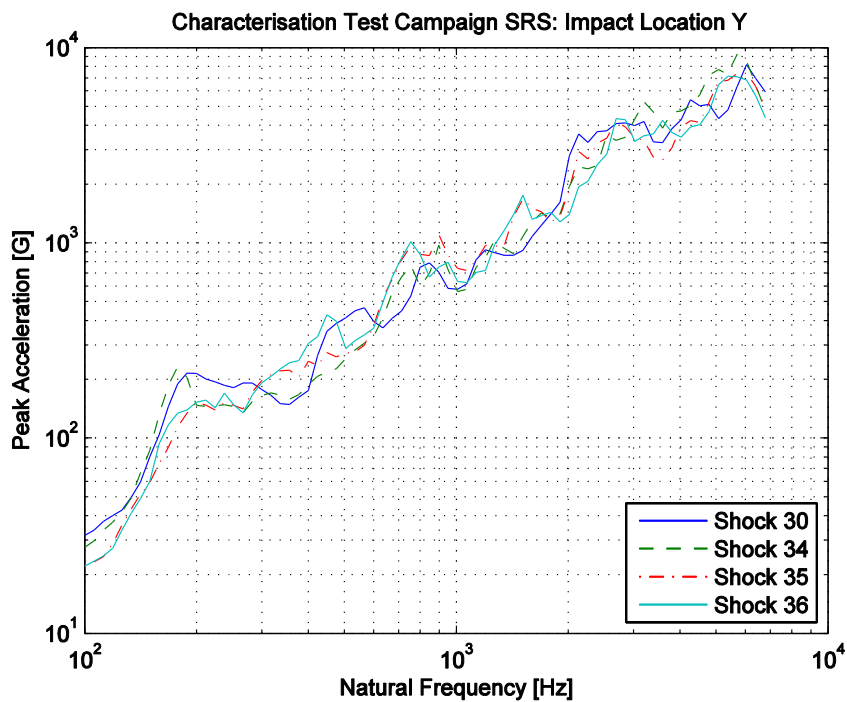


Figure 94 Influence of impact location shift in the  $y$ -direction

For the diagonal  $xy$ -direction interesting things started to happen. The results can be seen in **Figure 95**. The shift towards the corner of the plate attenuates the mode at 158 Hz but it also amplifies the modes around 1000 Hz so that the sought knee frequency arises.

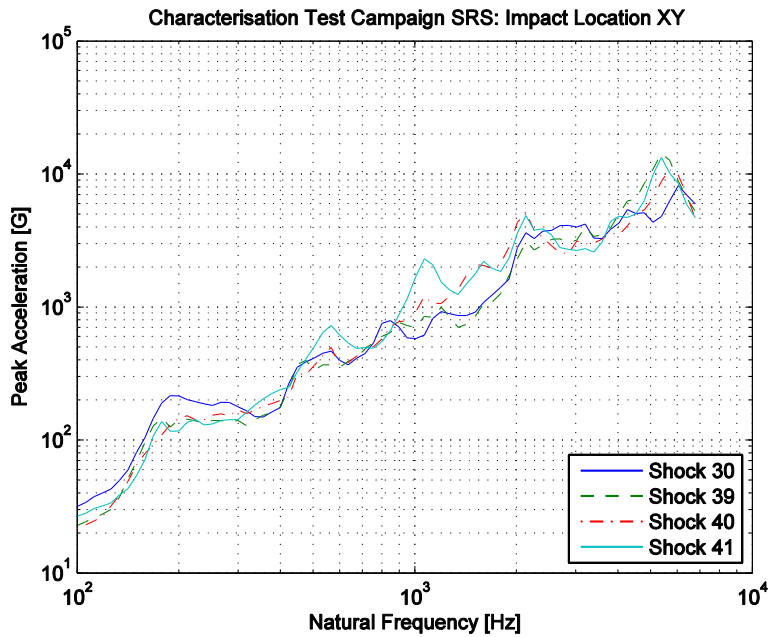


Figure 95 Influence of impact location shift in the diagonal  $xy$ -direction

#### 4.2.7 Foam type

Three different foam types had been selected for the STF. The foam is placed between the plate and the rest of the rig to emulate free boundary conditions. The softest foam was initially used in the BM but they were all tested. The influence of the foam was not simulated so the tests were purely experimental. The parameter was, however, expected to influence the SRS since the different foams in practice alters the boundary conditions of the plate which should have an effect on the overall shape of the SRS. The foam types tested were: Soft, Medium and Hard

As can be seen in **Figure 96** the shape was only marginally altered by the substitution of foam type. Since the difference was so small the medium foam was used instead of the soft one in the BM configuration since it was easier to handle.

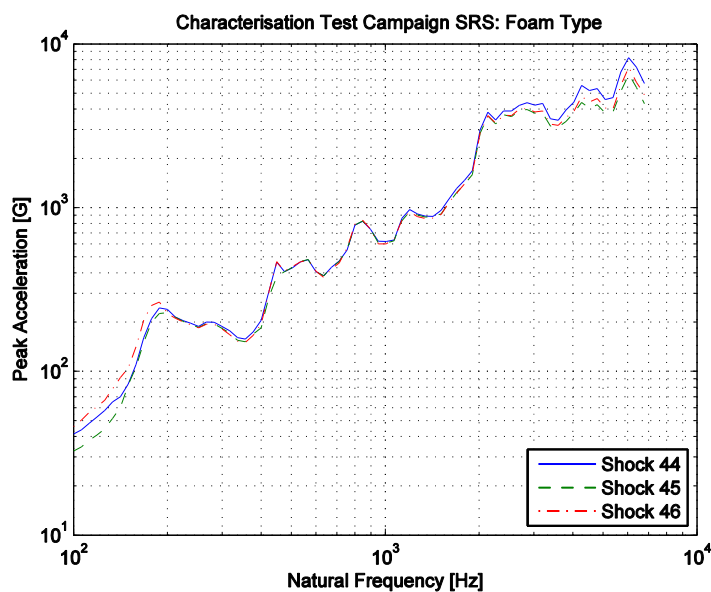


Figure 96 Influence of Foam Type

## 4.2.8 Boundary conditions of the plate

The boundary conditions can, excluding the different foam types, be altered by clamping the plate in different ways or by adding extra masses at certain locations. The possibilities are unlimited but two ways of restraining the plate were tested. The BM was to have the plate free and the other two tested ways were by clamping it with the STF's siderails and by using actual clamps and clamp the plate to the beams that the plate is resting on. This parameter was expected to alter the overall shape of the SRS. The settings tested were: Free, Siderails and Clamps.

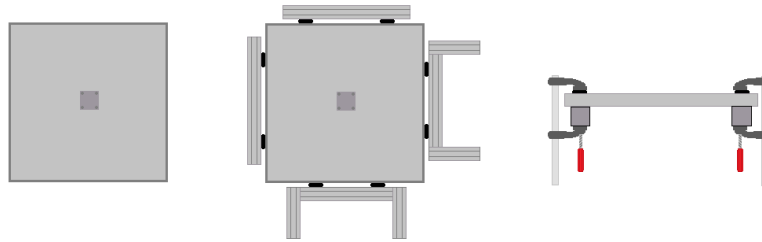


Figure 97 Resonant plate with its boundary conditions altered  
a) Free b) Siderails c) Clamps

The influence of clamping the plate with the siderails can be seen in **Figure 98**. It does not alter the response in any significant way but it is slightly lower overall.

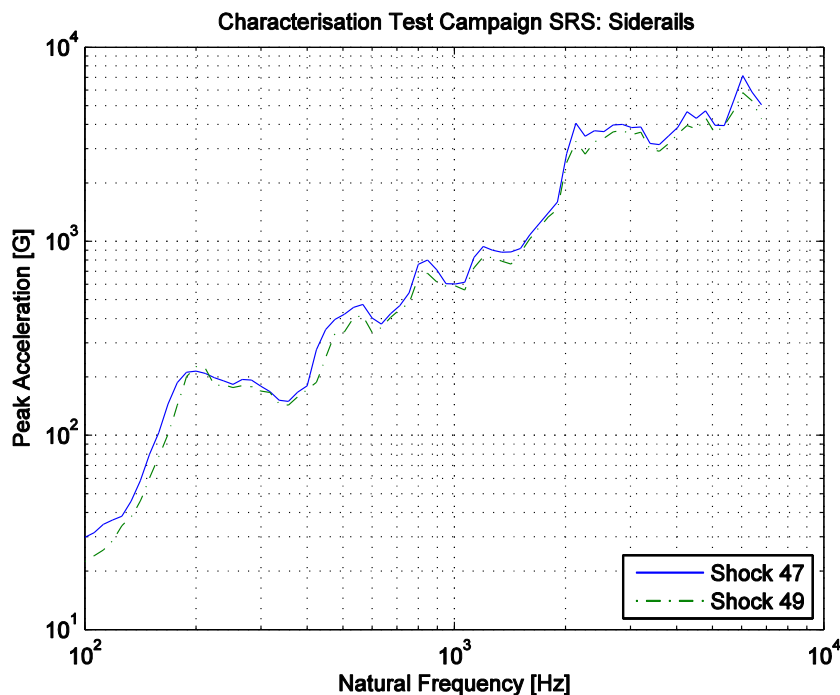


Figure 98 Influence of clamping the plate with the siderails

To fit the clamps on the plate the impact location had to be moved to  $-y$ , see **Figure 99**. Another measurement was taken before the plate was clamped to make sure that the influence of the clamping itself could be singled out.

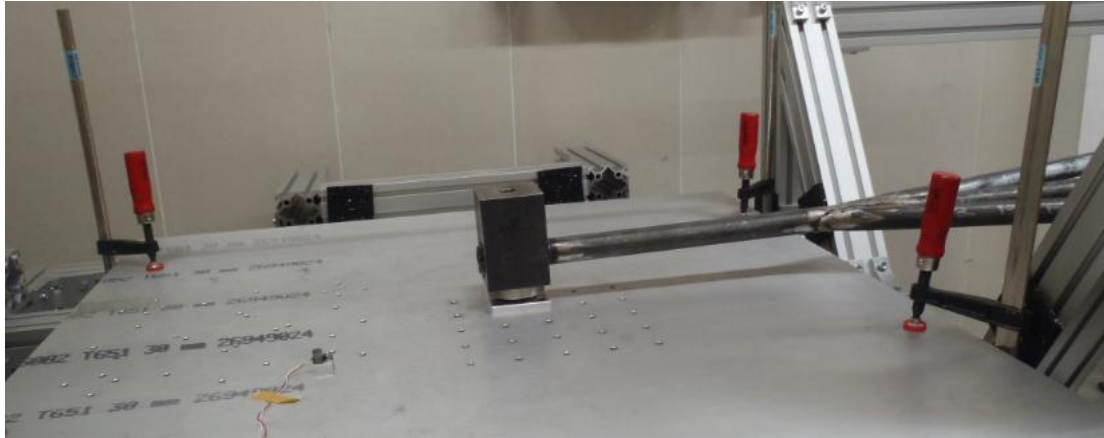


Figure 99 Resonant plate with clamps

The results can be seen in **Figure 100**. The mode at 158 Hz was attenuated and the levels were slightly lower for the high frequencies.

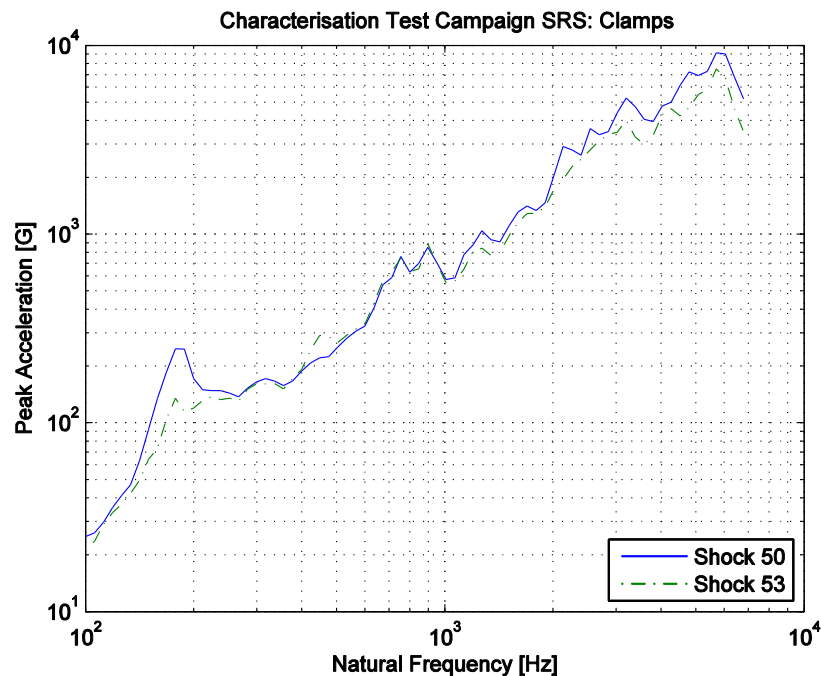


Figure 100 Influence of clamping the plate with clamps

#### 4.2.9 Mass dummy

It was expected that the mounting of a test specimen should have an effect on the SRS. The simulations did not give consistent results but research show that a small overall shift of the SRS to the left could be anticipated. Two different dummies were used, one “Heavy” and one “Light”. The heavy dummy was a part of the previous STF that has a mass of 26 kg. The light dummy was a 6.3 kg adaptor plate previously used for vibration testing. The other parameters were also tested to confirm that they had the same overall influence of the SRS as for the testing without a dummy. The dummy settings tested were: No dummy, Light and Heavy.

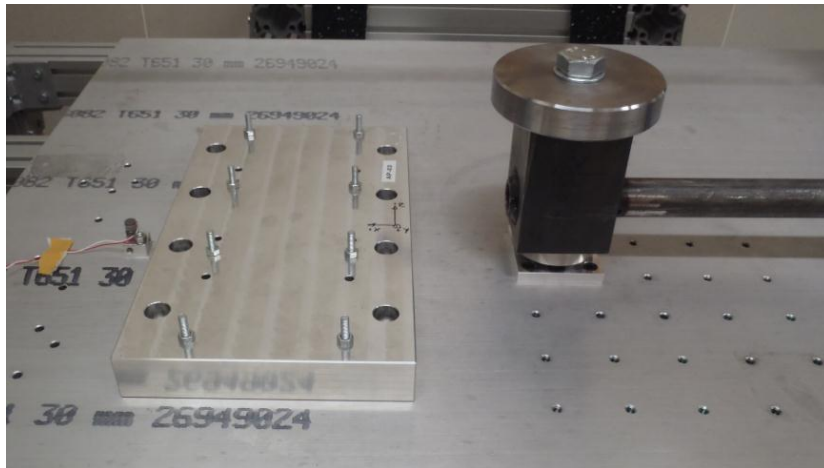


Figure 101 Light dummy mounted on resonant plate, 2 kg added to hammer mass

To fit the light dummy a new measurement location had to be used. The effect of adding the light dummy can be seen in **Figure 102**. The levels were attenuated for low- and mid-frequencies.

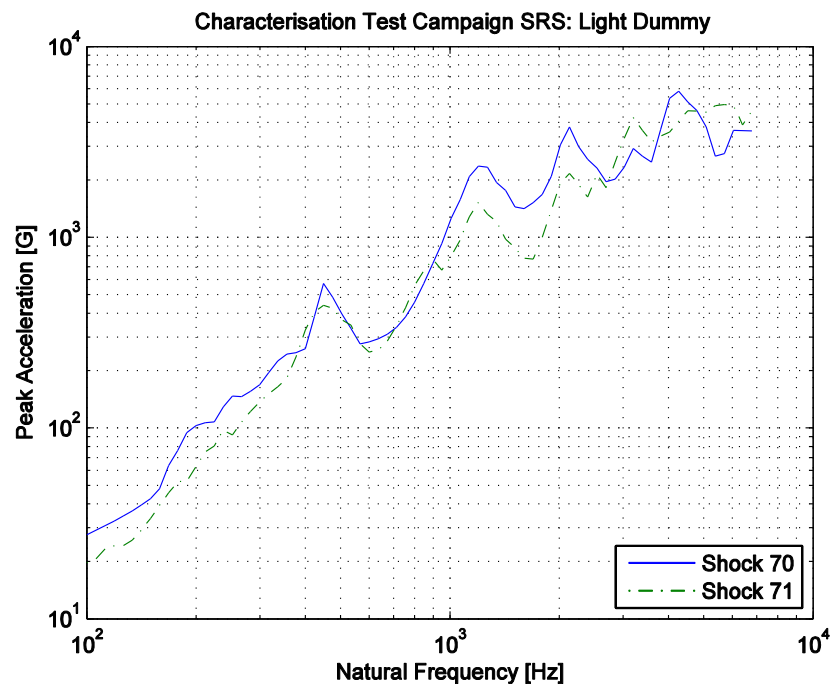


Figure 102 Influence of light mass dummy

Both the increase in impact velocity and addition of mass to the hammer had expected behaviours. Also the addition of a mechanical filter had the expected effect that the high frequencies are attenuated. The impact location shifts, however, did not show any improvement of the SRS.

To fit the heavy mass dummy on the plate the measurement location had to be moved again.

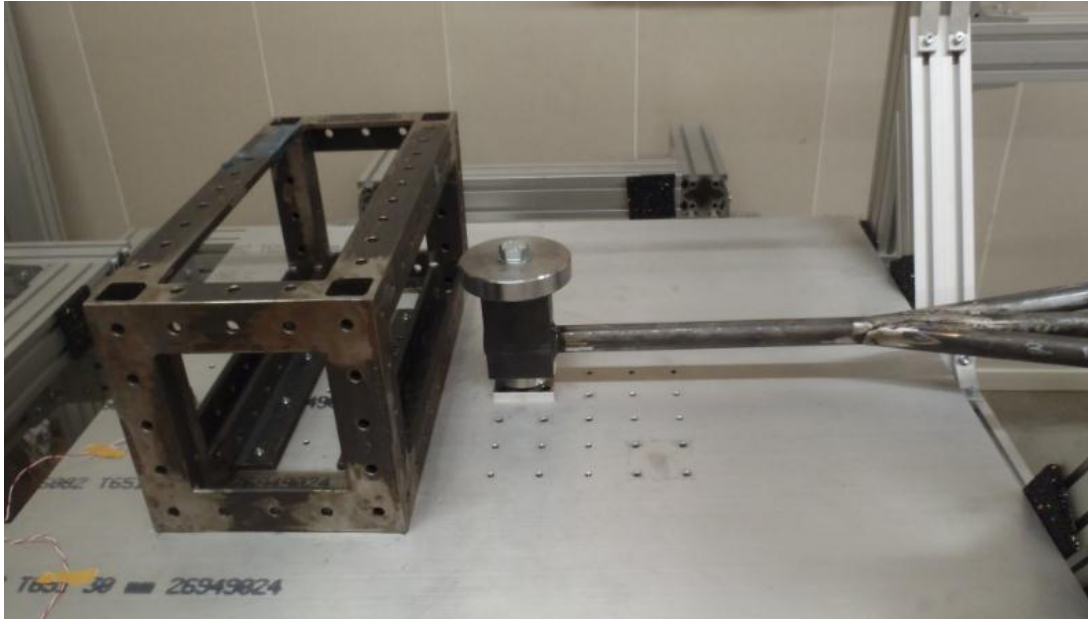


Figure 103 Heavy dummy on plate, 2 kg added to hammer mass

The effect of mounting the heavy dummy on the plate can be seen in **Figure 104**. The levels were lower everywhere but for the lowest frequencies and around 600 Hz. The testing showed that the shift of impact velocity, addition of mass to the hammer and addition of mechanical filters had the expected behaviours that were shown earlier.

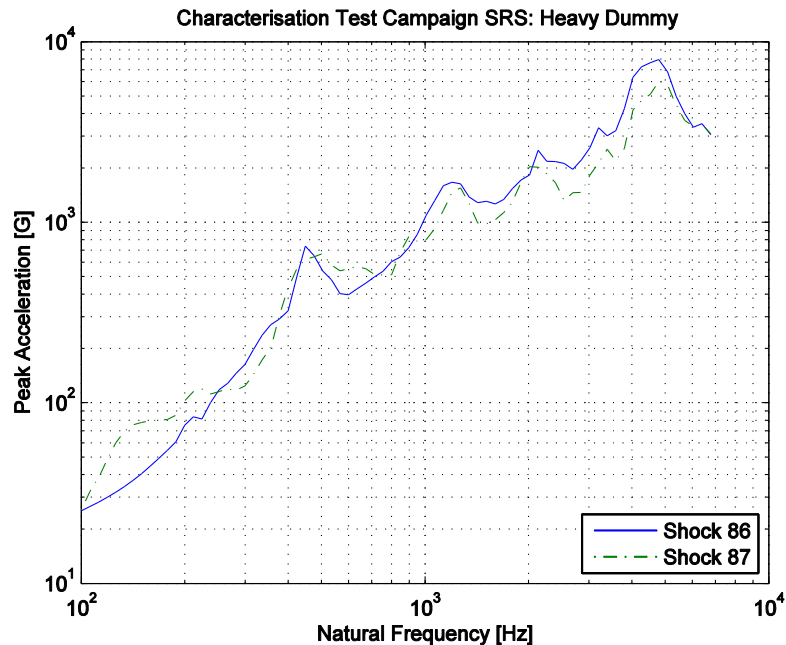


Figure 104 Influence of heavy dummy

#### 4.2.10 OOP/IP shift

This configuration change was expected to have a large influence on the SRS. The parameters were expected to have the same overall effect on the SRS for the IP configuration but the original shape of the SRS was expected to be different. The knee frequency was expected to lie at a higher frequency and there should be a different slope for the low frequencies. The shock levels in the OOP direction for the IP impact

direction were also measured since they can be substantial. This is since the plate is prone to be excited in its OOP bending modes also when it is impacted IP. The OOP impact does not have the ability to induce the IP compression waves in the same extent so for the OOP configuration this is not a problem.

- IP all else BM
- Measure OOP shock for IP impact
- Control testing of parameters

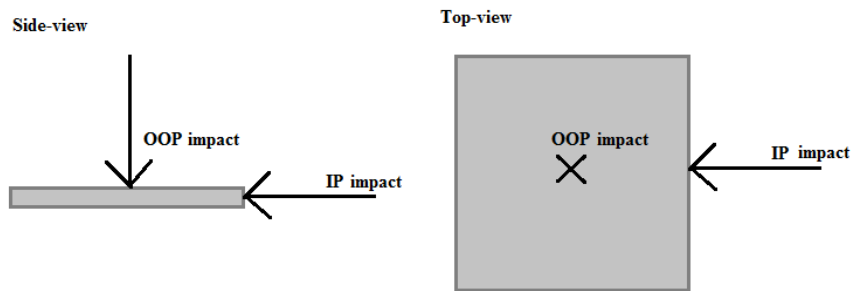


Figure 105 IP and OOP impacts

The OOP acceleration levels were indeed high. It is thus very important to check the OOP acceleration levels when qualifying equipment in the IP configuration so that the specimen is not being overtested in the OOP direction.

The results of the first IP shock for the IP acceleration levels can be seen in **Figure 106**.

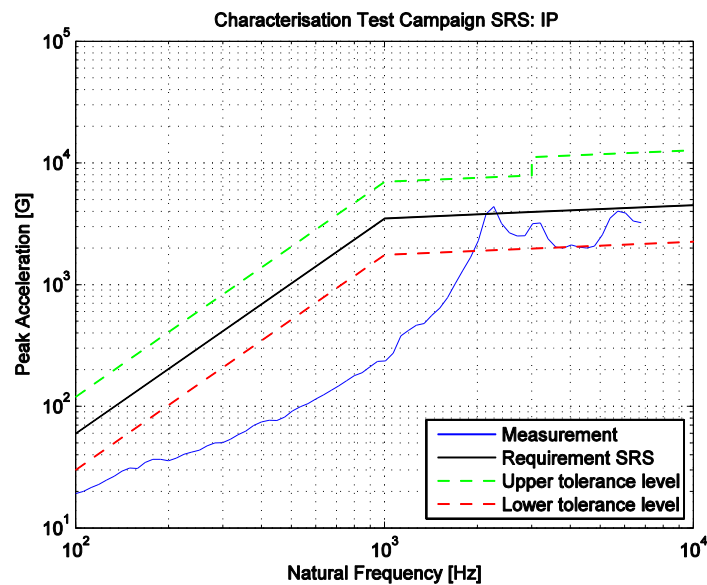


Figure 106 IP acceleration levels IP impact direction

The knee frequency was as expected at a higher frequency. Adding mass and increasing the impact velocity had expected influence on the SRS while shifting the impact location attenuated the highest frequencies but did not alter the shape of the SRS as such. The harder hammerhead attenuated the highest frequencies as for the OOP configuration but an unexpected result came from clamping the plate with the siderails. The shock levels were actually higher with the plate clamped than with the

plate free. A mechanical filter attenuated the levels overall and the effect of changing the anvil material was almost negligible.

The effect of mounting the heavy mass dummy on the resonant plate can be seen in *Figure 107*. The levels were lower overall but particularly for the knee frequency.

Both the addition of mass and increase in impact velocity worked as expected. A big dent had been formed on the anvil plate and it was clear that the testing here was at the limit of what the STF could handle.

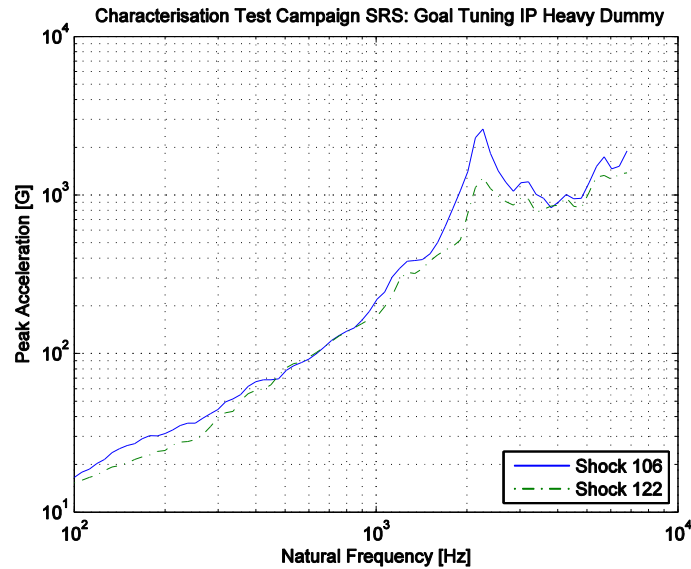


*Figure 107 Influence of mounting heavy mass dummy on plate*

### 4.3 Goal SRS tuning

The characterisation test campaign had the goal to capture the influence of each parameter on the SRS and in that way build up a toolbox for tuning the SRS in a desirable way. To test this toolbox it was used to try to tune the SRS into a shape that lies within the tolerance levels of the required SRS. The tolerances are not univocal between sources, see *Figure 19*, so the NASA tolerances were the first goal to try to reach since they are the most tolerant ones.

#### 4.3.1 No dummy OOP

Parameter	Plan configuration
Impact velocity	35°
Hammer mass	0 kg add-on
Anvil material	Medium, Al7075
Hammerhead material	Soft, SS303
Impact location	-3x-3y
Foam type	Medium
Boundary conditions	Free
Mass dummy	No dummy
Impact direction	OOP
Mechanical filter	Double foam pads on anvil

The first step was to select a configuration that was expected to come close to the goal SRS. This configuration was called the plan configuration. The result of the plan configuration can be seen in *Figure 108*. The overall levels were too low and it was not very smooth for high frequencies.

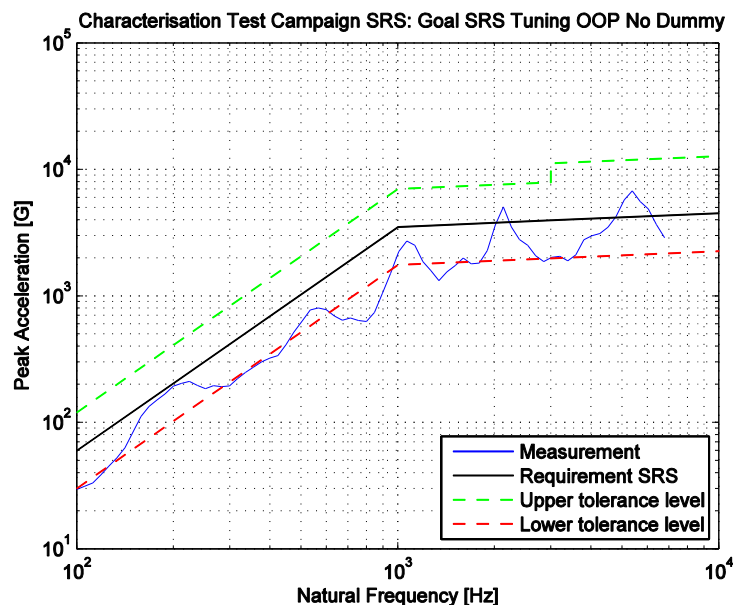


*Figure 108* Results of plan configuration, Shock 56

To smoothen the SRS for the high frequencies more mechanical filters were tested. Soft foam pads attenuated the high frequencies better than cardboard while hard pressed cardboard attenuated them too much. Extra mass was added to the hammer but the mode at 158 Hz reappeared so the mass was removed again.

To reach the required levels the impact velocity was instead increased. This almost put the SRS within the tolerances but another requirement is that more than 50% of the data points shall lie above the requirement. This was not fulfilled so higher levels were required. A charge angle of  $80^\circ$  was tested but this did not increase the overall levels but only a spike around 5500 Hz.

To increase the levels extra mass was again added to the hammer. 2 kg and 6 kg were tested. Both shocks were higher for the low frequencies but the 6 kg shock was actually a bit lower for the spike at 5500 Hz. The last shock looked quite good but it had two bulges that were over the tolerances. The one formerly mentioned around the mode at 158 Hz and one bulge at the modes around 5500 Hz. The plate was clamped to see if that could attenuate the bulges, see *Figure 109*. Shock 83 corresponds to the shock with the clamped plate. It did not kill the bulge around the mode at 158 Hz as expected but it did attenuate the one around 550 Hz and made the shock levels for the high frequency a bit too low. To counter this one of the foams on the anvil was removed which gave Shock 84.

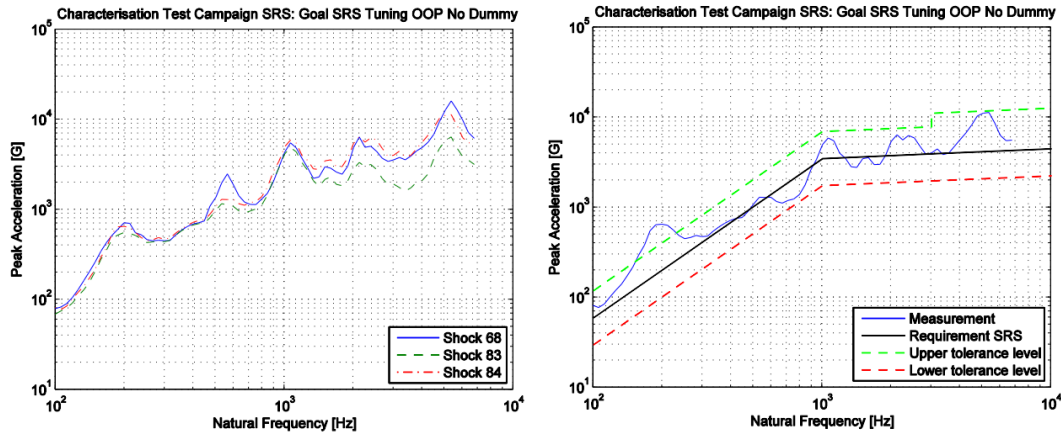


Figure 109 a) Clamping the plate b) Final shock OOP no dummy, Shock 84

Shock 84 was selected to be sufficient for the time being even though the bulge at the 158 Hz mode reached a bit over the upper tolerance.

### 4.3.2 Light dummy OOP

Parameter	Plan configuration
Impact velocity	45°
Hammer mass	6 kg add-on
Anvil material	Medium, Al7075
Hammerhead material	Soft, SS303
Impact location	Centre
Foam type	Medium
Boundary conditions	Free
Mass dummy	Light dummy
Impact direction	OOP
Mechanical filter	No

The result of the plan configuration can be seen in *Figure 110*. It was almost good enough but for two low small bulges around the knee frequency.

The impact velocity was increased by increasing the charge angle to 60°. The overall levels were slightly higher overall but a little bit too high for the highest frequencies. Another test was made with 10 kg on the hammer, see *Figure 111*.

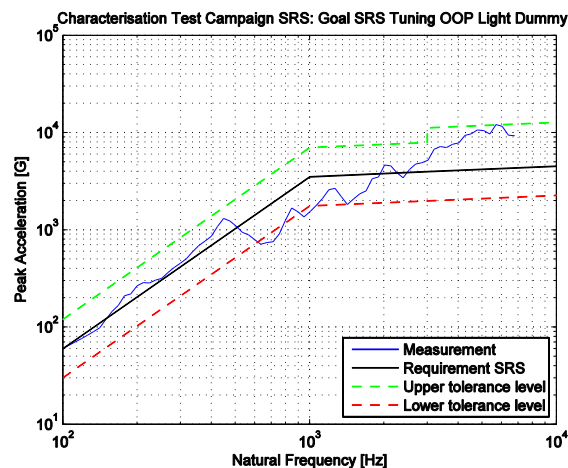


Figure 110 Plan configuration SRS

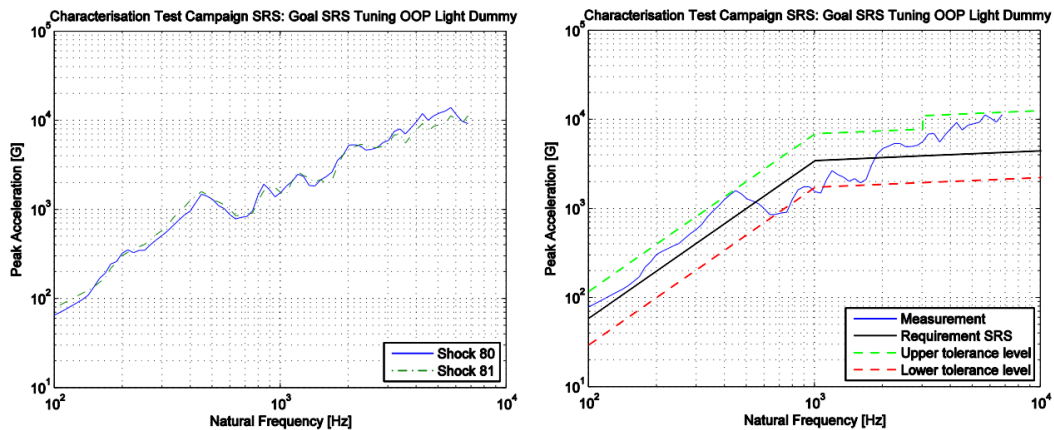


Figure 111 a) Increase of hammer mass b) Comparison of Shock 81 and goal SRS

The SRS was slightly higher for the low frequencies and slightly lower for the high frequencies. Shock 81 was considered to achieve the required SRS.

### 4.3.3 Heavy dummy OOP

Parameter	Plan configuration
Impact velocity	60°
Hammer mass	10 kg add-on
Anvil material	Medium, Al7075
Hammerhead material	Soft, SS303
Impact location	Centre
Foam type	Medium
Boundary conditions	Free
Mass dummy	Heavy dummy
Impact direction	OOP
Mechanical filter	Double foam

The result of the plan configuration can be seen in **Figure 112 a)**. It was a bit too high for the low frequencies. To get the low frequency levels down the mass of the hammer was decreased and one of the foam sheets was removed to see if it could raise the high frequency levels a bit. The levels got lower for the low frequencies but could not attenuate the bulge around 450 Hz. It was also a bit too high for the highest frequencies. The plate was clamped but that did only marginally affect the SRS. Another sheet of foam was added which gave the SRS in **Figure 112 b)**. It would need some extra attenuation for the bulge at 450 Hz but it was considered to be good enough to go on with the next step of the testing.

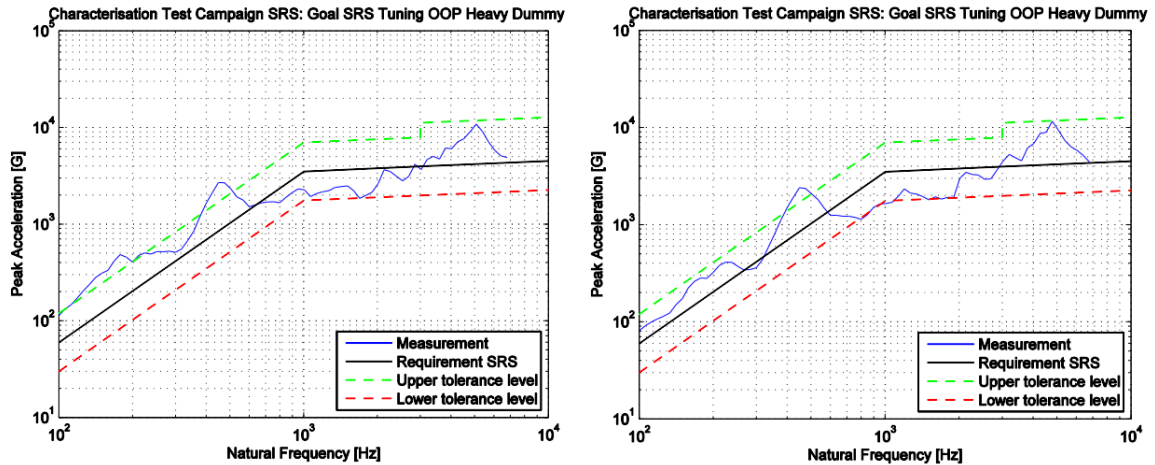


Figure 112 a) Result of the plan configuration test, Shock 91  
 b) Comparison of Shock 95 and goal SRS

#### 4.3.4 No dummy IP

Parameter	Plan configuration
Impact velocity	90°
Hammer mass	0 kg add-on
Anvil material	Medium, Al7075
Hammerhead material	Hard, SS630
Impact location	-x
Foam type	Medium
Boundary conditions	Free
Mass dummy	Heavy dummy
Impact direction	IP
Mechanical filter	No

The result of the shock with the plan configuration can be seen in *Figure 113 a*). It is evident that it is a more difficult challenge to reach the tolerances in this configuration. 4 kg extra mass was added to lift the curve for the lower frequencies. The plate was sliding into the siderail behind the plate upon impact so the back siderail was set in a position where it held the plate in place. That amplified the low levels somewhat but it was still too low. 2 kg extra was added to the hammer and the charge angle was increased to 100° to increase the impact velocity. The levels around the requirement SRS knee frequency were still a bit too low. It was tested both to increase the impact velocity and the hammer mass more but it did not improve the SRS any further.

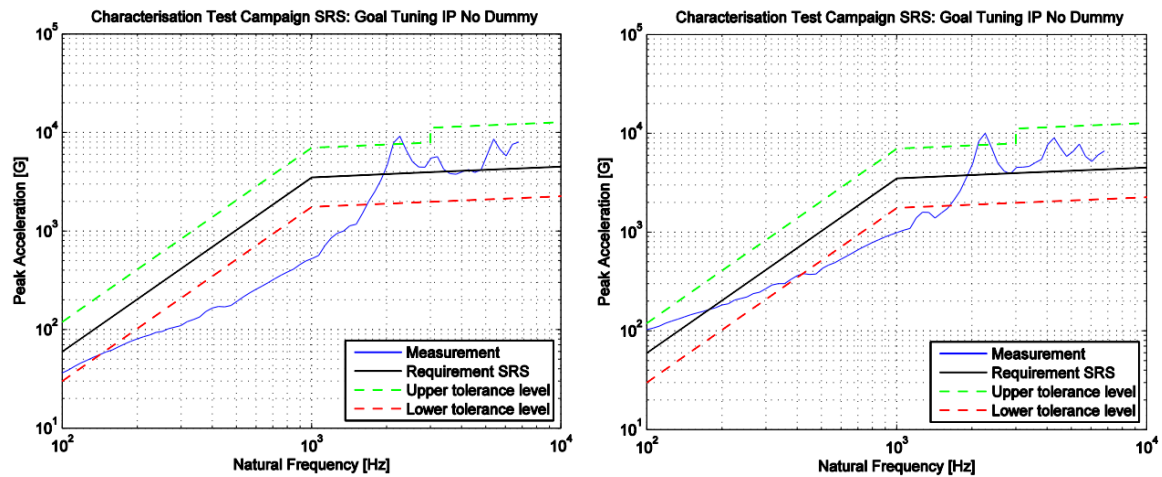


Figure 113 a) Result of the plan configuration shock. Shock 114  
 b) Comparison between Shock 117 and goal SRS

Shock 117 in **Figure 113** b) was the closest shock to the goal SRS that was achievable without further characterisation testing.

The time for testing was limited so to save time no testing were carried out for the light dummy IP.

#### 4.3.5 Heavy dummy IP

Parameter	Plan configuration
Impact velocity	90°
Hammer mass	6 kg add-on
Anvil material	Medium, Al7075
Hammerhead material	Hard, SS630
Impact location	Centre
Foam type	Medium
Boundary conditions	Back siderail
Mass dummy	Heavy dummy
Impact direction	IP
Mechanical filter	No

The levels were not high enough so the impact velocity was increased by increasing the charge angle to 120°, see **Figure 114** a). In this tests the anvil plate cracked from the impact, see **Figure 115**. The limit of the STF was thus both reached and crossed. It is possible that this was the straw that broke the camel's back and damage was already present. When testing close to these levels care should therefore be taken to not go over the limit and inflict damage to the STF. Shock 128 in **Figure 114** b) gave the best result for the time being for the heavy dummy IP.

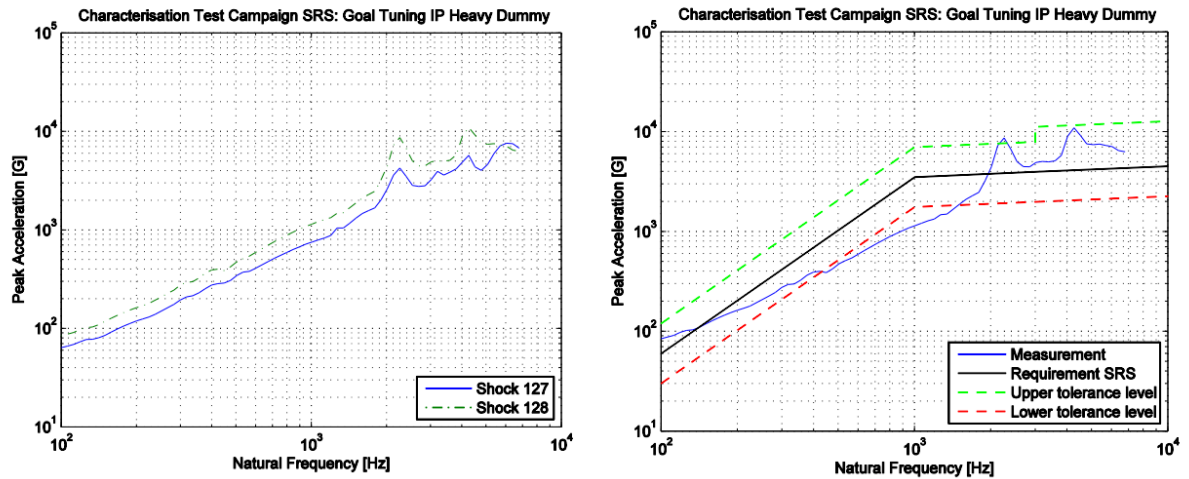


Figure 114 a) Shock 127 is the plan configuration SRS b) Shock 128 is the best shock achieved for the heavy dummy IP



Figure 115 Cracked anvil plate

As can be seen in **Figure 114** b) the levels are still a bit too low around the goal SRS knee frequency and it is not possible to push the STF further in the IP configuration. Either an additional way of altering the overall shape of the SRS needs to be found for the IP mode or the OOP mode will have to be used with an adaptor to be able to test the specimen in all directions.

## 5 Discussion

To evaluate the results of the STF development project the initial goals must be revisited.

### 5.1 Fulfilment of goals

The six goals of the project were defined in Section 2.1. The goals are discussed in individual sections below.

#### 5.1.1 Research the field and define requirements for a new STF

The phenomenon of shock and its importance in space missions were thoroughly examined to gain knowledge of the demands that a new STF would have to live up to. The required SRS did put the coming STF in the mid-field environment but the high acceleration levels for the heavy specimen were on the border and even considered unfeasible without the usage of explosives according to one expert [26]. Other sources [12], [15], [24] and [35] did, however, contradict that statement.

The requirements specification was produced by consulting ESA, NASA, MIL, ECSS and ISIS standards and has been revised continuously over the time of the project. A requirement review meeting was held at ISIS to make sure that the requirements specification covered all stakeholders and described a facility that would deliver what was expected. The fulfilment of the requirements is discussed in Section 5.3.

#### 5.1.2 Develop STF concepts based on the found requirements and the QuadPack

No usage of explosives was one of the first requirements to emerge so metal-to-metal impact was the only proven remaining option for exciting the shock environment. Still there was no lack in ideas on how to achieve this impact. A functional analysis was held to gain knowledge on the required functions of the STF which led to a set of five sub-functions that every concept would need to perform. During the analysis of existing mid-field metal-to-metal STFs and the brainstorming sessions these sub-functions were found to have strong mutual dependencies. Even with this limitation, however, the number of possible concepts had five digits. Many of these were of course unfeasible which would later be evident with input from simulations and experts.

The QuadPack was not in focus at the time since it defines limitations rather than possibilities. Not being able to test the QuadPack would be a killing argument but it should not initially stop a concept that might have useful fragments in it.

#### 5.1.3 Get data from simulations based on the requirements and concepts

The realisation of this goal overlapped with the realisation of the next one so they are discussed in the same section.

#### **5.1.4 Hold elimination process and trade-off studies based on requirements, simulation results and input from experts to select final concept**

The first major obstacle in the project was how to rationally select the best concept. The requirements were initially used to get rid of the obvious losers but to use the requirements alone was not sufficient. There were still more than a hundred concepts on the list. More knowledge was required to be able to say with certainty that one concept was better than another. This was a problem that required several different approaches to solve.

The first approach was to turn to shock experts all over Europe to gain understanding and get pragmatic advice. This was very fruitful and the number of surviving concepts could be narrowed down a lot.

The simulations were initially planned to be held after a concept had been chosen to confirm that the required shock levels could be reached. It was, however, used at an earlier stage so that the results could be used as input for the eliminations. The results from the simulations indicated the parameters which were important and their ranges. The surviving concepts were then developed to a level where it was known how and how well they could realise these parameters and ranges.

How well the actual STF results compared to the expected results from simulation and expert input is discussed in Section 5.2.

The last approach in selecting the final concept was a trade-off meeting at ISIS. Several engineers participated to define the most important criteria which led to the selection of a final concept.

#### **5.1.5 Design the concept details to a level where the STF can be manufactured**

The design of the final concept was developed in an iterative process where feed-back was gathered from review meetings at ISIS, additional simulations and from external experts. More time than expected was required from the time when the CAD-files of the to-be-manufactured custom parts were ready till the time of delivery from the manufacturer. A big part was that the manufacturing time in itself was long but that was to some extent expected. Unexpected was, however, the time it took to transfer the CAD-files to industrial standard drawings, to decide on the exact metal alloy for the different parts, to find a suitable manufacturer and to negotiate the price. It all went well, however, and no major issues occurred during the assembly process.

#### **5.1.6 Test the STF to verify that it gives predicted results**

The fulfilment of this goal requires a more exhaustive discussion and is therefore gone through in Section 5.2.

### **5.2 Expected and acquired results comparison**

Many of the parameters and behaviours of the STF were just as expected but there were, however, some discrepancies. For the expected behaviours see Section 3.2. In general it was much more difficult than expected to tune the SRS to a required shape.

The first tests of the STF showed that it was highly repeatable. This was a very good result. One of the first things noted was, however, that the distinctive knee frequency was shining with its absence. It was not until the impact location was altered that the sought shape appeared with a knee frequency at 1000 Hz. It can be argued that since no SRS from a real shock is as smooth as a typical requirement SRS, it is a bit arbitrary to say exactly where the knee frequency is located. In general, however, it was expected that there would be a stronger amplification of the modes around 1000 Hz. This also for the initial shocks with the BM impact location in the dead centre of the plate. The bulge in the shock just below 200 Hz that is evident in most of the SRSs before the impact location was altered corresponds to one of the first modes of the plate at 158 Hz, see **Figure 116**. It is reasonable to assume that this mode shape is aided by an impact in the dead centre of the plate. A shift away from the centre should hence attenuate this mode which seems to be the case, see **Figure 94** or any of the other results of shifting the impact location.

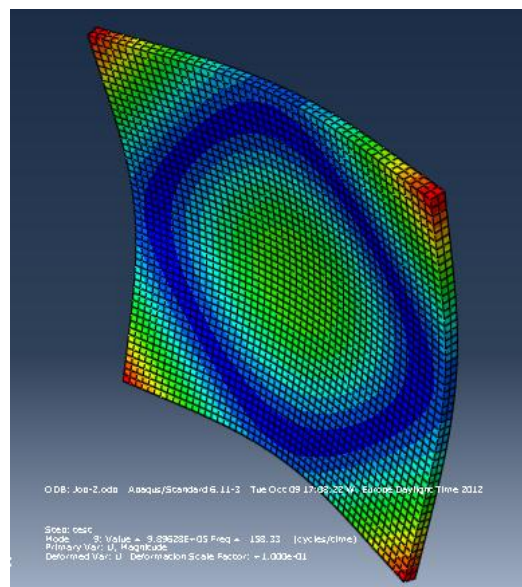


**Figure 116** Resonant plate mode at 158 Hz for free boundary conditions

This implies that the presence of the distinct knee frequency for the  $-3x-3y$  impact location could be related to that impact location being beneficial for the modes around 1000 Hz. The modes around 1000 Hz can be seen in **Figure 117**.

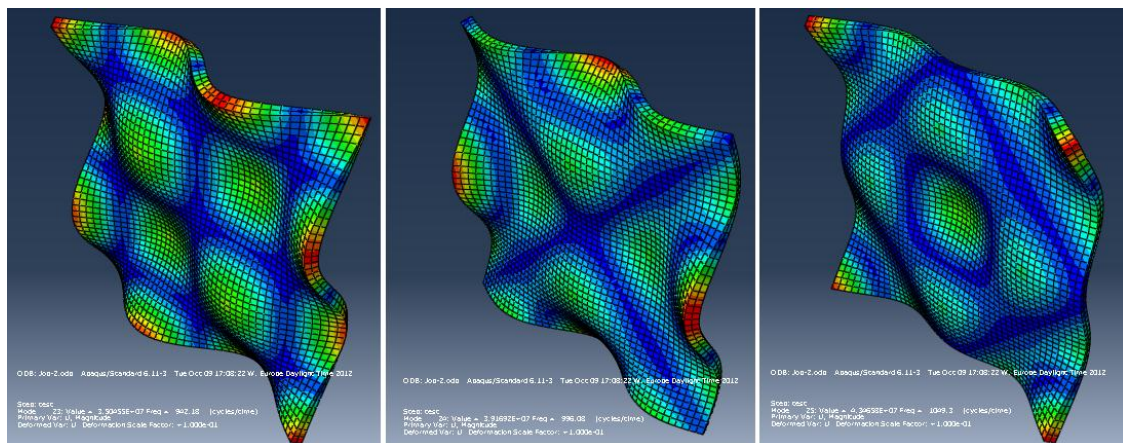


**Figure 117** Resonant plate mode shapes for the frequencies around 1000 Hz

For the leftmost mode it definitely makes sense that an impact diagonally off centre would amplify the mode but not as clearly for the rightmost mode and not at all for the middle one where the diagonal lines between the corners are nodal lines.

Also for different measurement locations the shapes of the SRSs were quite different. This is reasonable since one measurement location might lie on the nodal line of a mode while another measurement location might lie on an antinode. This was actually simulated, see *Figure 48*, but its importance was not recognised at first. This raises another argument for the theory on why the leftmost mode in *Figure 117* was extra apparent for the  $-3x-3y$  impact location. The measurement location for the OOP testing with no dummy was located at a position that corresponds well with an antinode of the mode in question, see *Figure 118*. The other two modes around 1000 Hz might have been more prone to get excited by other impact locations but because of the measurement location they were still not as apparent from the sensor's point of view.

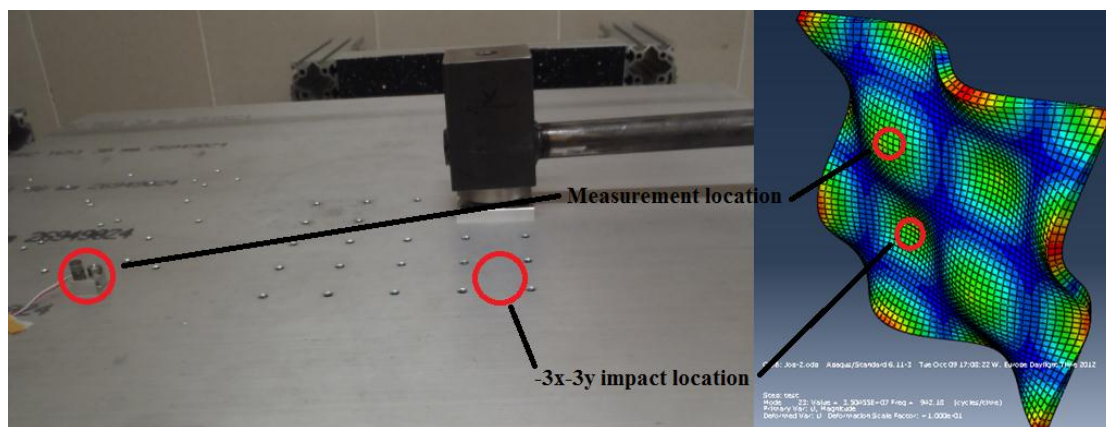


*Figure 118 Relationship between impact and measurement location and apparent modes in the SRS*

Before the testing with the light dummy the measurement location was moved to a new location to fit the dummy, see *Figure 101*. The shock levels were in this location measured without the influence of the dummy as Shock 70. This configuration compares better to the simulation configuration and the knee frequency at 1000 Hz was indeed more apparent here also for the centre impact location, see *Figure 102*. This impact and measurement location compares well with the rightmost mode in *Figure 117* and the measurement location also compares well with an antinode in the middle mode in the same figure.

Something that was expected to alter the shape of the SRS but did not was changing the boundary conditions of the resonant plate by exchanging the foam pad type the plate was resting on or by using different methods of clamping the plate. The exchange of foam had almost no influence whatsoever while the clamping of the plate was useful since it could kill certain mode spikes. It was, however, expected to have a larger influence.

The shift between OOP and IP configuration did as expected have a large effect on the SRS. The knee frequency was indeed pushed up to around 2000 Hz and since the other shape changing parameters did not work as good as expected it was very difficult to get the IP test configurations to end up within the required tolerances. In trying to push the shock levels to the goal the limit of the STF was found by cracking the anvil plate. This shock was almost within the tolerances but to fully reach the IP

goal SRS the shape must be altered somehow. Another way of solving the issue is to use the OOP configuration and then use an adaptor to enable testing in all directions. The IP configuration could then be used for SRS requirements where the knee frequency needs to be at a higher frequency. It is not uncommon to see requirements with the knee frequency at 1500Hz [29] or even 2000 Hz which is the case for the VEGA launch vehicle, see *Figure 17*. With this point of view the high IP knee frequency is a strength that makes the STF more versatile.

The overall acceleration levels were expected to be controlled by the impact velocity of the hammer. This is in turn set by the drop height which in the STF is controlled by the angle the hammer arm is raised. The expected behaviour was confirmed in the testing and maximum levels of around 6000 g at 1000 Hz and well over 10000 g for the highest frequencies were reached.

For the lower frequencies the slope of the SRS was expected to be controlled by the mass of the hammer. This was confirmed by the testing. For the heaviest configurations though the difference for the low frequencies was very small. At the high frequencies on the other hand the acceleration levels were lower. This was an unexpected result that could be used to control the high frequencies.

For the high frequencies in general the results were not as expected. The different anvil materials were expected to induce an effect for the high frequencies. The harder the material the higher the acceleration levels should be. The testing did, however, not show the presence of such behaviour for the three metal anvils. One reason might be that the materials were too similar since there, indeed, was a large difference when an anvil in a polymeric material was used. To add more control with this parameter more tests need to be made with more extreme materials such as copper, hardwood or polymeric materials.

Another parameter with expected control over the high frequencies was the material of the hammerhead. The same effect with harder material giving higher acceleration levels was expected but the result was surprisingly the opposite. The harder hammerhead induced lower acceleration levels for the higher frequencies. More than two materials are needed to confirm the pattern so further testing and research is required.

Since the expected parameter for controlling the high frequencies did not work as expected more testing was done with the influence of mechanical filters. A mechanical filter can be some type of material that is placed on the anvil. The influence of different foam pads, papers and cardboards were tested and they showed good and diverse ability to attenuate the high frequencies. Also for the mechanical filters there is a lot of knowledge to gain from further testing.

In general it is always true that further research is required to learn more about something and for the characterisation of a shock test facility more tests are always needed. For the characterisation of the THOR STF more than 150 shocks have been analysed so far. This should be compared to the characterisation test campaign of ESTECS's shock bench that included around 5000 shocks [29]. In addition to the earlier mentioned areas where more tests were required, more tests should also be done on, for example, the influence of adding extra oscillators or masses to the plate and the influence of adaptors.

The FE simulations should also be discussed. With the actual STF in place it is possible to validate the simulation results. Shock 70 was the configuration that was

most similar to a simulated configuration, namely setup 22. The configuration in Shock 70 is similar to the one in *Figure 101* but without the light dummy and the two kg extra mass on the hammer. Setup 22 was a simulation with the impact in the centre of the plate and the measurement location 34 cm away, see *Figure 119*.

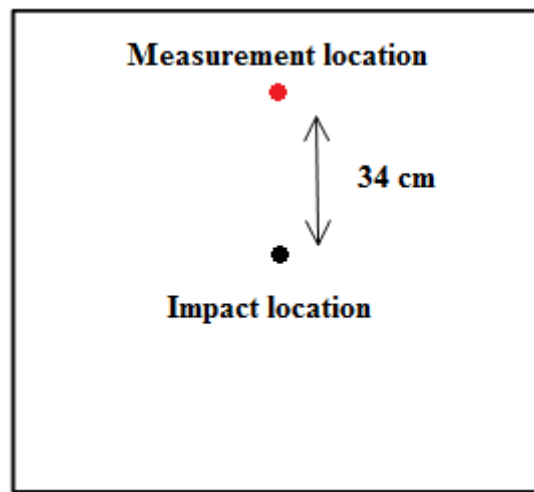


*Figure 119* Simulation Setup 22

The results are compared in *Figure 120*. The strong modes compare rather well but the simulation seems to be shifted to the left. It should be noted that the impact velocity in the simulated case was 0.7 m/s while it in the actual test was around 1.7 m/s.

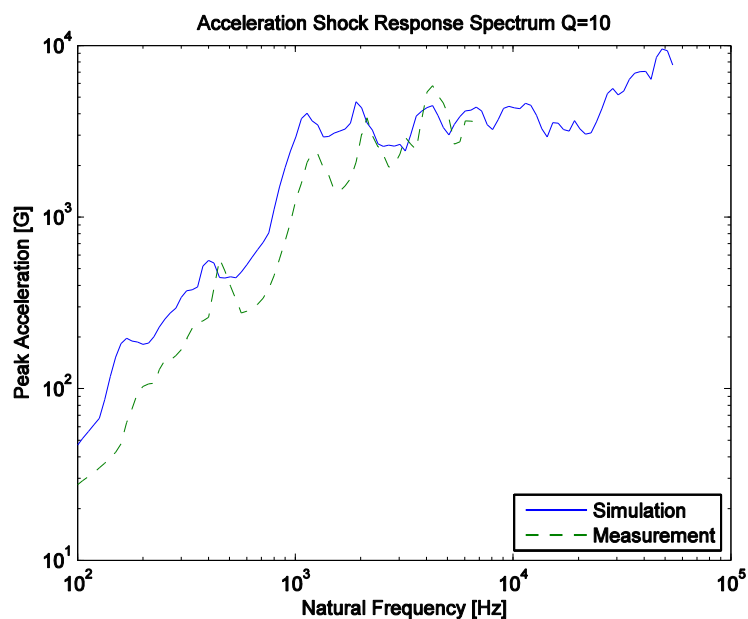


*Figure 120* Comparison of simulation of Setup 22 and measurement of shock test with the configuration Shock 70

For the IP configuration the results agreed even better, see *Figure 121*.

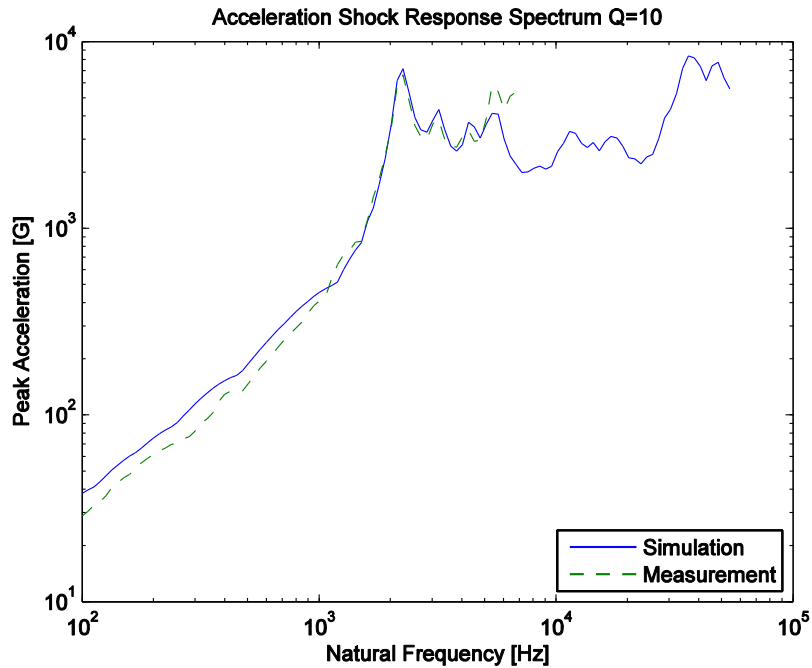


Figure 121 Comparison of simulation of Setup 3F and measurement of shock test with the configuration Shock 113

The impact velocity in the simulation was again 0.7 m/s while it was much higher for the real test. It was not measured but the charge angle was  $70^\circ$  in the IP configuration. The SRSs are very similar but for the slope at the low frequencies. This could be explained by a difference in the mass of the hammer since the exact mass of the actual hammer has not been determined.

If the discrepancies in impact velocity are neglected and only the shapes of the SRSs are considered it is interesting that the IP configuration has a higher correlation between the simulation and measurement than for the OOP configuration. A possible explanation is that it is the impact itself that is the troublemaker for the FE model. Close to the impact this can be apparent as somewhat non-physical behaviour and since the impact is further away from the area of interest in the IP configuration, this simulation suffers less from it.

To get even better simulation results another round can be made with data from the actual STF. These results can then be validated and improved as it goes. Several theses, articles and PhD reports have been made with this approach and the capabilities of the different FE codes are constantly improving.

### 5.3 Fulfilment of requirements

Around 90% of the requirements are already fulfilled according to the initial tests. The rest of them do, however, require some more testing before it can be said with confidence that they are fulfilled. They are the following requirements:

- The STF shall qualify the ISIS QuadPack with respect to shock
- The STF shall be able to introduce the required shock in all directions
- The data acquisition system shall have a specified sampling rate

- The level of noise shall be kept under a certain level
- The STF shall have a minimum usable lifetime
- The STF shall induce no plastic deformation in non-sacrificial parts
- The STF shall give repeatable and predictable results throughout its life

Explanations of each of the requirements are given below.

The QuadPack is a future product so it cannot be tested yet.

The required shock could not be introduced in the IP configuration with the present knowledge of the STF. The levels around the knee frequency were a bit too low. To reach the proper levels more tests to alter the shape of the IP SRS or with adaptors in the OOP configuration are required.

The DAQ module that was used in the test campaign was a test version of the DAQ that will later be used. This DAQ will have the required sampling rate.

The noise level has not been measured so it cannot be said with confidence that the limit level is not breached. The noise at impact does, however, cause disturbance for the neighbours so alternate location and/or noise reduction needs to be implemented.

The minimum usable lifetime of the STF is not directly available since it has not been tested for a long period of time yet.

For the highly energetic shock tests that pushed the limit of the STF's usable envelope the anvil cracked. After this a small deformation was visible on the resonant plate. For testing under this limit no deformation has occurred.

Future tests will have to determine if the STF has managed to stay as repeatable as it is today throughout its lifetime.

## 6 Conclusions

A new STF for qualification of space equipment has been developed. The project started with the mission statement:

ISIS wishes to verify that the developing deployment system QuadPack survives the shock environments related to space travel.

The aim was set for this target and the road there was divided into several goals, see Section 2.1. First of all the mechanical phenomenon of shock was examined and a thorough research of the engineering field of shock testing was carried out. From the knowledge gained the requirements specification for the new STF was defined and with that the first goal was reached.

The first part of the system engineering phase of the project was the development of STF concepts. A wide array of concepts was found through functional analysis, brainstorming and examination of existing solutions. This concluded the second goal.

To end up with the best possible concept as winner an extensive elimination process was held. Simulations were made, experts were contacted and meetings were held which led to a final concept and knowledge on how the STF would have to perform to reach the required shock levels. With this goal three and goal four were reached and a leading edge on goal five was attained.

The fifth goal was to design the details of the concept to a manufacturable level. This was done in an iterative process that finished with the assembly of the new STF without any major issues.

The sixth goal was realised by a characterisation test campaign that gave knowledge on the true performance of the STF. The parameters were tested and their actual influences on the SRS were examined.

The STF still needs to undergo additional characterisation testing but it has already shown a capacity of testing equipment up to 26 kg with control of the SRS for frequencies 100 Hz – 10 kHz. It can achieve levels over 3000 g at frequencies 1 kHz – 3 kHz. For smaller specimen the acceleration levels can reach up to 5000 g at 1 kHz and even higher for the highest frequencies.

### 6.1 Future work and recommendations

There are a lot of ways in which the STF can be further developed. Many of them come down to additional characterisation testing of the STF. New hammerheads and anvil plates in more diverse materials could be tested as well as a more extensive examination of the influence of mechanical filters. More efficient clamping types could be developed and tested together with the effect of tuning masses or secondary oscillators to see if it can attenuate specific modes. The usage of adaptors should be examined to enable improvement of the IP characteristics by using the OOP configuration and an adaptor.

A modal analysis of the actual plate could be done and compared to the simulated analysis to verify the modes. A mapping of the plate could also be made which gives indications of where a certain specimen should be placed for a beneficial shock

response. More mounting patterns could be added to the plate for generally good locations.

A new round of simulations could be held and improved iteratively by validation on the actual STF. With a validated model this can be used to shorten the trial and error time to reach a certain SRS requirement. In the long run this can be extended into a program that suggests the setting of the STF parameters for certain test specifications.

In the longer run different plates could be used for different requirements. This way the STF would not have to be pushed to its limit to give a response it is not prone to give. Other impactors such as a nail gun could be added for requirements that are not reachable with the pendulum hammer.

The DAQ chain should be updated with more sensors to shorten the time for testing. For each shock test the shock levels should be controlled in several directions and at several locations. The DAQ module should also be updated to a version that samples at the recommended speed. With these updated the DAQ software would also need an update.

More research and more testing are always required. Knowledge is a light burden to carry.

## References

- [1] J. E. Alexander, "Shock Response Spectrum - A Primer," *Sound & Vibration*, pp. 6 - 14, 2009.
- [2] Department of Defence, USA, "MIL-STD-810G, Test Method Standard," US Army Publications, 2008.
- [3] ESA, "ESSB-HB-E-005, ESA mechanical shock design and verification handbook," ESA, 2012.
- [4] NASA, "GSFC-STD-7000, General Environmental Verification Standard," NASA, Greenbelt, Maryland, 2005.
- [5] C. M. Harris and A. G. Piersol, *Harris' shock and vibration handbook*, McGraw-Hill, 2002.
- [6] NASA, "NASA-STD-7003A, Pyroshock Test Criteria," NASA, Washington, DC, 2011.
- [7] Arianespace, "Ariane 5 User's Manual Issue 5 Revision 1," Arianespace, 2011.
- [8] D. Dilhan, V. Cipolla and e. al, "Pyroshock Generation," in *European Conference on Spacecraft Structures, Materials and Mechanical Testing*, Noordwijk, 2005.
- [9] E. Filippi, H. Attouman and C. Conti, "Pyroshock Simulation Using the Alcatel ETCA Test Facility," in *Launch Vehicle Vibrations. First European Conference*, Toulouse, 1999.
- [10] C. De Fruytier, O. Verlinden and D. Wattiaux, "Pyroshock Simulation for Qualification of Space Electronic Equipment," in *Workshop on Spacecraft Shock Environment and Specification*, Noordwijk, 2008.
- [11] N. Siam, "Development of an Efficient Analysis Method For Prediction and Structural Dimensioning of Space Structures Subjected to Shock Loading," LTU-PB-EX, Kiruna, 2010.
- [12] E. Cavro and A. Girard, "Test Specifications and Facilities for Shock Environment Simulation," in *Workshop on Spacecraft Shock Environment and Specification*, Noordwijk, 2008.
- [13] Institute of Environmental Sciences, *Handbook for Dynamic Data Acquisition and Analysis*, Mount Prospect: Institute of Environmental Sciences.
- [14] NASA, NASA-HDBK-7005, *Dynamic Environmental Criteria*, NASA, 2001.

- [15] G. Schweickert, "The Dornier Shock Table - A New Facility for Shocktesting of Components," in *Environmental Testing for Space Programs*, Noordwijk, 1997.
- [16] D. Dilhan, A. Piquereau and e. al, "Definition and Manufacturing of the Pyroshock Bench," in *7th ESA/CNES International Workshop on Space Pyrotechnics*, Noordwijk, 2008.
- [17] T. Irvine, "An Introduction to the Shock Response Spectrum," 2010.
- [18] German Aerospace Center, Institute for Space systems, "Pyroshock test," DLR, Berlin, 2010.
- [19] B. Dahlenburg, "Untersuchung der Pyroschocksynthese mittels eines Bolzenschubgeräts zur Qualifizierung von Komponenten in der Raumfahrt," TU Berlin, Berlin, 2009.
- [20] ECSS, "ECSS-E-10 Part 1B, Space Engineering - System Engineering - Part 1: Requirements and Process," ESA Publications Division, Noordwijk, 2004.
- [21] NASA, NASA/SP-2007-6105 Rev1, NASA Systems Engineering Handbook, Washington, DC: NASA, 2007.
- [22] ECSS, "ECSS-E-10-03A, Space Engineering - Testing," ESA Publications Division, Noordwijk, 2002.
- [23] J. Leijon, Interviewee, *Shock expert, RUAG Space AB, Sweden*. [Interview]. May-August 2012.
- [24] M. Wagner, Interviewee, *Shock expert, ESTEC, ESA, Netherlands*. [Interview]. Jun-Aug 2012.
- [25] A. Bäger, Interviewee, *Shock Expert, DLR, Germany*. [Interview]. May-August 2012.
- [26] C. De Fruytier, Interviewee, *Shock Expert, Thales Alenia Space ETCA, Belgium*. [Interview]. May-August 2012.
- [27] ECSS, "ECSS-E-ST-10-02C, Space Engineering - Verification," ESA Requirements and Standards Division, Noordwijk, 2009.
- [28] A. Lacher, N. Jüngel and U. von Wagner, "Modelling of a Pyroshock Test Device," TU Berlin, Berlin, 2009.
- [29] S. Kiryenko, G. Piret and J. Kasper, "ESA/ESTEC Shock Bench Presentation," ESA/ESTEC, Noordwijk.
- [30] P. M. F.J. Harewood, "Comparison of the implicit and explicit finite element methods using crystal plasticity," *Computational Materials Science*, pp. 481-494,

2007.

- [31] I. N. Patrick Doelfs, "Using MSC.Nastran for Explicit FEM Simulations," München, 2004.
- [32] A. Calvi, *Spacecraft Structural Dynamics & Loads - An Overview*, Noordwijk, 2010.
- [33] A. Lacher, "Zur analytischen Beschreibung der Stoßantwort einfacher kontinuierlicher Strukturen mit Anwendung auf Pyroshocksimulationen," TU Berlin, Berlin, 2011.
- [34] T. J. Dwyer and D. S. Moul, *Pyro Shock Simulation: Experience with the MIPS Simulator*, Valley Forge: GE Astro Space Division.
- [35] A. Lacher, Interviewee, *Shock Expert, Technische Universität Berlin, Germany*. [Interview]. May-August 2012.
- [36] Abaqus 6.11, "Abaqus Theory Manual".
- [37] R. L. Mayes, *A Post Processing Algorithm to Add Damping to Undamped Model Responses*, Albuquerque, New Mexico: Sandia National Laboratories.
- [38] D. O. Smallwood, "An Improved Recursive Formula for Calculating Shock Response Spectra," Sandia National Laboratories, Albuquerque, New Mexico.
- [39] J. Kasper, Interviewee, *Shock expert, EADS Astrium, Germany*. [Interview]. May-August 2012.
- [40] Endevco, "Problems in High-Shock Measurement," Endevco.
- [41] A. S. Chu, "Zeroshift of Piezoelectric Accelerometers in Pyroshock Measurements," in *57th Shock & Vibration Symposium*, 1987.
- [42] J. Wijker, *Mechanical Vibrations in Spacecraft Design*, Berlin Heidelberg: Springer-Verlag, 2004.

## Appendix A – Brainstorming Results

In this step every imaginable sub-solution is hunted. No revealed solution is to be overlooked since even the unlikeliest of solutions might have a grain of success in them. For the sake of completeness they will all be documented here together with the existing solutions.

### Impactor

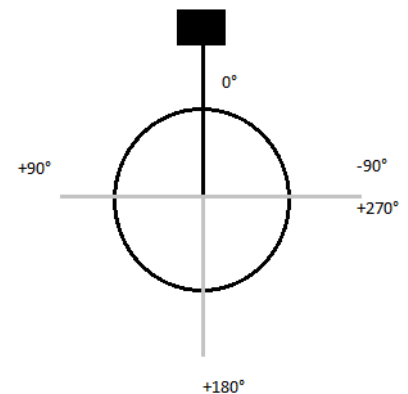
The sub-solutions to the excite function are closely linked to the solution of the charge energy function. If held apart too much the impactor would only be an object with mass that is accelerated in some way so the solutions of these two sub-functions are partly invading each other's territories.

- Drop hammer

Some kind of mass (cylinder, ball, cuboid, etc.) that more or less guided falls on the receiver. It could have exchangeable masses, impact geometries and impact materials. It could also be dropped from adjustable heights and impact at different positions.

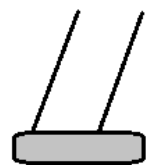
- Pendulum hammer

Some kind of mass similar to that stated above that is connected to a structure via a rigid link. Can be charged to a maximum of  $0^\circ$  (see schematic to the right) and will from its elevated position fall down and strike the receiver at  $+90^\circ$ ,  $-90^\circ$ ,  $+180^\circ$  or  $+270^\circ$  depending on configuration. Can thereby be used both for in plane and out of plane excitation.



- Ram hammer

A kind of pendulum hammer connected to a structure via two lines which keep it levelled. Also here the mass, height, material, geometry and impact location can be altered for tuning.

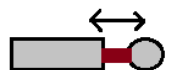


- Combination of hammers
- Pneumatic gun

Some kind of mass (rod, ball, etc.) is being accelerated by high pressure gas and impacts the receiver. Release pressure and position can be easily altered.

- Pneumatic piston

A similar solution to the one above but the piston that impacts the receiver is held by its housing like in a hydraulic cylinder. In addition to the release pressure and the impact position it is also easy to alter the material of the impact head. It could also be used on a hammer shaft for leverage.



- Regular hammer

Easy and cheap and it is simple to alter all the spatial parameters of the stroke. The downside however is that it is very hard to achieve good repeatability.

- Nail gun

A commercial nail gun (e.g. Hilti) can be used to excite the STF. It is highly repeatable but care must be taken so that personnel and material is not damaged.

- Rocket sled hammer

A mass is attached to a sled and accelerated with rockets along a track where it eventually impacts the receiver. It shares a lot of advantages with the other hammers but requires a rocket which is a disadvantage.

- Bowling ball rails

A bowling ball is rolled along a rail where it eventually impacts the receiver. Similar to drop and pendulum hammer with many adjustable parameters.

- Sliding weight

A weight slides along a guiderail and eventually hits the receiver. It is similar to drop hammer in advantages and disadvantages. This can be charged in a lot of different ways.

- Hammer on torque axle

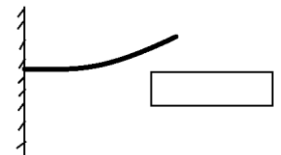
A hammer attached to an axle with a torsion spring, electric engine or other machine that gives angular speed. Can strike both in and out of plane and can be adjusted in the same way as the pendulum hammer with the height exchanged for engine power or angular displacement. It does not have a maximum limit in the same way as the pendulum hammer.

- Bullet shot on anvil

Some kind of weapon is fired onto the receiver. It is highly repeatable but dangerous both for personnel and material.

- Beam

An elastic cantilever beam is displaced and released onto the receiver. Displacement, impact position and anvil material can be easily adjusted.



- Motorised small car/wagon

A small car (RC-type or wire controlled) with adjustable speed is driven to collide with the receiver

- Inclined rail with train

A train is released from some elevation along a rail and is brought to impact the receiver. Similar to bowling ball rails in adjustable parameters.

- Magnet

A magnetic object is accelerated along magnetic rails and brought to collide with the receiver. It is basically a rail gun. Might be expensive but is also likely to be highly repeatable and adjustable.

- Hammer with adjustable shaft length

This is similar to the pendulum hammer but with an adjustable shaft. This should shift the limit in height of the pendulum hammer to a higher level.

### Charge energy

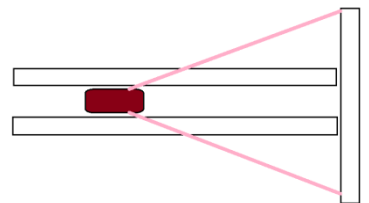
As mentioned above, most of these solutions are directly dependent on the impactor solutions so these two sub-functions will be merged before the concept generating phase.

- Height (Potential energy in different hammers)
- Air/Gas/Pneumatic pressure
- Muscle power (Regular hammer)
- Gunpowder (Bullet shot on anvil)
- Electricity (Torque engine, Magnet)
- Hydrocarbons (Torque engine)
- Compression spring



This is the first solution for this sub-function without an implied solution from the impactor. Potential energy is stored in a spring and used to accelerate a mass onto the receiver.

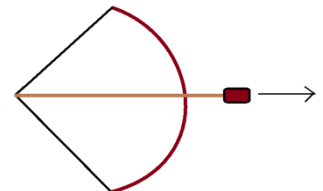
- Rocket fuel (Rocket sledge hammer)
- Torsion spring (Torque hammer)
- Elastic beam (Potential strain energy)
- Bungee cords



Energy is charged in bungee cords and used to accelerate a mass onto the receiver.

- Crossbow

Energy is charged in a bow and used to accelerate a mass onto the receiver.



- Magnetic force (Potential energy in magnet)

If constant magnets are used in the magnet solution instead of electromagnets.

- Combined spring and height

If the height is insufficient extra energy could be charged with some kind of spring. This could also be some kind of add-on when needed, comparable in that sense to the hammer with adjustable shaft length.

### Receiver

This sub-function is tightly linked with the Fasten QuadPack function.

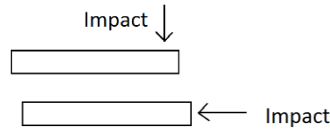
- Anvil

It is possible that all the sub-solutions below will be provided with anvils to be used as sacrifice elements and take the potential deformation of the impact.

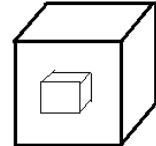


- Resonant plate

- Resonant beam
- Resonant bar
- Resonant bi-plate
- Tunable resonant plate
- Tunable resonant beam
- Tunable resonant bar
- Plate between hammer and anvil
- Compounded structure from above parts
- Box



Box made of either resonant plates or resonant beams; the specimen can be fastened on either side of the structure.



- Triangular plate
- Round plate

Different shape of the plates could be used on the same STF when different shock environments are required.

- Bi-plate with interchangeable spacers

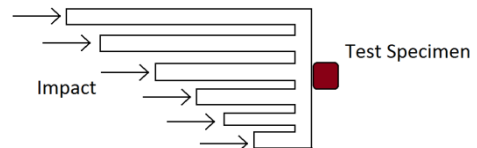
No spacers could also be a setting.

- L-bar/beam

One of several possible compounded structures to achieve required frequency.

- Structure with different impact locations

Structure made to have different responses excited



depending on impact location.

- Minimal



### Fasten QuadPack

This is the holder that the QuadPack needs to fasten to. As mentioned earlier this sub-solution is directly dependent on the solution for the receiver. The fastening shall be made with the QuadPack's original fastening elements and it shall bring about the opportunity to test the QuadPack in all directions if the receiver does not do that itself. Basically there are two configurations.

- Directly on receiver
- On fixture/bracket/fastening adaptor

This adaptor shall allow the QuadPack to geometrically fit on the STF and to be tested in all directions if the receiver in itself does not do that. It could also be a way of

making the STF useable for more equipment in the future if the receiver does not allow enough altering. Several adaptors one STF.

### Connect holder to environment

This is the third of the more independent sub-solutions.

- Guide rails

The rails are fastened to the floor, wall or a scaffold and steers the motion of the Exciter into the receiver. The receiver is distanced from the environment with springs or foam pads.

- Resting on foam pad on table
- Adaptable clamping plate

The clamping plates clamp the structure dependent on required natural frequency. The plates in turn are mounted on a solid base.

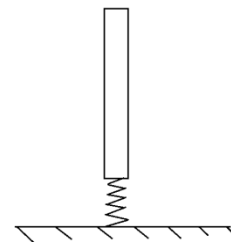
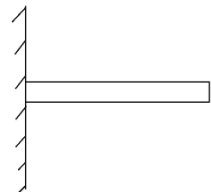
- Bolts with springs
- Hanging in ropes

All the hanging configurations could be hung from either the roof or a scaffold. They could also be hung both vertically or horizontally.

- Hanging in chains
- Hanging in bungee cords
- Hanging in springs
- Cantilever structure

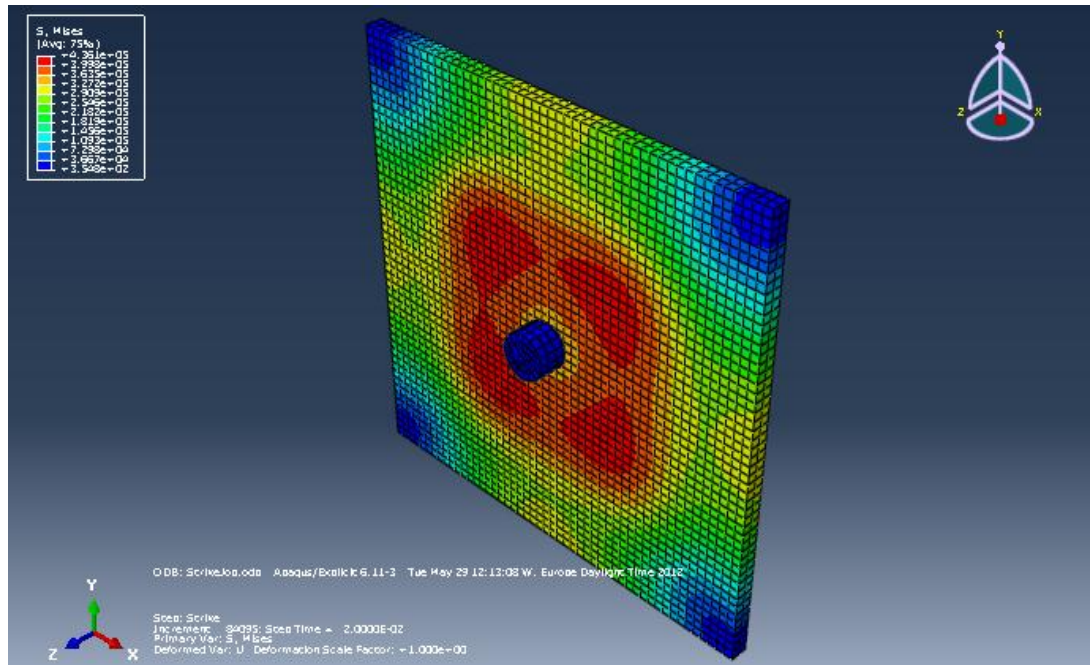
This boundary condition realises the sub-function automatically.

- Standing on wheels
- Resting on foam pad on floor
- Standing on low friction surface
- Springs in ground



## Appendix B – Analysis information

The simulations were made with the FEA software Abaqus. The calculations were made with Abaqus Explicit while the pre- and post-processing were made with Abaqus CAE.



### Appendix B 1 Impact simulation setup

#### Plate

1000 x 1000 x 30 mm

Aluminium with:

Young's modulus: 71.1 GPa

Poisson's' ratio: 0.33

Density: 2650 kg/m<sup>3</sup>

Number of elements: 8978

Type of elements: C3D8R, 8 node linear brick element

Free boundary conditions

#### Hammer

Cylinder with spherical impact surface

Radius of curvature: 200 mm

Steel with:

Young's modulus: 210 GPa

Poisson's' ratio: 0.3

Mass: 5 kg

Density: 7800 kg/m<sup>3</sup>

Number of elements: 594

Type of elements: C3D8R, 8 node linear brick element

### Impact

Modelled as initial velocity rather than free fall

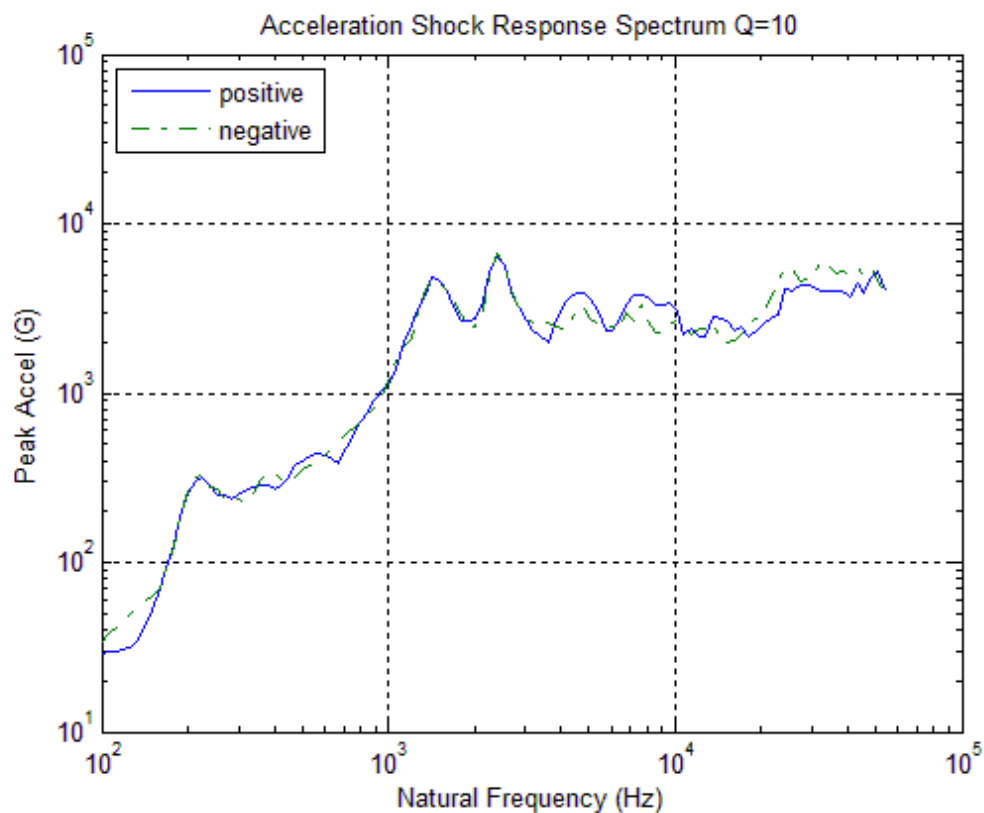
Damping not included

Stable time increment: Typical  $2.55e-7$  s

Contact property: Tangential behaviour

Friction formulation: Penalty

Friction coefficient: 0.3



### Appendix B 2 Positive and negative side SRS

SRSs were calculated with Matlab using the acceleration time histories and the Smallwood algorithm.

## Appendix C – Sustainable development

Throughout the project a sustainable development mind-set has been kept. Already in the requirement capture phase this had an impact where three sustainable development goals were defined:

- The STF should have as small impact on the environment as possible
- Recyclable material should have priority
- The amount of combustion gasses should be kept at a minimum

Later in the trade-off studies one of the killer arguments was:

- Sustainable, as small impact on the environment as possible

This led to that concepts which could not be implemented in a sustainable way were more prone to be eliminated. Sustainable was also one of the few criteria in the numerical trade-off where the final concept was selected.

The STF is designed with MK-profiles which is a standardised system. This makes most parts of the STF reusable when it is no longer needed. The majority of the parts are made of aluminium so when they cannot be reused anymore they can be recycled by melting them and making new parts. The foam pads used are made out of recycled foam pieces and both of the test dummies are reused parts.

The STF does only need power supply for the laptop in the data acquisition system. The data acquisition box and the sensor are USB-powered so if the laptop has a full battery no external power needs to be supplied for testing. Energising of the STF is done by human power and gravity so no combustion is used.

## Appendix D – Characterisation test campaign, plan and annotations

This appendix is the characterisation test campaign plan with the difference that the observations and records made during the actual characterisation test campaign has been added. Everything added after the test campaign has been given this green colour.

The characterisation test campaign is one of the most important phases in the development of a STF. In the characterisation test campaign the actual performance of the STF is examined and its potential is established. It is in this phase that the true influences of the parameters are measured and experience is gained on how to use them to tune the SRS. The testing in chapter 3 is carried out to build up a versatile toolbox for tuning the SRS to a certain shape. This toolbox is then to be used in chapter 4 to tune the SRS to within the requirements for six different test configurations.

### Tunable Parameters

The parameters whose influences are to be tested are:

- Impact velocity
- Hammer mass
- Anvil material
- Hammerhead material
- Impact location
- Foam type
- Boundary conditions of resonant plate

In addition to these parameters the STF will also be tested for:

- Repeatability
- Influence of mass dummy
- OOP/IP shift in impact direction

With all these parameters it would take more than 90 000 shocks to test all configurations. It is not feasible to do so many tests so to bring the number down a starting configuration is used as a benchmark. The parameters are then tested one at a time to see how they alter the SRS from the benchmark SRS and this behaviour is assumed to be present for all configurations. There are a few exceptions from this rule, namely the IP and OOP configuration shift and the usage of a mass dummy. The shift between IP and OOP configuration is expected to alter the SRS significantly so the STF needs to be tested for both configurations thoroughly. It is also important to test how the STF behaves when using a test specimen mass dummy so the influence of this will also be thoroughly examined.

### Starting Configuration

The starting settings of the different parameters are selected to make the test process as streamlined as possible. The selected values can be seen in the table below. A more elaborate discussion on the individual parameters are given in the chapter **Testing**.

Parameter	Benchmark setting
Impact velocity	15°
Hammer mass	0 kg add-on
Anvil material	Medium, Al7075
Hammerhead material	Soft, SS303
Impact location	Centre
Foam type	Soft
Boundary conditions	Unclamped
Mass dummy	No dummy
Impact direction	OOP

The configuration with these settings is henceforth called the benchmark configuration (BM).

### Testing

Before the testing commences the first step is of course to make sure that all the sub-systems work as they are supposed to do. The motion of the hammer shall be as expected and the DAQ chain shall be online. Functional tests of these are the first things that are done.

Sub-function	Working?	Observations
Hammer motion	OK	Anvil comes loose, make sure to check before testing
DAQ chain	OK	

The alignment of the setup and the readiness of the DAQ chain is something that is subsequently checked before every shock. Before every parameter is tested the BM is tested again to ensure long term repeatability. **The shocks that were not saved got the shock identification number 0.**

To determine how a parameter influences the shock results it is important to isolate the parameter to as large extent as possible. This way it can be said with confidence that it is the parameter in question that has the shown effect. Another basic assumption that must hold true for the tests to be performed with confidence is the repeatability of the STF. The repeatability is therefore the first and one of the most important characteristic tested on the STF.

### Repeatability

Two consecutive shocks with the same settings of the tunable parameters shall give the same resulting shock and SRS. Two consecutive shocks are considered to be the same if their SRS curves lies within 1 dB of each other. If necessary the BM will be updated in this process.

If conducted properly the STF is predicted to give repeatable results.

Shock identification number	Configuration	Observations	Comments on results
1	BM	Long hammer arm gives a lot of leverage, risk of bending charge angle plate bolt	Acceleration time history does not show expected exponential damping. Interesting to see if foam/clamping has influence

2	BM	Anvil surface still smooth	
3	BM	Everything still attached well	Looks very good! Almost identical.
		Ear protection is a must	S1, S2, S3 Saved without maximax shortcut in data

### Impact velocity

The impact velocity is a continuously variable parameter but to impose some structure on the testing it is tested in discrete steps. The impact velocity is controlled by the drop height of the hammer. The maximum height is around 1.5 m in the OOP configuration and around 3 m in the IP configuration. The BM is in the OOP configuration so it is in this configuration that the initial tests will be held.

The STF is equipped with a system to ensure that the same drop height can be used for consecutive shocks. It is, however, not graded as height in meters but instead as the angle of the pendulum hammer arm. The BM for the impact velocity is a charge angle of 15°. In this test round the levels that will be tested are:

- 15° → 1.7 m/s (BM to ensure long term repeatability)
- 30° → 3.4 m/s
- 45° → 4.2 m/s
- 60° → 4.9 m/s
- 75° → 5.3 m/s

Parameter	Benchmark setting
Impact velocity	15°
Hammer mass	0 kg add-on
Anvil material	Medium, Al7075
Hammerhead material	Soft, SS303
Impact location	Centre
Foam type	Soft
Boundary conditions	Unclamped
Mass dummy	No dummy
Impact direction	OOP

The expected results are that the shape of the SRS will stay constant while the overall shock level will rise when the drop height is increased.

Shock identification number	Configuration	Observations	Comments on results
4	BM 15°		Looks good. This will be the benchmark shock since S4 has the maximax shortcut in the data. A comparison program was written to simplify comparison.
5	BM 15°		

6	30°	Anvil still smooth as a baby bottom	Already above req. SRS for freq. over 2000 Hz. Expected effect with overall raise
7	45°		Significantly smaller raise from 6→7 than for 5→6. Obs! Log scales and circular movement
8	60°	Plate “jumps” out from rubber pads	Even smaller difference
9	75°	Anvil smooth. Everything still attached	19000g max

### Hammer mass

The hammer has a “naked” mass which is the minimum mass it has without any add-on masses. There are five add-ons each weighing 2 kg which can be added in steps. The BM is without any add-on masses. The configurations that will be tested are:

- 0 kg add-on (BM to ensure long term repeatability)
- 2 kg
- 4 kg
- 6 kg
- 8 kg
- 10 kg

Parameter	Benchmark setting
Impact velocity	15°
Hammer mass	0 kg add-on
Anvil material	Medium, Al7075
Hammerhead material	Soft, SS303
Impact location	Centre
Foam type	Soft
Boundary conditions	Unclamped
Mass dummy	No dummy
Impact direction	OOP

It is expected that an increase in hammer mass will have an effect on the frequencies under the knee frequency in the SRS. With a heavier hammer the shock levels should get higher for the lower frequencies which in effect straighten out the SRS curve.

Shock identification number	Configuration	Observations	Comments on results
10	BM 0 kg		Long term repeatability: Small difference at the lowest and highest frequencies
11	2 kg		Expected effect for freq. <1000 Hz. Also lower for freq. >3000 Hz

12	4 kg		Goes lower than S11 for the lowest freq. Not expected. Redo
13	4 kg	Tightened mass bolt extra	Same as S12
14	6 kg		Similar to S12. Specially for low freq.
15	8 kg	Differences between pos. and neg. SRS are increasing	Slightly higher for lower freq.
16	10 kg		Lower for high freq. Otherwise similar to S15
17	10 kg, 20°		Expected result, Overall heightening of SRS

### Anvil material

The anvil plate has been manufactured in three different materials. They range from the “Soft” Al6082, over the “Medium” Al7075, to the “Hard” stainless steel SS304. The medium anvil Al7075 is in the BM instead of the softest one since it will get more shocks than the other two and a softer anvil is more prone to deformation. All three anvils will be tested:

- Medium Al7075 (BM to ensure long term repeatability)
- Soft Al6082
- Hard SS304

Parameter	Benchmark setting
Impact velocity	15°
Hammer mass	0 kg add-on
Anvil material	Medium, Al7075
Hammerhead material	Soft, SS303
Impact location	Centre
Foam type	Soft
Boundary conditions	Unclamped
Mass dummy	No dummy
Impact direction	OOP

The expected results are that the anvil material will influence the SRS for the frequencies over the knee frequency. The shock levels are expected to be higher for the harder anvil and lower for the softer material. Attention will also be kept to spot distinctions that might be visible in the time plane.

Shock identification number	Configuration	Observations	Comments on results
18	BM Medium, 20°	20° by mistake	Hence higher than S4
19	BM Medium		Small differences for the lowest freq.
20	Soft	Some kind of smudge has formed under plate. Easier to	Almost no difference!

		change plate if charge angle plate bolt is loosened before the arm is lifted. Arm can also be tied up to be out of the way	
21	Hard		Slightly higher for high freq.
22	9 A4 standard papers on anvil		Lower overall but particularly for high freq.
23	Newly manufactured plastic anvil		After the mode at almost 200 Hz which actually was higher here, there is a dip but after 400 Hz the levels hold around 300 g

### Hammerhead material

The hammerhead has been manufactured in two materials, the “Soft” SS303 and the “Hard” SS630. The softer hammerhead is the BM and they will both be tested:

- Soft SS304 (BM to ensure long term repeatability)
- Hard SS630

Parameter	Benchmark setting
Impact velocity	15°
Hammer mass	0 kg add-on
Anvil material	Medium, Al7075
Hammerhead material	Soft, SS303
Impact location	Centre
Foam type	Soft
Boundary conditions	Unclamped
Mass dummy	No dummy
Impact direction	OOP

The expected results are similar to those for the anvil plate. The harder hammerhead is expected to give a SRS that has higher levels for the frequencies over the knee frequency.

Shock identification number	Configuration	Observations	Comments on results
24	BM Soft	Starting to see a barely visible dent on medium anvil, no sign of wear on soft anvil	Looks a bit higher than BM (S4). Do again
25	BM Soft		Almost identical to S24
26	Hard	Aluminium residue on hammerhead	The harder hammerhead has lower response for high frequencies. Unexpected,

			verify
27	Hard		Lies between S25 and S26 but it is still lower than S25 for high frequencies
28	Hard		
29	Soft with very soft pink foam on anvil		Lower for high frequencies!

### Impact location

There are 16 different impact locations for the OOP impact direction. The OOP configuration is the BM configuration. The BM for the impact location is the dead centre of the square plate. In the simulations no consistent rule could be found for the behaviour of the SRS when the impact location was altered so the testing here is of an experimental nature. Ten different locations will be tested. From the centre location tests will be made by taking three steps to the left, three steps down and three steps diagonally between these directions. The directions are given as they are seen by the hammer, see the figure below where the impact locations are shown.

The impact locations that will be tested in this round are hence:

- Centre (BM to ensure long term repeatability)
- -x
- -2x
- -3x
- -y
- -2y
- -3y
- -xy
- -2xy
- -3xy

Parameter	Benchmark setting
Impact velocity	15°
Hammer mass	0 kg add-on
Anvil material	Medium, Al7075
Hammerhead material	Soft, SS303
Impact location	Centre
Foam type	Soft
Boundary conditions	Unclamped
Mass dummy	No dummy
Impact direction	OOP

Shock	Configuration	Observations	Comments on results
-------	---------------	--------------	---------------------

identification number			
30	BM Centre		A bit higher than S4 for medium freq. Identical to S24 though. Indicating some settling time.
31	-x	The first peak in the SRS $\approx 200$ HZ is more "squeezed"	SRS "pushed/shifted" to the left overall
32	-2x		For mid to high freq. the SRS is shifted a bit up and to the left compared to S31
33	-3x	Pos/neg SRS still looking good	In comparison to S32 this setup enhances some modes (500, 1500, 3000, 4000 Hz) and dampens others (200, 2000 Hz)
n/a	n/a	Overall the x movement of the impact location dampens the low freq. and enhances the mid freq.	Closer to a knee freq. at 1000 Hz
34	-y	Dampens the mode at 200 HZ almost precisely as S 31	For the rest of the SRS it has almost opposite effect compared to S31
35	-2y	Mode at 200 Hz gone.	Mid freq. up, high freq. down compared to S34 and S30. Quite smooth for low freq.
36	-3y	+ and - SRS shows some difference, do again	S36 and S37 pretty much identical.
37	-3y	Same. Some differences at low freq.	Higher mode at 450 Hz lower at 800-900 Hz compared to S35
38	-xy	Spike at 5000Hz $>10000$ g	Do again $\rightarrow$ Identical to S39 go on
39	-xy	Lower for low freq.	Spike at 5-6 kHz
40	-2xy		Higher than S39 between 1000-3000 Hz lower spike at 5-6 kHz
41	-3xy	Good slope overall for low freq. and good knee freq. at 1000 Hz	Still spike at 5-6 kHz. Enhancement of modes at 1000 Hz and 500-600 Hz in comparison to S40
n/a	n/a	The impact location amplifies and dampens different modes	The results inspired an extra look on the modal analysis of the plate
42	-3xy, 20°, soft foam on anvil		The extra impact velocity was nulled by the foam. The foam could not kill the spike

			at 5-6 kHz
43	-3xy, 30°, black foam on anvil		Also could not attenuate the spike, but we are starting to get somewhere. Result is almost within NASA tolerances

### Foam type

Three different foam types have been selected for the STF. The foam is placed between the plate and the rest of the rig to emulate free boundary conditions. The softest foam is the BM but they will all be tested. The influence of the foam has not been simulated so the tests are purely experimental. It is, however, expected to influence the SRS since the different foams in practice alters the boundary conditions of the plate. This should have an effect on the overall shape of the SRS.

- Soft (BM to ensure long term repeatability)
- Medium
- Hard

Parameter	Benchmark setting
Impact velocity	15°
Hammer mass	0 kg add-on
Anvil material	Medium, Al7075
Hammerhead material	Soft, SS303
Impact location	Centre
Foam type	Soft
Boundary conditions	Unclamped
Mass dummy	No dummy
Impact direction	OOP

Shock identification number	Configuration	Observations	Comments on results
44	BM Soft	Slightly, <1 dB higher overall	
45	Medium		No real difference from S44
46	Hard		A little bit higher for low freq.

Since there is no difference the medium foam will henceforth be used as benchmark since it is more convenient to work with.

### Boundary conditions of the plate

The boundary conditions can, excluding the different foam types, be altered by clamping the plate in different ways or by adding extra masses at certain locations. The possibilities are unlimited but two ways of restraining the plate will be tested. The BM is to have the plate unclamped (free) and the other two ways are clamping it with

the STF's siderails or by using actual clamps and clamp the plate to the beams that the plate is resting on. This parameter is expected to alter the overall shape of the SRS.

- Free (BM to ensure long term repeatability)
- Siderails
- Clamps

Parameter	Benchmark setting
Impact velocity	15°
Hammer mass	0 kg add-on
Anvil material	Medium, Al7075
Hammerhead material	Soft, SS303
Impact location	Centre
Foam type	Medium
Boundary conditions	Unclamped
Mass dummy	No dummy
Impact direction	OOP

Shock identification number	Configuration	Observations	Comments on results
47	BM Free		Almost identical to S30
48	Siderails	Very different sound. Acc. Time history looks a bit better	A small spike for the mode at 158 Hz, otherwise the same
49	Siderails harder		Slight attenuation at lower frequencies
50	BM -y	New BM so that the clamps will fit	
51	BM -y clamps	Zeroshift	Do again
52	BM -y clamps	Better	Slightly lower everywhere but for mode 400-500Hz
53	Clamp without the rubber pads		Clamps kill the mode at 158 Hz and slightly dampens the high frequencies
54	Rubber instead of foam under plate		Attenuates the mode at 158 Hz, amplifies the mode at 400-500 Hz, otherwise the same
55	Clamps, rubber under plate		Slightly lower for high freq.

To avoid a lot of configuration changes the no dummy OOP goal will be tested before the influence of adding a dummy is tested.

### Mass dummy

It is expected that the mounting of a test specimen will have an effect on the SRS. The simulations did not give consistent results but research show that a small overall shift of the SRS to the left can be anticipated. Two different dummies will be used, one “Heavy” and one “Light”. The heavy dummy is a part of the previous STF that has a mass of 26 kg. The light dummy is a 6.3 kg adaptor plate previously used for vibration testing. The other parameters will be tested to confirm that they have the same overall influence of the SRS as for the testing without a dummy. If that is not the case the parameter in question will be examined further.

- No dummy (BM to ensure long term repeatability)
- Light
- Heavy
- Control testing of parameters
- Further testing of parameters not showing expected behaviour

Parameter	Benchmark setting
Impact velocity	15°
Hammer mass	0 kg add-on
Anvil material	Medium, Al7075
Hammerhead material	Soft, SS303
Impact location	Centre
Foam type	Medium
Boundary conditions	Unclamped
Mass dummy	No dummy
Impact direction	OOP

Shock identification number	Configuration	Observations	Comments on results
69	BM		Almost identical to S47
70	BM switch measurement location	To fit light dummy, first this location was tested without any dummy	Quite different from S69, S70 is the BM for testing with the light dummy
71	Light	Not very tight bolts on dummy, hard to torque. Sound is very different	Lower for low freq. and 1000-2500 Hz
72	Light, 25°	Tightened the screws somewhat	Expected behaviour
73	Light, 25°, 2kg		Expected behaviour
74	Light, 35°, 2kg, foam		Lower for high freq.
75	Light, 25°, 2kg, -3xy	Very different	Lower for mid freq. higher for high and mode at 158 Hz
76	Light, 45°, 6kg, foam	Time history looks better now	Compared to S74 higher everywhere but around knee frequency

77	Light, 45°, 6kg, foam, -y		Lower for high freq. Not the way to go.
78	Light, 45°, 6kg, foam, -x	Goal SRS testing for the light dummy was carried out before the switch to the heavy dummy	Very similar to S76
85	BM switch measurement location	To fit heavy dummy, first this location was tested without any dummy	Spike at 450 Hz and 4500 Hz
86	Again, as above	Time history looks good	As S85
87	Heavy	Different sound	Compared to S86 higher for low freq. lower for high freq.
88	Heavy, 25°	Time history looks good, +- also	Expected behaviour
89	Heavy, 25°, 2 kg		Higher for low freq. as expected
90	Heavy, 45°, 2 kg, Foam on anvil		A bit lower overall but for 1200 Hz and 2000 Hz

The goal SRS tests will be done before the OOP/IP shift so that this configuration change will only have to be done once.

### OOP/IP shift

This configuration change is expected to have a large influence on the SRS. The parameters are expected to have the same overall effect on the SRS for the IP configuration but the original shape of the SRS is expected to be different. It is also important to measure the shock levels in the OOP direction for the IP impact direction since these can be substantial. This is since the plate is prone to be excited in its OOP bending modes also when it is impacted IP. The OOP impact does not have the ability to induce the IP compression waves in the same extent so for the OOP configuration this is not a problem.

- IP all else BM
- Measure OOP shock for IP impact
- Control testing of parameters
- Further testing of parameters not showing expected behaviour

Parameter	Benchmark setting
Impact velocity	15°
Hammer mass	0 kg add-on
Anvil material	Medium, Al7075
Hammerhead material	Soft, SS303
Impact location	Centre
Foam type	Medium
Boundary conditions	Unclamped
Mass dummy	No dummy
Impact direction	OOP

Shock identification number	Configuration	Observations	Comments on results
96	IP BM 20°	Sensor still OOP	No levels to talk about
97	Sensor OOP, 45°, 2 kg		
98	Sensor OOP, 90°, 2 kg		Spike at high freq. not over NASA tol.
99	IP BM, 25°, 2 kg		Looks like the simulation results
100	40°, 2 kg		As expected
101	40°		Lower for low freq. as expected. Also higher for the highest freq.
102	40°, -x		Lower for high freq.
103	40°, -2x		Very similar to S102
104	40°, -x, hard hammerhead	It will be hard to fit both the slope of the low freq. and the knee freq. for the IP configuration	Lower for high freq. compared to S102.
105	40°, -x, hard hammerhead, soft anvil		Slightly mini lower for high freq.
106	40°, hard hammerhead, soft anvil		Slightly lower than S105 for high freq.
107	40°, hard hammerhead, soft anvil, siderails	Different sound	Higher for high and low freq. Do again.
108	40°, hard hammerhead, soft anvil, siderails		It is higher! Again.
109	40°, hard hammerhead, soft anvil, siderails	Dent on anvil	As S108
110	40°, hard hammerhead, soft anvil, 4 kg		Higher than S106 for both high and low freq.
111	40°, hard hammerhead, -x		

112	55°, hard hammerhead, -x		
113	70°, hard hammerhead, -x		
122	40°, hard hammerhead, heavy		Compared with S101 lower overall. Much lower for high freq.
123	60°, hard hammerhead, heavy	Hammer arm visibly vibrating	Higher overall as expected
124	90°, hard hammerhead, heavy		Higher overall
125	120°, hard hammerhead, heavy		Higher overall but not much
126	90°, hard hammerhead, heavy, 2 kg		As expected higher for low freq.
127	90°, hard hammerhead, heavy, 6 kg	Cracked anvil plate	

### Goal SRS

After the behaviours of the parameter tuning have been unravelled it should be possible to use these tools to get a SRS within the tolerances of the goal SRS. This should be done for both the OOP and the IP configuration, for both the mass dummies and without a dummy. In total that is six cases.

- No dummy, OOP
- Light, OOP
- Heavy, OOP
- No dummy, IP
- Light, IP
- Heavy, IP

Before the testing commences the conclusions drawn on the earlier testing should be used to plan a configuration that is believed to give the correct response for each of the six cases.

### No dummy OOP

Plan:

Parameter	Benchmark setting
Impact velocity	35°
Hammer mass	0 kg add-on
Anvil material	Medium, Al7075
Hammerhead material	Soft, SS303

Impact location	-3xy
Foam type	Medium
Boundary conditions	Unclamped
Mass dummy	No dummy
Impact direction	OOP
Mechanical filter	Double foam on anvil

Shock identification number	Configuration	Observations	Comments on results
56	Plan		As S43 but lower for high freq., Still high spike
57	Cardboard on anvil	First complaint from neighbours	Foam is better at attenuating the high freq.
58	Plan	Tested a normal hammer first which damaged the anvil slightly	As S56, anvil damage did not influence results
59	Hard pressed cardboard on anvil		158 mode is back, high freq. strongly attenuated
60	2kg, no foam	Forgot foam on anvil	Higher overall and sharper spikes
61	2kg, no foam	Zeroshift!	
62	2 kg, no foam	Still has sharper spikes	Higher for low freq. and smoothness is gone there. The modes are amplified at 158 Hz, 550 Hz and 1000 Hz. The mode at 5500 Hz is , however, lower.
63	2 kg		Higher for low freq. incl. mode at 158 Hz. Attenuates high freq. levels well.
64	45°	Except for a small bulge at 800 Hz OK for NASA tolerances	Higher overall but with smaller spike at 5500 Hz.
65	60°	Bulge at 800 still under	Same tendency as for S 64
66	80°	Turned around pink foam	Only difference is that spike is back at 5500 Hz
67	60°, 2 kg	Higher spikes. Spike at 158 and 5500 over tol.	
68	60°, 6 kg	158 Hz levels shifted right. 550 Hz higher, 5500 Hz lower.	50% over req. SRS. Needs to kill spikes at 158 and 5500 Hz
83	60°, 6 kg, clamps	Remembered this tool later in the process, hence higher shock identification number.	Did not kill the bulge at 158 Hz but it did get the one at 550 Hz

84	60°, 6 kg, clamps, one foam on anvil	OK for NASA tolerances except for bulge at 158 Hz
----	--------------------------------------	---

Since adding mass to the plate can attenuate certain modes the next step in the testing process was started.

### Light OOP

Plan:

Parameter	Benchmark setting
Impact velocity	45°
Hammer mass	6 kg add-on
Anvil material	Medium, Al7075
Hammerhead material	Soft, SS303
Impact location	-3xy
Foam type	Medium
Boundary conditions	Unclamped
Mass dummy	Light dummy
Impact direction	OOP
Mechanical filter	No

Shock identification number	Configuration	Observations	Comments on results
79	Plan		Higher than S76 for high freq.
80	60°		Slightly higher overall
81	60°, 10 kg		OK for NASA tolerances
82	60°, 10 kg, clamps		A little lower for high freq.

### Heavy OOP

Plan:

Parameter	Benchmark setting
Impact velocity	60°
Hammer mass	10 kg add-on
Anvil material	Medium, Al7075
Hammerhead material	Soft, SS303
Impact location	-3xy
Foam type	Medium
Boundary conditions	Unclamped
Mass dummy	Light dummy
Impact direction	OOP
Mechanical filter	Double foam

Shock identification number	Configuration	Observations	Comments on results
91	Plan		Too high for low freq.
92	6 kg, only 1 foam on anvil		Lower for low freq. Higher for high freq.
93	4 kg, 1 foam		Lower for low, almost OK
94	4 kg, 1 foam, clamps		Almost identical to S93
95	4 kg		Lower for high freq. OK for NASA

### No dummy IP

Plan:

Parameter	Benchmark setting
Impact velocity	90°
Hammer mass	0 kg add-on
Anvil material	Medium, Al7075
Hammerhead material	Hard, SS630
Impact location	-x
Foam type	Medium
Boundary conditions	Unclamped
Mass dummy	No dummy
Impact direction	IP
Mechanical filter	No

Shock identification number	Configuration	Observations	Comments on results
114	Plan		
115	4 kg	Sent the plate into the back siderail	
116	4 kg, backrail		A little bit higher overall
117	6 kg, 100°, backrail	Whole STF moves	Higher for low freq. Go back to 90°
118	10 kg, backrail		Higher for low freq., lower for high freq.
119	0 kg, centre, backrail, 120°	Big dent on anvil	Compared to S118 lower for low freq. and higher for high freq.
120	0 kg, centre, backrail, foam on anvil	Punched hole in the foam	Lower overall

121	0 kg, centre, backrail, hard cardboard on anvil		Everything low
-----	---	--	----------------

S117 is the best I can do at the time being. Due to a limited amount of time the light dummy was not tested. It is assumed that anything that is possible with the heavy dummy is also possible with the light dummy.

### Heavy IP

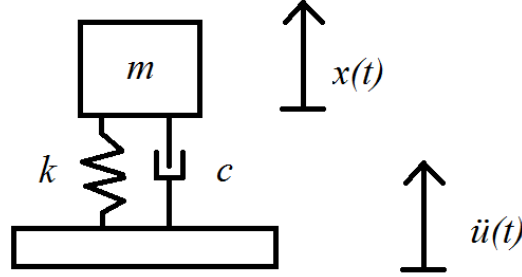
Plan:

Parameter	Benchmark setting
Impact velocity	120°
Hammer mass	6 kg add-on
Anvil material	Medium, Al7075
Hammerhead material	Hard, SS630
Impact location	Centre
Foam type	Medium
Boundary conditions	Backrail
Mass dummy	Heavy dummy
Impact direction	IP
Mechanical filter	No

Shock identification number	Configuration	Observations	Comments on results
128	Plan	Complaint on the noise. Deformation of resonant plate visible at IP impact location	A bit too low around knee freq. Pushed shock test facility to its max.

## Appendix E – Calculation of the peak acceleration of a SDOF system

The maximum acceleration response  $\ddot{x}(t)$  for a SDOF system with an arbitrary natural frequency from an enforced acceleration  $\ddot{u}(t)$ , see **Appendix E 1**, can be derived as follows [42]:



*Appendix E 1 SDOF system with spring constant  $k$ , damping constant  $c$  and mass  $m$*

Firstly the natural frequency  $\omega_n = \sqrt{\frac{k}{m}}$ , the critical damping  $c_{\text{crit}} = 2\sqrt{km}$ , the damping ratio  $\zeta = \frac{c}{c_{\text{crit}}}$  and the damped angular frequency  $\omega_d = \omega_n\sqrt{1 - \zeta^2}$  are introduced. The quality factor formerly mentioned is  $Q = \frac{1}{2\zeta}$ .

A relative displacement  $z$  is also introduced as

$$z = x - u \quad (1)$$

The equation of motion expressed in  $z(t)$  then becomes

$$\ddot{z} + 2\zeta\omega_n\dot{z} + \omega_n^2z = -\ddot{u} \quad (2)$$

Which together gives

$$\ddot{x} = \ddot{z} + \ddot{u} = -2\zeta\omega_n\dot{z} - \omega_n^2z \quad (3)$$

Solving **Equation (2)** with  $z(0) = \dot{z}(0) = 0$  gives

$$z(t) = -\int_0^t e^{-\zeta\omega_n\tau} \frac{\sin\omega_d\tau}{\omega_d} \ddot{u}(t-\tau) d\tau = -\int_0^t e^{-\zeta\omega_n(t-\tau)} \frac{\sin\omega_d(t-\tau)}{\omega_d} \ddot{u}(\tau) d\tau \quad (4)$$

Differentiation with respect to time gives

$$\dot{z}(t) = -\int_0^t e^{-\zeta\omega_n(t-\tau)} \cos(\omega_d(t-\tau)) \ddot{u}(\tau) d\tau - \zeta\omega_n z(t) \quad (5)$$

Which in turn, after applying **Equation (3)** gives

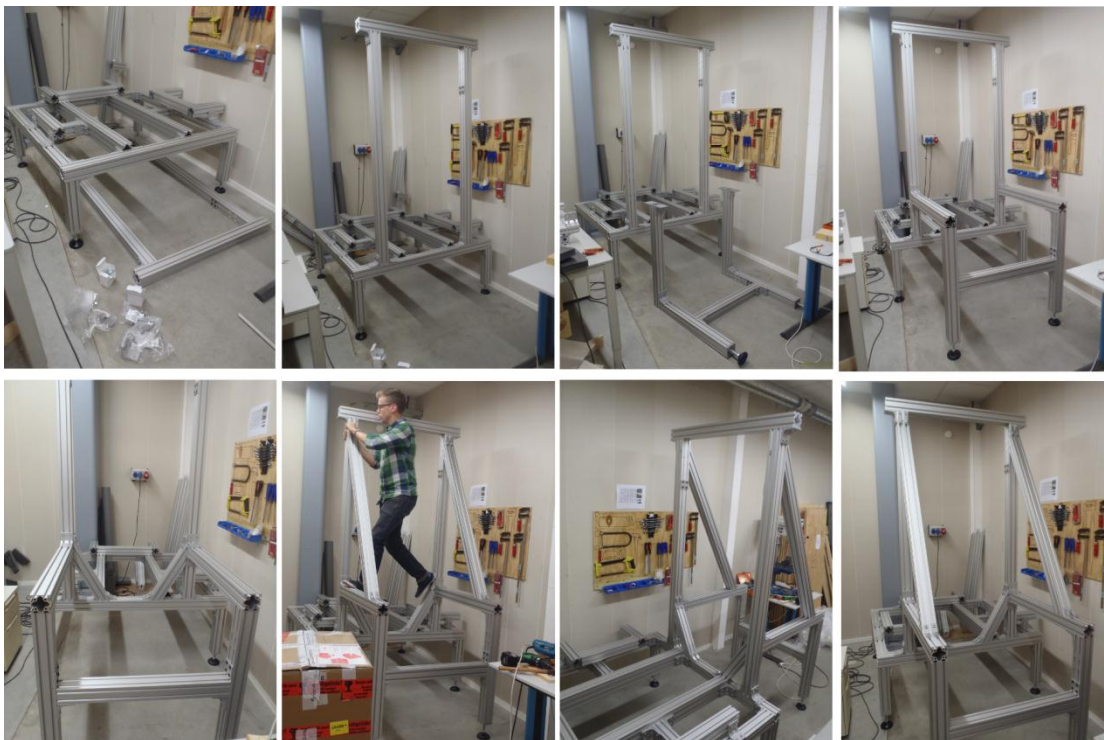
$$\ddot{x}(t) = 2\zeta\omega_n \int_0^t e^{-\zeta\omega_n(t-\tau)} \cos(\omega_d(t-\tau)) \ddot{u}(\tau) d\tau + \omega_n(2\zeta^2 - 1)z(t) \quad (6)$$

The maximum acceleration  $\ddot{x}$  can now be calculated by inserting arbitrary natural frequency  $\omega_n = 2\pi f$ .

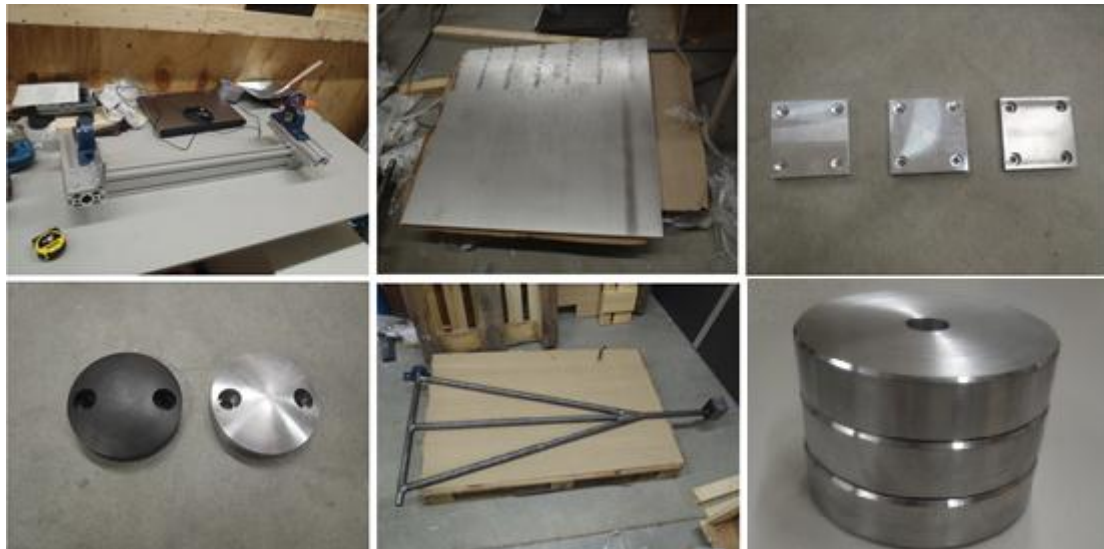
## Appendix F – Assembly of STF



*Appendix F 1 Assembly of MK parts 2, note the size of the facility*



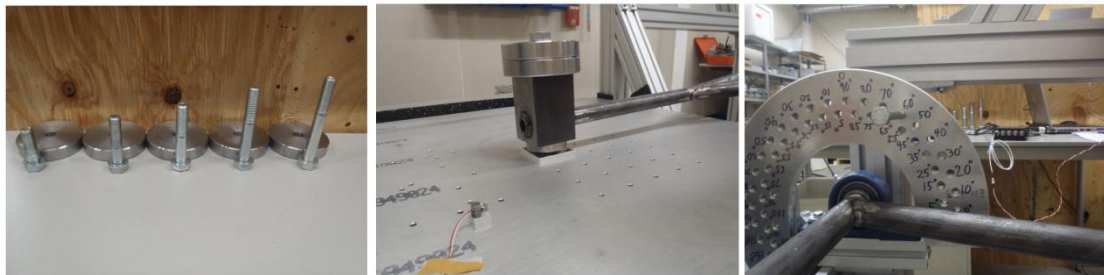
*Appendix F 2 Assembly of MK parts 2, note the size of the facility*



*Appendix F 3 a) Bearing solution b) Resonant plate c) Anvil plates  
d) Hammerheads e) Hammer arm f) Hammer add-on masses*



*Appendix F 4 a) Assembled bearing solution, charge angle plate and hammer arm  
b) Resonant plate in position c) Hammer assembly mounted on rig*



*Appendix F 5 a) Hammer masses with fasteners b) Hammer masses mounted on arm  
c) Charge angle plate mounted on rig*